

CHEMODYNAMICS OF COMPLEX WASTE MIXTURES:  
APPLICATIONS TO CONTAMINATION AND REMEDIATION  
OF SOILS AND AQUIFER MEDIA

By

DIONYSIUS C.M. AUGUSTIJN

A DISSERTATION PRESENTED TO THE GRADUATE SCHOOL  
OF THE UNIVERSITY OF FLORIDA IN PARTIAL FULFILLMENT  
OF THE REQUIREMENTS FOR THE DEGREE OF  
DOCTOR OF PHILOSOPHY

UNIVERSITY OF FLORIDA

1993

Copyright 1993

by

Dionysius C.M. Augustijn

## ACKNOWLEDGEMENTS

This dissertation means the conclusion of almost four years of doctoral research. During these years I have received assistance from many people, which I greatly appreciate. First, I would like to thank my committee members, Dr. Nkedi-Kizza, Dr. Rhue, Dr. Graham, and Dr. Hatfield, for there helpful comments and suggestions during my doctoral program.

I would like to thank my colleague students in the lab, Linda Lee, Itaru Okuda, Cheryl Bellin, and Dongping Dai. They were the reason for a very pleasant atmosphere in the lab, and made working there enjoyable. I would like to give special thanks to Linda Lee, who, with her unlimited energy, was always there to provide assistance with analytical problems. I also like to thank the OPS workers in the lab who have assisted me in my experimental research, especially Robin Wilson and Cathy Liang.

I would like to thank Ron Jessup for his invaluable assistance with the modeling part of this dissertation. The numerous discussions we had on the black board, helped me to develop a better conceptualization of soil physics and solute transport. Over the years, I have considered Ron as my second advisor.

Several other people have contributed to the work presented in this dissertation. In particular, I would like to thank Lynn Wood from the U.S. EPA Kerr

lab. in Ada, OK, who initiated the ideas and funded the research presented in Chapter 5. Additional financial support from the Electric Power Research Institute and Environmental Protection Agency is also greatly acknowledged.

I would like to thank my family and my wife's family, who, over the long distance, were always supportive to the work I was doing. I would like to give a very special thanks to my wife Ellen-Wien, her love and support were essential during my time in Florida.

Finally, I would like to thank Dr. Suresh Rao, who has been an outstanding advisor to me. I appreciate the combination of freedom and guidance he has given me during my Ph.D. The many intellectual and challenging discussions we had have given me a broader view on science, and have helped me to mature in a professional sense.

The help, advice, and friendship of all these people and more is greatly appreciated; without them none of this would have been possible.



## TABLE OF CONTENTS

ACKNOWLEDGEMENTS .....	iii
LIST OF TABLES .....	viii
LIST OF FIGURES .....	x
ABSTRACT .....	xii
CHAPTER 1 INTRODUCTION .....	1
Preface .....	1
Overview of the Problem .....	3
Migration of Organic Immiscible Liquids .....	3
Release and Transport of Contaminants .....	7
Nonequilibrium Conditions .....	12
Basic Transport Equations .....	14
Discussion .....	16
CHAPTER 2 DISSOLUTION FROM COMPLEX WASTE MIXTURES ...	19
Introduction .....	19
Dissolution Mechanisms .....	21
Model Development .....	24
Transport Equations .....	24
Initial and Boundary Conditions .....	28
Experimental Procedure .....	30
Experiments With Decane/PCE/Naphthalene Mixtures .....	31
Experiments With Coal Tar .....	34
Results and Discussion .....	35
DPN Mixture .....	35
Coal Tar .....	42
Conclusions .....	35

CHAPTER 3 SORPTION DYNAMICS IN CONTAMINATED SOILS: MECHANISMS, MODELS, AND PREDICTIVE APPROACHES . . .	47
Introduction . . . . .	47
Sorption Mechanisms . . . . .	48
Particulate organic matter and organic matter associated with mineral surfaces . . . . .	51
Organic matter in micropores of porous particles . . . . .	54
The Fractal Nature of Soil Organic Matter . . . . .	57
Sorption Nonequilibrium Models . . . . .	66
Film-Diffusion Model . . . . .	67
Pore-Diffusion Model . . . . .	69
First-Order Mass-Transfer Models . . . . .	72
Other Sorption Nonequilibrium Models . . . . .	73
Predicting Sorption Rate Coefficients . . . . .	77
Log $k_2$ -Log K Relationship Revisited . . . . .	77
Dependency of $k_2$ on Other Model Parameters . . . . .	85
Degree of Nonequilibrium . . . . .	89
Mass Transfer Rates in Contaminated Soils . . . . .	92
Sorption Transfer Rates in Contaminated Soils . . . . .	92
Experimental Procedure . . . . .	93
Preparation of the Soils . . . . .	95
Data Analyses . . . . .	99
Results and Discussion . . . . .	100
CHAPTER 4 REMEDIATION OF SOILS CONTAMINATED WITH COMPLEX WASTE MIXTURES: SOLVENT FLUSHING . . . . .	110
Overview of Remediation Techniques . . . . .	110
Cosolvency Theory . . . . .	116
Cosolvent Effects on Solubility . . . . .	116
Cosolvent Effects on Sorption . . . . .	119
Cosolvent Effects on Nonequilibrium Conditions . . . . .	120
Parameter Estimation . . . . .	123
Cosolvency Power . . . . .	123
Solubility . . . . .	125
Equilibrium Sorption Coefficient . . . . .	126
Nonideality Coefficients . . . . .	126
Sorption Nonequilibrium Parameters . . . . .	127
Applications . . . . .	127
Case 1: Solvent Flushing of a Low-Level Contaminated Soil . . . . .	129
Case 2: Solvent Flushing of Soils Contaminated with Single-Component OILs . . . . .	142

Case 3: Solvent Flushing of Soils Contaminated with Multi-Component OILs .....	145
Discussion of Solvent Flushing as a Potential Remediation Techniques	148
Hydrologic considerations .....	148
Selection of Cosolvents .....	149
Heterogeneity .....	150
External factors .....	155
CHAPTER 6 SUMMARY AND CONCLUSIONS .....	157
APPENDIX A NUMERICAL SOLUTION FOR MULTI-COMPONENT ELUTION .....	161
APPENDIX B COMPILATION OF SORPTION NONEQUILIBRIUM DATA FROM THE LITERATURE .....	174
REFERENCE LIST .....	180
BIOGRAPHICAL SKETCH .....	193

## LIST OF TABLES

Table 1-1	Expressions for the solute mass in each phase and their equilibrium relationship with the concentration in water . . . . .	17
Table 2-1	Composition of DPN mixture and column parameters used for model simulation . . . . .	38
Table 2-2	Composition of coal tar and column parameters used for model simulation . . . . .	38
Table 3-1	Comparison of the volume of micropores and soil organic matter (SOM) . . . . .	56
Table 3-2	Data for determination of a fractal dimension for two different soils . . . . .	63
Table 3-3	Nondimensional solute transport equations for four different sorption nonequilibrium models . . . . .	74
Table 3-4	Summary of estimated transport parameters for the four different sorbents studied . . . . .	101
Table 4-1	Summary of equations to estimate important parameters related to the cosolvency theory . . . . .	124
Table 4-2	Parameter values for the elution of naphthalene and anthracene with methanol-water mixtures from Eustis fine sand . . . . .	138

Table 4-3 Parameter values used for the simulation of elution profiles from  
a soil contaminated with a single-component OIL . . . . . 138



## LIST OF FIGURES

Figure 1-1 Schematic overview of soils contaminated with organic immiscible liquids .....	6
Figure 1-2 Schematic representation of the phase distribution in five different regions of a contaminated soil .....	8
Figure 2-1 Phase diagram for the solubility of naphthalene in decane/PCE mixtures .....	36
Figure 2-2 Simulated elution profiles for PCE and naphthalene from a decane/PCE/naphthalene mixture for ideal and nonideal behavior under equilibrium conditions .....	39
Figure 2-3 Simulated (fitted) and experimental elution profiles for PCE and naphthalene from a decane/PCE/naphthalene mixture .....	41
Figure 2-4 Elution profiles for six different tar-constituents from a column packed with a tar-treated sand .....	43
Figure 2-5 Measured versus predicted equilibrium solute concentrations for water in contact with coal tar ID#4 .....	45
Figure 3-1 Schematic representation of the three possible forms of organic matter in soils .....	50
Figure 3-2 Schematic representation of the chemical structure of soil organic matter (a) and the distribution of polar and hydrophobic domains in this hypothetical structure (b) .....	53
Figure 3-3 Three examples of fractal objects, and the calculation of the fractal dimension from their basic structure .....	58
Figure 3-4 Plot for determination of the fractal dimension of the Menger sponge, by filling the pores or paving the internal surfaces with sequence of balls with increasing radii .....	61
Figure 3-5 Plot of sorption data for determining of the fractal dimension of Tampa and Eustis soils .....	64
Figure 3-6 Correlation between the reverse first-order, mass-transfer rate coefficient ( $k_2$ ) and equilibrium sorption coefficient ( $K$ ) .....	78
Figure 3-7 Correlation between the first-order, mass-transfer rate coefficient ( $k$ ) and the equilibrium sorption coefficient normalized to the organic carbon fraction ( $K_{oc}$ ) .....	82
Figure 3-8 Correlation between the fraction of instantaneous sorption ( $F$ ), and the equilibrium sorption coefficient normalized to the organic carbon fraction ( $K_{oc}$ ) .....	84

Figure 3-9 The dependence of the first-order, mass transfer rate coefficient on the retardation factor (R), flowrate (T), and fraction of instantaneous sorption (F) .....	87
Figure 3-10 Representation of the degree of nonequilibrium ( $\mu$ ) as a function of the Damkohler number ( $kL/v$ ), retardation factor (R), fraction of instantaneous sorption (F), and Peclet number (P) .....	91
Figure 3-11 Comparison of the mass-transfer rates found for three types of contaminated soils with the rate coefficients reported for natural systems .....	103
Figure 3-12 Experimental breakthrough curve of benzene through a column packed with coal tar/sand mixture .....	105
Figure 3-13 Results of the batch time-study for sorption of benzene by the coal tar/sand mixture .....	107
Figure 4-1 Schematic of the possible options for remediating soils and aquifers contaminated with organic immiscible liquids .....	111
Figure 4-2 Schematic representation of the in situ solvent flushing technique .....	115
Figure 4-3 Simulated elution profiles of naphthalene for 20% and 50% methanol fractions .....	132
Figure 4-4 Simulated concentration profiles within the column for naphthalene at two different pore volumes (pv) in the solution (a) and sorbed phase (b) at a methanol fraction 20% .....	134
Figure 4-5 Experimental data (filled circles) and independent model predictions (solid lines) for naphthalene elution curves at three different cosolvent fractions .....	139
Figure 4-6 Experimental data (symbols) and independent model predictions (lines) for the binary solute elution experiments at two different cosolvent fractions .....	141
Figure 4-7 Simulated concentration and mass removal profiles for elution from a single-component OIL .....	143
Figure 4-8 Experimental (filled circles) and predicted (lines) elution profiles for six different coal tar constituents and 25% methanol .....	146
Figure 4-9 Experimental (filled circles) and predicted (lines) elution profiles for six different coal tar constituents and 50% methanol .....	147
Figure 4-10 Results of Monte Carlo simulations for variable velocity .....	154

Abstract of Dissertation Presented to the Graduate School  
of the University of Florida in Partial Fulfillment of the  
Requirements for the Degree of Doctor of Philosophy

CHEMODYNAMICS OF COMPLEX WASTE MIXTURES:  
APPLICATIONS TO CONTAMINATION AND REMEDIATION  
OF SOILS AND AQUIFER MEDIA

By

Dionysius C.M. Augustijn

August 1993

Chairperson: Dr. P.S.C. Rao

Major Department: Soil and Water Science

Many ground water contamination problems originate from sites contaminated with complex waste mixtures. Complex waste mixtures of environmental concern studied here are multi-component, organic immiscible liquids, such as coal tar. The release and transport of organic chemicals in saturated media contaminated with such complex waste mixtures are controlled by two major processes: dissolution and sorption. These processes were discussed at a mechanistic level, in relation to their impact on contamination and remediation of soils and aquifer media.

A model was developed, based on Raoult's law, for describing multi-component dissolution from complex waste mixtures under equilibrium and nonequilibrium conditions. Model simulations and experimental data showed that with depletion of more-soluble components, the concentration of all other



constituents increases due to changes in mole fraction. Nonideal conditions also increase contaminant concentrations, but can generally be ignored at the field scale.

Rate-limited sorption of nonpolar organic compounds is controlled by two possible mechanisms: intra-organic matter diffusion and retarded intra-particle diffusion. Several models that describe sorption nonequilibrium, based on different conceptualizations of sorption dynamics, were discussed. The theoretical and experimental basis for the reported log-log, inverse, linear relationship between the first-order, mass-transfer rate coefficient and equilibrium sorption coefficient, which can be used to predict local-scale nonequilibrium, was critically evaluated. Sorption rates measured for three different contaminated matrices revealed that mass-transfer rates for some complex wastes may be significantly smaller than those observed for natural sorbents.

Cosolvents enhance the solubility, reduce sorption, and enhance the rate of approach to sorption equilibrium. Such effects have an important impact on the release and transport of organic contaminants when cosolvents are present at the waste-disposal site, or are introduced as part of a site remediation strategy. The cosolvency theory was used to develop several predictive models, which were used to evaluate solvent flushing as a potential remediation technique.

## CHAPTER 1 INTRODUCTION

### Preface

Many industrial waste disposal/spill sites are characterized by the presence of complex waste mixtures. The release of contaminants from these sites has formed a serious threat to human health and vulnerable ecosystems. Research is needed to be able to assess the problems associated with soils and aquifer media contaminated with complex waste mixtures.

Complex waste mixtures of environmental concern studied here are multi-component, organic immiscible liquids such as gasoline, diesel fuel, and coal tar. The separate organic fluid phase created by the complex waste mixtures is often referred to as nonaqueous-phase liquid (NAPL), or organic immiscible liquid (OIL)<sup>1</sup>. The problems associated with soils contaminated with these products are very complex. In most cases, the amount, composition, and distribution of the OIL is not exactly known. Furthermore, the chemistry and physics of systems containing multi-

---

<sup>1</sup> The term nonaqueous-phase liquid was introduced in the mid to late eighty's. When dealing with heavily contaminated soils, high concentrations of chemicals may change the properties of the water phase such that it behaves significantly different from dilute aqueous solutions. In these systems, the term NAPL may not be the most appropriate description of the separate organic phase, therefore preference will be given to the term OIL in this dissertation.

component OILs is very complicated because of the possible interactions between constituents, and the presence of a separate fluid phase. These aspects form the core of this dissertation.

In evaluating a contaminated site, some of the most important questions are: what contaminant concentrations can be expected in the air and water phases; how far have the contaminants spread; and what action should be taken to restore the site or prevent further contamination? To answer these questions, another set of more specific questions needs to be addressed. In relation to sites contaminated with complex waste mixtures, some of these questions are as follows:

- (1) What are the major processes that control the release and transport of organic chemicals, and what are the mechanisms that determine the rate of these processes?
- (2) How can these processes be modeled, and what methods are available to determine or estimate the model parameters?
- (3) What is the relative importance of local- and large-scale processes?

The purpose of this work is to clarify some of these questions, and help develop a better understanding of the complexity associated with these contaminated soils. This will be done first by reviewing the problem at a larger scale: how do immiscible liquids migrate through soils; what may be the expected distribution of phases; and what are the primary processes controlling the release and transport of organic chemicals in these soils? Then, the chemodynamics of organic chemicals in soils contaminated with complex waste mixtures will be discussed in more detail,

focusing on the chemical and physical aspects of dissolution and sorption. Finally, the effect of organic cosolvents on the release and transport of organic chemicals will be discussed and applied as a potential remediation technique.

In the following sections, the general complexity of soils and aquifer media contaminated with complex waste mixtures will be discussed. At the end of this chapter, the basic solute transport equation will be derived, which forms the basis for the models developed in the following chapters.

### Overview of the Problem

#### Migration of Organic Immiscible Liquids

The migration of OILs is important in understanding the final distribution of the complex mixture in the subsurface. When an OIL is introduced into the subsurface, it will migrate downward through the vadose zone as a distinct liquid due to a gravitational and a potential gradient. Lateral spreading also occurs due to the effect of physical heterogeneity (e.g., layering) and capillary forces (Schwille, 1984). As the OIL progresses downward, part of it gets trapped in the pore spaces and will become immobilized due to capillary forces. The immobilized portion that is retained by the soil is referred to as the residual saturation of OIL. Whether the OIL reaches the saturated zone as a free-moving liquid depends on the amount introduced, the area of infiltration, and the residual saturation. Once the OIL reaches the saturated zone, further migration is determined by its density. OILs lighter than water (light OIL) will float on top of the capillary fringe and spread



laterally in the direction of the declining water table. OILs with a density greater than water (dense OIL) will stay on top of the capillary fringe until a sufficient pressure is developed to overcome the surface tension of the capillary fringe, and penetrate into the saturated zone. When groundwater is displaced by the pressure of the moving OIL, the OIL-water interface may become unstable as manifested by "fingers" of OIL penetrating through the aquifer (Schwille, 1988). As the dense OIL migrates downward through the saturated zone, it again leaves a residual saturation behind. This residual saturation is generally much higher than the residual saturation in the vadose zone (Wilson et al., 1990). The OIL migrates downward until it encounters a less permeable layer, and then spreads laterally in accordance to the slope of this less permeable stratification, forming pools of OIL. This lateral spreading could be in a direction different than that of regional groundwater flow. Accumulation of the OIL may occur at any location in the porous medium (saturated or unsaturated zone) where the OIL encounters zones of lower permeability. The distribution of OIL becomes more complicated when the soil or aquifer consists of discontinuous laminae of different permeabilities.

In contrast to dense OIL, light OIL accumulates at the top of the capillary fringe. If the mass of OIL becomes sufficiently large, a depression in the water table may be created. Due to seasonal fluctuations or pumping activities the elevation of the water table moves up and down. This periodic vertical displacement results in trapping of the light OIL in capillary spaces below the average depth of the groundwater table (Pfannkuch, 1984; Hunt et al., 1988).

The OIL phase forms a source of contaminants. Groundwater that comes in contact with the OIL will dissolve some of the OIL and carry the dissolved chemicals away from the source in the direction of the water flow, thus creating a contaminant plume. The contaminants dissolved in the aqueous phase may be retained by the solid phase, reducing their rate of transport. In the vadose zone, an envelope of organic vapors can develop around the source when compounds evaporate from the OIL or soil water. These vapors may diffuse through the vadose zone and escape at the surface or contaminate upstream regions of pristine groundwater. Water infiltrating through the vadose zone will dissolve some of the OIL constituents, and cause a periodic influx of organic chemicals into the saturated zone. Figure 1-1 shows a schematic of the final distribution of a dense and light OIL as discussed above.

Transport of OILs in subsurface systems can be described by multiphase flow models. A growing body of literature is presently available, in which various mathematical models are presented that described the migration of OILs in saturated and unsaturated media (cf., Corey, 1986; Abriola, 1989). These transport models vary from those based on simple sharp-interphase or piston-flow assumptions (e.g., Van Dam, 1967) to more sophisticated models in which the flow equations for each of the fluid phases are simultaneously solved, including hysteresis in displacing patterns (Lenhard et al., 1989). Although these multiphase transport models can be used to get a general idea of how OILs migrate through porous media, their practicality may be limited. In general, transport of OILs is limited to a relative

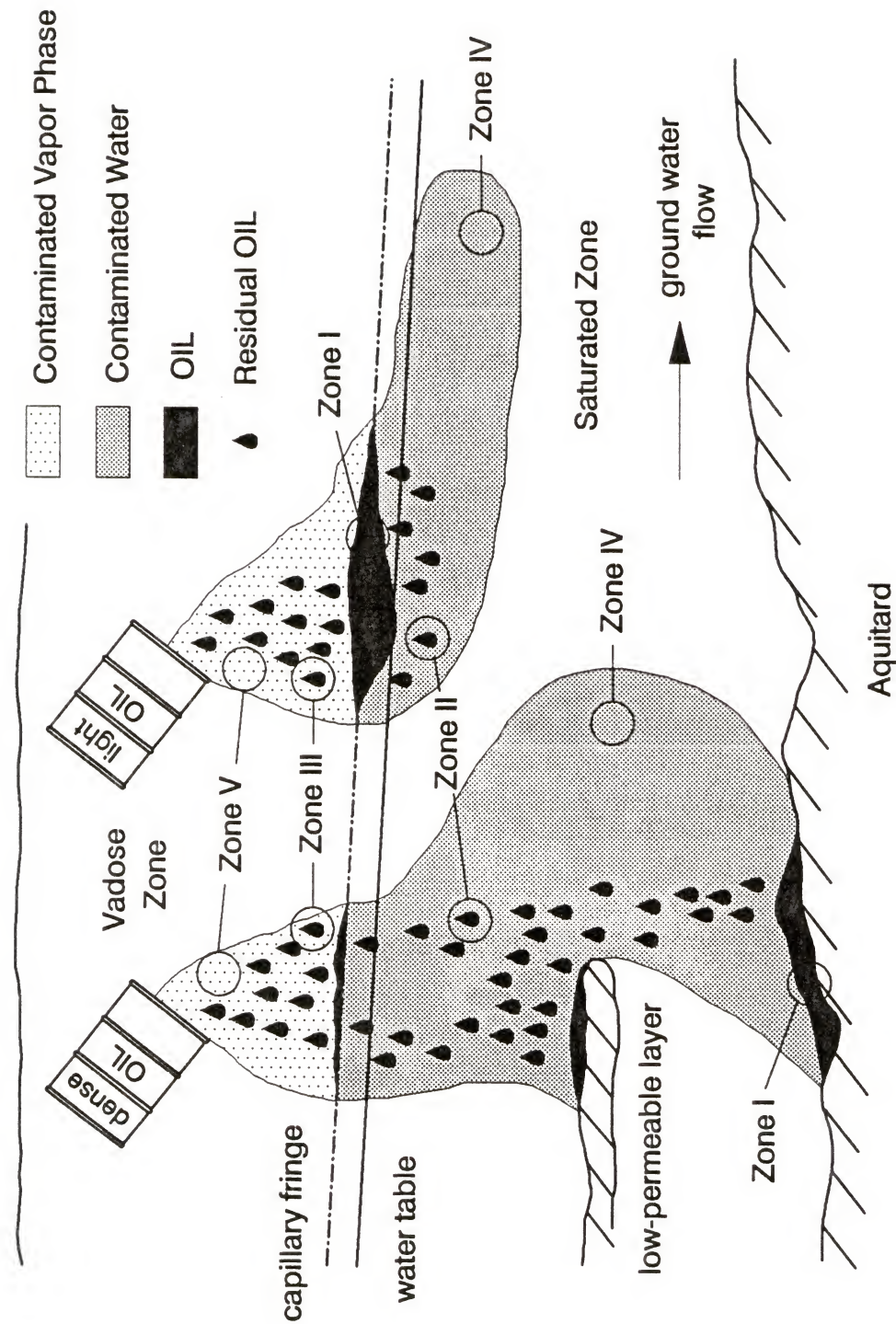


Figure 1-1 Schematic overview of soils contaminated with organic immiscible liquids.



small volume of the total contaminated zone. In most cases, the wetting history and soil heterogeneity are unknown in most cases, making the prediction of the transport and distribution of OILs very difficult. Furthermore, depending on the characteristics of the porous medium and OIL, the transport of the OIL as a separate fluid phase may take place in a relative short time period. It is the release of constituents from the residual OIL and pools of OIL that determines the long term (over several decades or centuries) contamination problem.

#### Release and Transport of Contaminants

The release and transport of organic chemicals in OIL-contaminated soils is controlled by three major processes: dissolution, volatilization, and sorption. Degradation of the chemical may also be an important process, but will not be considered in this study.

In Figure 1-1, five different zones are distinguished in which each of these processes play a different role. Zone I is the region in which the OIL is a free moving liquid; Zones II and III represent the regions containing residual OIL in the saturated and unsaturated zone, respectively; Zone IV represents the contaminant plume in the saturated zone; and Zone V represents the contaminated vapor phase in the vadose zone. Zone I through III are considered as the source and near-field region of the contaminated site, whereas Zones IV and V are referred to as far-field regions. Dissolution is the primary process controlling the release of organic contaminants at the source; sorption is the dominant process in the far-field; and volatilization is only important in the vadose zone. Figure 1-2 shows schematics of the distribution of phases in each of these zones, which will be discussed individually.



## Source/Near-Field Region



## Far-Field Region

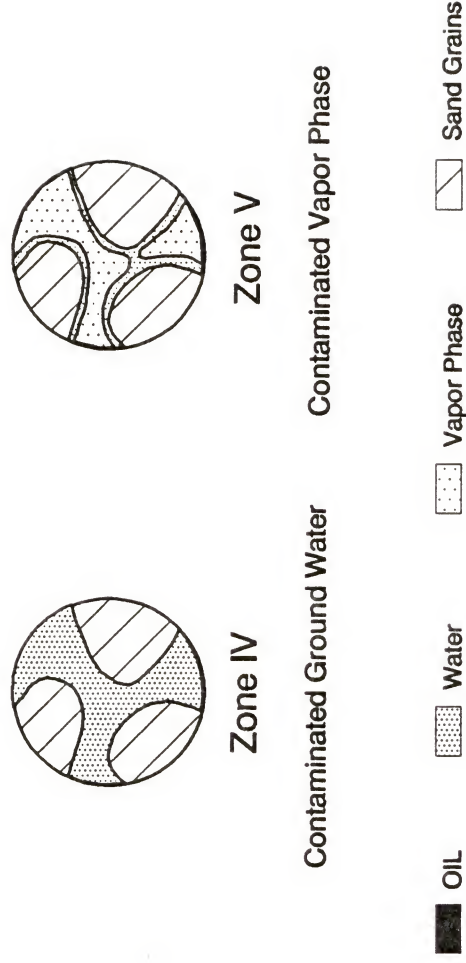


Figure 1-2 Schematic representation of the phase distribution in five different regions of a contaminated soil.

Zone I. This zone is the region in which free-moving OIL is present, and occurs where the OIL has accumulated due to a reduced permeability for the OIL, such as the water table or a low-permeable stratification. In this zone, the volumetric OIL content exceeds the residual saturation, but will almost never occupy all pore spaces. The solute concentration in the air and water phases present in this zone, are most likely in equilibrium with the OIL and sorbed phases. It is, however, the contact between this region and the flowing groundwater that determines the release of organic contaminants. This contact area is often very limited compared to the total volume of the pool and is usually considered as a planar area. A review of the specific problems associated with dense OILs is given by Huling and Weaver (1991).

Zone II. The region in which the OIL is trapped as residuals in the saturated zone is indicated by Zone II. The entrapment of an immiscible liquid occurs when the capillary pressure exceeds other forces acting on the liquid. The capillary pressure is the result of a combination of adhesive forces between the liquid and solid phases, and cohesive forces within the fluid itself. The capillary force is proportional to the interfacial tension and the strength of fluid wetting to the solid surface, and inversely proportional to the pore size. Hence, the residual saturation depends on several factors such as the media's pore-size distribution; wettability; fluid viscosity and density ratios; interfacial surface tension; gravity and buoyancy forces; and hydraulic gradients (Mercer and Cohen, 1990).

The residual saturation is expressed as the fraction of pore spaces occupied by the OIL. At the stage of residual saturation, the OIL phase is discontinuous and

may occur as single droplets or ganglia (Chatzis et al., 1983; Schwille, 1988; Wilson et al., 1990). The residual saturation can vary widely. Values have been reported from less than a percent for low viscous fluids and high permeable media (Schwille, 1984), to as high as 60% for gasoline in an initially dry, fine sand (Hoag and Marley, 1986). The residual saturation is highest in heterogeneous media (Wilson et al., 1990).

For most minerals, water is the wetting fluid, i.e., water preferentially covers the mineral surfaces. Soil organic matter, however, prefers contact with the organic liquid due to hydrophobic forces. Therefore, in surface soils, the solid matrix may have an intermediate preference for wetting by water or OIL. For this reason, the distribution of residual OIL in subsurface systems may be different from the distributions observed for experimental media in which the solid surfaces are preferably wetted by water.

Zone III. This zone represents the regions in the unsaturated zone that contain residual OIL. Air is the least preferential wetting fluid for mineral surfaces; hence, the most likely sequence of phase distributions in the vadose zone is mineral/water/OIL/air. Since the OIL is a discontinuous phase at residual saturation, both OIL and water may contact the air phase.

The unsaturated zone is a very dynamic component of the subsurface hydrology. During wetting and drying cycles, the air and water contents can vary considerably, changing contact areas between the different phases almost continuously. Dissolution of the residual OIL will be important when water

percolates through the vadose zone. Sorption and desorption will determine the rate at which the OIL constituents move down once they are dissolved. Water infiltration at the surface causes periodic inputs of contaminants into the saturated zone. If the site is covered by structures that prevent any infiltration of water, this source of contamination for groundwater is essentially eliminated.

Zone IV. Zone IV represents the contaminant plume in the saturated zone, originating from the OIL phases present in the zones described previously. The size and shape of the plume depend on the time the complex mixture was introduced in the soil, the groundwater flow rate, heterogeneity of the soil, and sorption. Sorption is the primary process that controls the relative rate at which the contaminants are being transported. Different chemicals experience different affinities for the solid phase, which lead to chromatographic separation of the chemicals in the contaminant plume.

Zone V. The contaminated vadose zone free of OIL is indicated by Zone V. As was discussed under Zone III, the vadose zone is a very dynamic system in which the phase distribution frequently changes. During the periods that air exists as a continuous phase, transport through the vapor phase may be important for volatile organic compounds. Transport of organic vapors is controlled by diffusion, advection due to density differences (Falta et al., 1989; Mendoza and Frind, 1990), or advection due to pressure gradients caused, for example, by infiltrating water. In these cases, the vapor phase acts as a medium in which contaminants are slowly being transported from OIL contaminated regions to the atmosphere, groundwater, or other regions of



the unsaturated zone. At low water contents, sorption of organic vapors at the air/water interface (Pennell et al., 1992), and onto mineral surfaces becomes more important (Rhue et al., 1989; Chiou, 1990; Pennell et al., 1992), affecting the rate of transport through the vapor phase.

### Nonequilibrium Conditions

Nonequilibrium conditions have an important impact on contaminant concentrations, the spreading of contaminants, and the efficiency of remediation techniques. In many cases, some type of nonequilibrium exists caused by either large-scale heterogeneity or rate-limiting processes at the local scale, or both.

The heterogeneous character of most porous media causes the hydraulic conductivity to be spatially variable, which results in a heterogeneous distribution of groundwater velocities. The concentration gradients created by the nonuniform velocity distribution can result in rate-limited diffusion between different flow domains, causing nonequilibrium conditions. The presence of an OIL phase also reduces the hydraulic conductivity for water and enhances this type of nonequilibrium.

At the local scale, nonequilibrium conditions occur when the contact time between phases is not sufficient to complete the process that leads to an equilibrium distribution of the chemicals in all phases. The time required by a process to reach equilibrium can be determined by a chemical reaction rate or a diffusion process. Chemical processes such as dissolution, volatilization, adsorption, and degradation, are generally considered rapid, but may require some finite time for completion.

The rate of many processes, however, is controlled by diffusion. Dissolution of multi-component OILs, for example, involves diffusion of the constituents through the OIL phase toward the OIL-water interface, dissolution at the interface, and diffusion away from the OIL-water interface. Sorption is also considered to be controlled by diffusion. Two mechanisms have been proposed to describe rate-limited sorption: intra-sorbent diffusion, and retarded intra-particle diffusion. The first mechanism views sorption as diffusion of solutes into the sorbent matrix, the second mechanism views sorption as diffusion into the micropores of porous particles in which the solutes are instantaneously sorbed.

The contact area between phases has an important effect on nonequilibrium. Small contact areas between phases results in short contact times, which increases the potential for nonequilibrium conditions. For this reason, the distribution of the OIL phase is very important, since it determines the contact area between OIL and water. High groundwater velocities also reduce the contact time, and will therefore also enhance nonequilibrium conditions.

In OIL-contaminated soils, conditions observed at a larger scale may be different from the conditions at the local scale. For example, if dissolution of the OIL is instantaneous, but dilution of contaminated water with fresh water leads to concentrations well below expected equilibrium concentrations, the observations at a larger scale may be misinterpreted as nonequilibrium conditions. On the other hand, when dissolution is rate-limited at the local scale, but the contact between OIL and water extends over a large distance, apparent equilibrium conditions may be

reached at the aquifer scale. In these cases, it is again important to know what the distribution of the OIL phase is to be able to assess the current situation and predict further developments.

### Basic Transport Equations

In this dissertation various models will be developed to examine the release and transport of organic chemicals in contaminated soils. The basic equation for solute transport used in this study is derived from the mass balance equation which states that the change in mass in a volume element of the system is equal to the difference between the influx and outflux of solutes in all directions. For an infinitesimally small volume and time, the mass balance or continuity equation can be written as

$$\frac{\partial M}{\partial t} = -\nabla \cdot J \quad (1-1)$$

where  $M$  is the total solute mass in the system ( $\text{g}/\text{cm}^3$  soil);  $t$  is time (hr); and  $J$  is the solute flux ( $\text{g}/\text{cm}^2$  hr).

The solute flux ( $J$ ) is composed of two major components: an advective flux and a dispersive flux. Advection refers to the transport of solutes with the bulk of the water phase. The advective solute flux ( $J_a$ ) can therefore easily be described by:

$$J_a = q C \quad (1-2)$$

where  $q$  is the Darcy flux (cm/hr), and  $C$  the solute concentration in water (g/ml). Dispersion of the solutes is caused by molecular diffusion and mechanical dispersion as a result of local velocity distributions. The effects of these two processes are combined in the so called hydrodynamic dispersion coefficient,  $D_h$  (cm<sup>2</sup>/hr):

$$D_h = D_e + D_m \quad (1-3)$$

where  $D_e$  is the effective molecular diffusion coefficient (cm<sup>2</sup>/hr), defined as:

$$D_e = \lambda D_o \quad (1-4)$$

and  $D_m$  is the mechanical dispersion coefficient (cm<sup>2</sup>/hr), defined as (Biggar and Nielsen, 1976):

$$D_m = \epsilon v^n \quad (1-5)$$

where  $\lambda$  is a complexity factor ( $0 \leq \lambda \leq 1$ ) that accounts for the sinuous and tortuous nature of the pore network;  $D_o$  the molecular diffusion coefficient (cm<sup>2</sup>/hr) of the solute in bulk water;  $\epsilon$  the dispersivity (cm);  $v$  the pore water velocity (cm/hr); and  $n$  an empirical constant, often assumed to be 1. While molecular diffusion may play an important role at low velocities, the mechanical dispersion becomes dominant at higher velocities. In some cases, a third term is included in  $D_h$  to account for the dispersion caused by solute transfer between domains of different pore water velocities (Davidson et al., 1983). In many case, however, it is more appropriate to account for this effect in a separate term (Van Genuchten and Wierenga, 1976).

The dispersive flux ( $J_d$ ) is written as a function of a concentration gradient even though it has no theoretical basis, but has proven to be an expedient and



adequate way to describe dispersion phenomena:

$$J_d = -\theta D_h \nabla C \quad (1-6)$$

Combining equations 1-6 and 1-2 with the continuity equation (Equation 1-1) gives the most general solute transport equation:

$$\frac{\partial M}{\partial t} = \nabla(\theta D_h \nabla C) - \nabla(qC) \quad (1-7)$$

In this study, only one-dimensional, steady flow (in the x-direction) in a saturated, homogeneous medium will be considered, which simplifies Equation 1-7 to:

$$\frac{\partial M}{\partial t} = \theta D_h \frac{\partial^2 C}{\partial x^2} - q \frac{\partial C}{\partial x} \quad (1-8)$$

This equation describes solute transport in the mobile aqueous phase; all other phases are considered stagnant and of constant volume in space and time. Equation 1-8 forms the basis for the models developed in the following chapters. The total solute mass (M) in this equation is the sum of the solute mass in all phases. Expressions for the solute mass in each phase are given in Table 1-1. This table also gives the equilibrium relationships between the solute concentration in each phase and the solute concentration in water.

### Discussion

The release and transport of organic chemicals in soils contaminated with multi-component OILs is a very complex problem. The distribution of the OIL phase depends primarily on the history of contamination, and the physical and chemical

Table 1-1 Expressions for the solute mass in each phase and their equilibrium relationship with the concentration in water.

Air phase	$M^a = \theta_a C^a$	$C^a = H C^w$
Water phase	$M^w = \theta_w C^w$	---
Sorbed phase	$M^s = \rho S$	$S = K C^w$
OIL phase	$M^o = m$	$m = C^w N_o / S^w$

$C^a$  is the solute concentration in air ( $\text{g}/\text{cm}^3$ );  $C^w$  the solute concentration in water;  $H$  the Henry's constant;  $K$  the equilibrium sorption coefficient ( $\text{cm}^3/\text{g}$ );  $M^a$  the solute mass in the air phase ( $\text{g}/\text{cm}^3$ );  $M^w$  the solute mass in water ( $\text{g}/\text{cm}^3$ );  $M^s$  the solute mass in the sorbed phase ( $\text{g}/\text{cm}^3$ );  $m$  and  $M^o$  the solute mass in the OIL phase ( $\text{g}/\text{cm}^3$ );  $N_o$  the total number of moles in the OIL phase ( $\text{moles}/\text{cm}^3$ );  $S$  the sorbed concentration ( $\text{g}/\text{g}$ );  $S^w$  the liquid solubility ( $\text{moles}/\text{cm}^3$ );  $\theta_a$  the volumetric air content ( $\text{cm}^3/\text{cm}^3$ );  $\theta_w$  the volumetric water content ( $\text{cm}^3/\text{cm}^3$ ); and  $\rho$  the dry bulk density of the soil ( $\text{g}/\text{cm}^3$ ).

characteristics of the complex waste mixture and the porous medium. At a contaminated site, the distribution of the OIL is often associated with high uncertainty, which makes it very difficult to predict the release of organic contaminants from the OIL phase. In many cases, simplifying assumptions need to be made to be able to model such complicated systems. In this study, the behavior of contaminants will primarily be discussed at the local scale. The models that will be presented in the following chapters are developed for one-dimensional, homogeneous media, which are only representative for a small portion of the total contaminated volume. The purpose of these studies is to investigate the mechanisms and rates of local-scale processes. The knowledge gained from this type of research is essential to assess the importance of local-scale processes in a larger, more complicated system.

## CHAPTER 2 DISSOLUTION FROM COMPLEX WASTE MIXTURES

### Introduction

Dissolution of OILs is receiving increasingly more attention. To date, most dissolution studies were focused on single-component OILs (cf., Van der Waarden et al., 1971; Fried et al., 1979; Hunt et al., 1988; Miller et al., 1990; Powers et al., 1992). More recently, some researchers have also studied the more complex problem of multi-component dissolution (Abriola and Pinder, 1985; Corapcioglu and Baehr, 1987; Kaluarachchi and Parker, 1990; Mackay et al., 1991; Zaladis et al., 1991; Borden and Piwoni, 1992). In most of these studies, multi-component dissolution was described by a constant partition coefficient between the OIL and water phases. This may be a reasonable estimation for the more-soluble constituents, but for the less-soluble constituents, the partition coefficient is affected by the changing composition of the OIL, as will be demonstrated in this chapter. Mackay et al. (1991) developed a model in which the partition coefficient changed as a function of the OIL composition, and showed that the trends observed in model simulations were consistent with experimental data. Their model, however, was developed for a zero-dimensional system, i.e., the OIL and aqueous phases were assumed to be homogeneous. In this chapter a more realistic, one-dimensional model will be developed.

Nonideal conditions, due to molecular interactions in the OIL phase, have generally been ignored, or included in the partition coefficient. If the composition of the organic mixture is known, the activity coefficients in the OIL phase can be estimated by various methods. In this chapter, the UNIFAC model will be used to estimate the activity coefficients and the results incorporated into the one-dimensional dissolution and solute transport model to account for nonideal behavior.

The potential for nonequilibrium conditions in soils contaminated with OILs were discussed in Chapter 1. In most studies mentioned above, equilibrium conditions were assumed. Borden and Pivoni (1992) developed an equilibrium and nonequilibrium model, and concluded that both models described their data equally good. Only when most of the OIL mass was removed from the column, the concentrations leveled off which is indicative for nonequilibrium conditions. Wise et al. (1992) tried to explain this behavior by assuming a nonlinear isotherm, which is equivalent to a change in partition coefficient with decreasing solute concentration in the solution phase. A more realistic explanation, probably, is the increasing importance of rate-limiting processes once the constituent is almost depleted. In addition, dilution effects may become apparent when a constituent is depleted from the smaller ganglia but not from the larger ganglia. Nonequilibrium conditions can be described by various models. In this chapter, a first-order mass-transfer model will be used, which has also been used to describe dissolution from single-component OILs (Hunt et al., 1988; Sleep and Sykes, 1989; Miller et al., 1990; Powers et al., 1991).



The purpose of the work in this chapter is to present a more complete description of the multi-component dissolution process that contributes to a better understanding of the dissolution dynamics of complex waste mixtures, and is helpful in estimating the release of organic chemicals from complex waste mixtures in contaminated soils.

### Dissolution Mechanisms

Dissolution is defined as the transfer of chemicals from their original phase to a dissolved stage in the contacting solution. For a single-component OIL, the organic chemical dissolves from its pure substance. The availability of the compound for dissolution at the OIL-water interface is unlimited, making the dissolution process itself the only rate-limiting step. In contrast, for multi-component OILs, the constituents first have to diffuse through the organic phase toward the OIL-water interface, under influence of a concentration gradient, before dissolution can take place.

Even though dissolution may be considered rapid, it is certainly not instantaneous. This conclusion is based on the observation that some time is required to dissolve a pure, liquid compound, even under well-stirred conditions. Since dissolution is an interfacial phenomenon, the dissolution rate is directly proportional to the contact area between the solution and OIL phases. The dissolution rate of multi-component OILs depends on the surface to volume ratio of the OIL phase. For a given surface area, the diffusion path length for the

constituents increases with increasing volume of OIL, consequently the dissolution rate decreases with decreasing surface to volume ratio of the OIL phase.

Determination of the contact area between the solution and OIL phases depends on the spatial distribution of the phases, and is an essentially impossible task. Several studies have shown the complexity of the size and shape (i.e., the morphology of the ganglia), and the spatial distribution of the OIL phase (Chatzis et al., 1983; Schwille, 1988; Wilson et al., 1990; Powers et al., 1992). When the medium is preferentially wetted by water, the OIL will be trapped in the larger pore throats, while a thin film of water remains between the solid surface and the OIL phase. Wilson et al. (1990) observed from glass micromodels that flow occurs in these thin films. In natural systems, however, the mineral surfaces may be intermediately wetted by OIL and water, causing these thin films of water to be discontinuous (see Figure 1-2, Zone II). Discontinuous films will not contribute to flow, reducing the contact area between the OIL and mobile ground water. In addition, the irregular surfaces of soil minerals may cause large drag forces and also diminish the flow in these thin films of water, reducing the effective contact area between the OIL and water phases.

An additional complexity related to dissolution is the temporal changes. When the OIL consists of only organic compounds with significant aqueous solubilities (e.g., gasoline), the ganglia will shrink as the dissolution process proceeds. As the ganglia shrink, the interfacial area between OIL and water becomes smaller, reducing the dissolution rate (Hunt et al., 1988). On the other hand, with shrinking

ganglia, the volume of water between the solid surface and OIL phase increases, and at some point regains flow. This increases the effective surface area between the OIL phase and mobile water. When the size of the ganglia decreases, the capillary forces acting on the ganglia will also change, causing a redistribution of the OIL phase, which is accompanied by a change in contact area. For complex mixtures consisting of a large portion of essentially insoluble compounds, here referred to as "pitch", changes in size and shape of the ganglia can be ignored. The complexity of the processes described above has lead to the use of simple first-order mass-transfer models in which all spatial and temporal complexity is contained in the first-order mass-transfer rate coefficient.

The concept that dissolution is controlled by diffusion through a stagnant boundary layer (Pfannkuch, 1984), generated many empirical relationships between the dimensionless representation of the first-order mass-transfer rate coefficient (Sherwood number) and several hydrodynamic parameters such as Reynolds number and Schmidt number (see for example the data compiled by Powers et al., 1991). For multi-component OILs, diffusion through the organic phase could become more rate limiting. In this case, the dissolution process is mechanistically very close to desorption, and traditional sorption models could be used to describe the phase partitioning of solutes between the immobile OIL phase and water. When significant amounts of mass dissolve away, the composition of the complex mixture changes, and the morphology of the ganglia is altered. This, in turn, may affect the molecular diffusion of the chemicals in the organic phase.



## Model Development

### Transport Equations

The equilibrium partitioning of a chemical between water and a multi-component OIL can be described by the following equation (Leinonen and Mackay, 1973; Banerjee, 1984; Vadas et al., 1991):

$$C_i = \gamma_i X_i S_i \quad (2-1)$$

where  $C$  is the concentration in the aqueous phase ( $\text{g}/\text{cm}^3$  water);  $\gamma$  the activity coefficient in the OIL phase;  $X$  the mole fraction in the organic phase;  $S$  the liquid solubility in water ( $\text{g}/\text{cm}^3$  water), which is equal to the reciprocal value of the activity coefficient in water; and subscript  $i$  refers to the  $i^{\text{th}}$  component. Under ideal conditions, the activity coefficient is equal to 1, and Equation 2-1 reduces to Raoult's law:

$$C_i = X_i S_i \quad (2-2)$$

When the behavior of organic chemicals in the organic mixture is nonideal, the activity coefficients can be predicted by the UNIFAC model (Banerjee and Howard, 1988). When solutes, that would be solids in their standard state, are dissolved in an OIL phase, like most polyaromatic hydrocarbons in gasoline and coal tar, the solubility in Equations 2-1 and 2-2 represents the super-cooled liquid solubility. The super-cooled liquid solubility is higher than the crystal solubility since the extra energy required to overcome the intermolecular forces within the solid structure are eliminated. The super-cooled liquid solubility can be calculated as follows (Prausnitz, 1969):

$$\ln S_l - \ln S_s = \frac{\Delta H_f}{RT} \left( \frac{T}{T_m} - 1 \right) \quad (2-3)$$

where  $S_l$  is the super-cooled liquid solubility (g/ml);  $S_s$  the crystal solubility (g/ml)  $\Delta H_f$  the heat of fusion (J/mole);  $R$  the gas constant (8.31 J/mole °K);  $T$  the temperature (°K); and  $T_m$  the melting point (°K).

In soils where a complex mixture is present, the total mass of a component is given by the sum of the mass in the solution, sorbed, and OIL phases. The interactions between the OIL phase and solid matrix of the soil make it very difficult to distinguish between the sorbed and OIL phases. In most contaminated soils and aquifer media, the amount of native organic carbon is probably also negligible compared to the high mass of organic carbon introduced with the OIL. Therefore, the sorbed and OIL phases will be treated here as a single phase in which natural soil organic matter is considered part of the pitch. Given these considerations, the total mass ( $M$ ) of component  $i$  is given by:

$$M_i = \theta C_i + m_i \quad (2-4)$$

where  $\theta$  is the volumetric water content (cm<sup>3</sup> water/cm<sup>3</sup> soil); and  $m_i$  the mass of the  $i^{\text{th}}$  constituent in the OIL phase (g/cm<sup>3</sup> soil). Substitution of Equation 2-4 into the general one-dimensional solute-transport equation in a homogeneous medium (Equation 1-8) gives:

$$\theta \frac{\partial C_i}{\partial t} + \frac{\partial m_i}{\partial t} = \theta D_h \frac{\partial^2 C_i}{\partial x^2} - q \frac{\partial C_i}{\partial x} \quad (2-5)$$

where  $t$  is the time (hr);  $D_h$  the hydrodynamic dispersion coefficient ( $\text{cm}^2/\text{hr}$ );  $x$  the distance (cm); and  $q$  the Darcy flux ( $\text{cm}/\text{hr}$ ). In Equation 2-5, it is assumed that  $\theta$  can be considered constant over time and space. This may only be true for small time scales, or for OILs that consist for a large portion of essentially insoluble components. Under ideal conditions, the relation between the mass in the organic phase and concentration in the solution phase can be described by Raoult's law (Equation 2-2). The mole fraction ( $X$ ) can be written as:

$$X_i = \frac{m_i}{MW_i N_o} \quad (2-6)$$

Hence, the equilibrium concentration in the solution face is give by:

$$C_i = \frac{m_i}{N_o} \frac{S_i}{MW_i} \quad (2-7)$$

where  $m$  is the mass of a constituent in the OIL phase ( $\text{g}/\text{cm}^3$ );  $MW$  the molecular weight ( $\text{g}/\text{mole}$ ); and  $N_o$  the total number of moles in the organic phase.  $N_o$  is defined as:

$$N_o = \frac{m_p}{MW_p} + \sum \frac{m_i}{MW_i} \quad (2-8)$$

where subscript  $p$  refers to the pitch, if present. Note that when  $(m_p/MW_p) \gg (\sum m_i/MW_i)$ ,  $N_o$  is constant and Equation 2-8 reduces to the description of a linear sorption isotherm where the equilibrium sorption coefficient ( $K$ ) is equal to:

$$K_i = \frac{f_p MW_i}{MW_p S_i} \quad (2-9)$$

where  $f_p$  is the mass fraction of the pitch in the soil, which is closely related to the analytically more easy to determine fraction of organic carbon ( $f_{oc}$ ). Rearrangement of Equation 2-7, and substitution into Equation 2-5, gives, for equilibrium conditions:

$$\theta \frac{\partial C_i}{\partial t} + \frac{MW_i}{S_i} \frac{\partial (N_o C_i)}{\partial t} = \theta D_h \frac{\partial^2 C_i}{\partial x^2} - q \frac{\partial C_i}{\partial x} \quad (2-10)$$

For nonequilibrium dissolution, the change of mass in the OIL phase will be described by the commonly used first-order mass-transfer model (Hunt et al., 1988; Sleep and Sykes, 1989; Miller et al., 1990; Powers et al., 1991):

$$\frac{\partial m_i}{\partial t} = \theta k_i (C_i - C_{eq}) \quad (2-11)$$

where  $k$  is the first-order mass-transfer rate coefficient ( $\text{hr}^{-1}$ ), which describes the rate of dissolution, which involves the diffusion through the organic phase, the dissolution rate at the interface between the solution and OIL phases, and the diffusion away from the interface. It is expected that  $k$  depends on the properties of the chemicals, and will therefore be different for each compound. The equilibrium concentration ( $C_{eq}$ ) in Equation 2-11 is given by Equation 2-7. Substitution of Equations 2-7 and 2-11 into the general one-dimensional solute-transport equation gives, for nonequilibrium conditions:

$$\theta \frac{\partial C_i}{\partial t} = \theta D_h \frac{\partial^2 C_i}{\partial x^2} - q \frac{\partial C_i}{\partial x} - \theta k_i \left( C_i - \frac{m_i}{N_o} \frac{S_i}{MW_i} \right) \quad (2-12)$$

### Initial and Boundary Conditions

The solute transport equation will be solved for a finite medium (e.g., a column). This requires an initial condition, and two boundary conditions. For convenience, the system was assumed to be initially at equilibrium. This means that the initial concentration can be described by Equation 2-7. When a contaminated soil is analyzed for its compounds, the total mass in solution and OIL phase is determined. To calculate the distribution of mass between the solution and OIL phases from this amount, a numerical iteration scheme is required. If most of the mass, however, is located in the OIL phase,  $m$  can be assumed equal to the total mass, and  $C$  can be calculated directly from Equation 2-7.

For the top boundary ( $x=0$ ), it is assumed that at  $t=0$  a solution free of contaminants is introduced. This means that the flux-averaged concentration in the column inlet is equal to zero, or in mathematical form:

$$qC_i - \theta D_h \frac{\partial C_i}{\partial x} = 0 \quad t > 0; \quad x = 0 \quad (2-13)$$

The bottom boundary condition for a finite medium, is described by:

$$\frac{\partial C_i}{\partial x} = 0 \quad t > 0; \quad x = L \quad (2-14)$$

### Nondimensional Equations

For comparison between different systems it is often convenient to express transport parameters in a nondimensional form. Introducing the following nondimensional parameters:



$$p = \frac{vt}{L} \quad (2-15)$$

$$P = \frac{vL}{D_h} \quad (2-16)$$

$$X = \frac{x}{L} \quad (2-17)$$

$$\omega_i = \frac{k_i L}{v} \quad (2-18)$$

where  $p$  is the pore volume;  $v = q/\theta$  the pore water velocity (cm/hr);  $L$  the length of the column (cm);  $P$  the Peclet number;  $X$  the relative distance (cm);  $\omega$  the Damkohler number which is the ratio of the residence time of water ( $L/v$ ) and the characteristic time for the dissolution process ( $k$ ). All other parameters are as defined before.

Using these dimensionless parameters, the transport equations for equilibrium conditions can be rewritten as:

$$\frac{\partial C_i}{\partial p} + \frac{MW_i}{\theta S_i} \frac{\partial(N_o C_i)}{\partial p} = \frac{1}{P} \frac{\partial^2 C_i}{\partial X^2} - \frac{\partial C_i}{\partial X} \quad (2-19)$$

$$m_i = \frac{N_o MW_i C_i}{S_i} \quad (2-20)$$

and for nonequilibrium conditions:

$$\frac{\partial C_i}{\partial p} - \frac{1}{P} \frac{\partial^2 C_i}{\partial X^2} - \frac{\partial C_i}{\partial X} - \omega_i \left( C_i - \frac{m_i}{N_o} \frac{S_i}{MW_i} \right) \quad (2-21)$$

$$\frac{\partial m_i}{\partial p} - \theta \omega_i \left( C_i - \frac{m_i}{N_o} \frac{S_i}{MW_i} \right) \quad (2-22)$$

Note that the concentrations are not normalized. The boundary conditions can be transformed to:

$$C_i - \frac{1}{P} \frac{\partial C_i}{\partial X} = 0 \quad p > 0; \quad X = 0 \quad (2-23)$$

$$\frac{\partial C_i}{\partial X} = 0 \quad p > 0; \quad X = 1 \quad (2-24)$$

The transport equations for equilibrium and nonequilibrium conditions were solved using a Crank-Nicolson central finite difference method (Wang and Anderson, 1982), with an iteration procedure to calculate the number of moles remaining in the OIL phase. The complete numerical procedure for equilibrium conditions is given in Appendix A.

### Experimental Procedure

To validate the model described in previous sections, experiments were conducted with two types of multi-component OILs: (1) a synthetic mixture of decane, tetrachloroethene (PCE), and naphthalene, which will later be referred to as the DPN mixture; and (2) coal tar. The DPN mixture was chosen as a model for

a complex mixture whose composition is exactly known. Compounds from three different chemical groups (alkane, chlorinated hydrocarbon, and polycyclic aromatic hydrocarbon) were selected to investigate the effect of nonideality, which is more likely to occur for chemicals that are different. Decane was selected to represent a low-solubility compound comparable to pitch material. Naphthalene was included in this mixture as an example of a solid dissolved in an organic liquid. Coal tar was chosen as an example of a complex waste mixture of environmental concern.

#### Experiments With Decane/PCE/Naphthalene Mixtures

First, the mutual solubilities of the three compounds were investigated. From some preliminary experiments, it was found that decane and PCE were completely miscible, and that naphthalene had a limited solubility in decane, PCE, or decane-PCE mixtures. To measure the solubility of naphthalene in different mixtures of decane and PCE, excess of naphthalene crystals were added to 4.5 ml amber vials containing the following volume ratios of decane and PCE: 4:0; 3:1; 2:2; 1:3; and 0:4 (ml:ml). The vials were heated slightly and sonicated for approximately 15 minutes, and then put on a rotator overnight. The next day, the samples were centrifuged (2500 rpm), and 0.25 ml of the supernatant was sampled and diluted with 3 ml of methanol for analyses on a gas chromatograph with flame ionization detector (GC-FID; Shimadzu GC-14A). All samples were done in duplicate. The temperature in the laboratory during the entire experiment was approximately 20 °C.

The density of each mixture used in the solubility study was measured by sampling 0.25 ml from the supernatant of the centrifuged vials with an accurate

syringe, and weighing the mass of this aliquot on an analytical balance (Mettler H45AR). The density of the DPN mixture behaved ideally, which means that the density of the mixtures was equal to the sum of masses for each component, divided by the sum of volumes for each component.

Based on the solubility study, a mixture of 60% decane, 30% PCE, and 10% naphthalene (mole basis) was selected to conduct a column experiment. The density of this particular mixture was 0.90 g/ml. Prior to the column experiment, batch partition experiments were performed to investigate the nonideal behavior of this mixture. Five mixtures with different ratios of decane, PCE, and naphthalene were prepared. These mixtures were selected based on the expected depletion pattern for multiple extractions. One ml of each mixtures was combined in a 4.5 ml amber vial with 3 ml of an aqueous 0.01 N  $\text{CaCl}_2$  solution. One ml decane, one ml PCE and excess naphthalene crystals were also combined with 3 ml water to measure the solubilities of the pure compounds. The samples were rotated for at least 24 hours and analyzed on the GC-FID. All experiments were, again, performed in duplicate.

For column experiments, a homogeneous distribution of the OIL is required to obtain representative data. This can be established best by creating a residual saturation of OIL in the column. Also, the mass of OIL in the column should be small to avoid experiments that take too long (weeks or months). For these reasons, a small, stainless-steel column was selected (length: 5.0 cm; diameter: 0.48 cm). For a small column like this, the potential for significant boundary flow along the walls of the column is very high. This could result in relative large dispersion coefficients



(small Peclet numbers) or even bimodal breakthrough curves. The assumption made here, however, was that the presence of residual OIL would partially interrupt the flow along the walls and establish more homogeneous conditions. The column was packed with glass beads (0.35-0.71 mm), and saturated with degassed water (0.01 N  $\text{CaCl}_2$ ). Glass beads were used to eliminate sorption.

After the column was completely saturated (i.e., no change in weight occurred), a miscible-displacement experiment was performed with a nonreactive tracer (pentafluorobenzoic acid, PFBA) to determine the pore volume and Peclet number of the column. The column was then disconnected, and several pore volumes of the DPN mixture were introduced into the column with a glass syringe, opposite to the direction in which the water flowed.

After the injection of the mixture, the column was flushed for several pore volumes in the original flow direction with an aqueous 0.01 N  $\text{CaCl}_2$  solution that was previously equilibrated with the same DPN mixture. This solution was used to avoid dissolution from the mixture during the immiscible OIL displacement. The column was then connected back to the pump and the elution experiment was initiated by pumping a clean 0.01 N  $\text{CaCl}_2$  through the column at a flow rate of 0.1 ml/min, which was the lowest possible, accurate flow rate. This flow rate translated to a pore-water velocity of 83 cm/hr, which would probably be too fast to maintain equilibrium conditions. During the elution experiment, samples were collected periodically and analyzed on the GC-FID as soon as possible. After the concentrations had dropped significantly, the experiment was terminated.

Another miscible-displacement experiment was performed to determine the pore volume and Peclet number of the column still containing most of the residual OIL. The same flow rate was used as for the elution experiment, to avoid possible displacement of the OIL by increased flow rates. The concentrations of decane, PCE and naphthalene in the column effluent were very small and relatively constant, so they would not interfere with the response of the UV detector. The difference between the measured pore volumes from the PFBA-experiment prior to adding the OIL to the column, and after the elution experiment was finished, was used to determine the volume of residual OIL. This method was used since the pore volume of the column was too small to determine the residual saturation accurately by weight or volume measurements.

#### Experiments With Coal Tar

For the coal tar experiments, a few drops of pure, liquid coal tar (equal to 0.176 g) was added to 120 g of the 0.3-0.5 mm fraction of a builder sand. The coal tar used in this study was provided by the Electric Power Research Institute and was the same one as used by Lee et al. (1992b) and identified with ID# 4. The tar and sand were thoroughly stirred until the coal tar was homogeneously distributed on the sand grains. Imaging with an optical microscope revealed that the coal tar was smeared into thin films surrounding the sand grains with some accumulation in the crevices on the mineral surfaces. After stirring the tar and sand, the mixture was immediately packed into a glass column (Kontes) of 15 cm long and 2.5 cm in diameter, and slowly saturated with a degassed 0.01 N  $\text{CaCl}_2$  solution. The attraction

forces between the tar and quartz were strong enough, such that the tar was not displaced by water. When the first effluent appeared at the outlet of the column, the flow was stopped. Although, some air may still have been trapped in the column by this method, gravimetric measurements showed that the medium was close to saturation. After the column was equilibrated for a day, the flow was resumed to initiate the elution experiment. The nominal flow rate was 0.5 ml/min, which translates to a pore-water velocity of 15 cm/hr. Effluent samples were collected periodically and analyzed on GC/mass spectrometer (Varian Saturn II). When some of the most soluble components (naphthalenes) were virtually depleted, the experiment was terminated.

## Results and Discussion

### DPN Mixture

The results of the solubility study are shown in Figure 2-1 in the form of a phase diagram. The measured solubilities of naphthalene in various decane/PCE mixtures are indicated by the black circles. Left from the regression line through the data points naphthalene is present as a solid. The solubility of naphthalene was also calculated with UNIFAC version 5 (Hansen et al., 1991), and are indicated by open circles. The asterisk in Figure 2-1 indicates the composition of the DPN mixture used in the column experiment. The dotted line represents the compositional change upon multiple extractions, assuming ideal behavior of the mixture. The triangle markers indicate the compositions of the samples used in the partition study. The

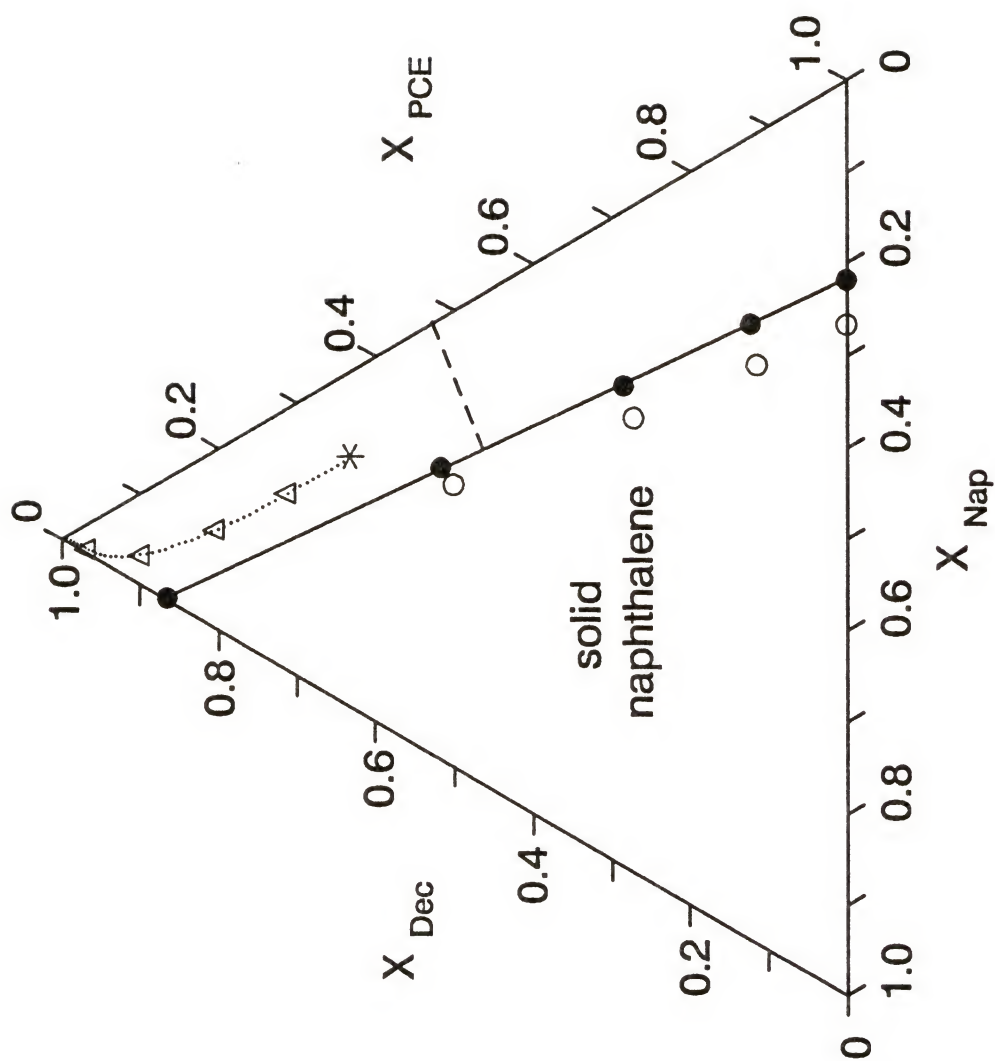


Figure 2-1 Phase diagram for the solubility of naphthalene in decane/PCE mixtures.



dashed line represents the composition at which the density of the mixture is equal to the density of water (1 g/ml). Above this line, the mixture is a light OIL and will float on top of water, while below this line the mixture is a dense OIL and would sink to the bottom of the aquifer when introduced into the saturated subsurface.

The partition study showed deviations from 1 for the activity coefficients of PCE ( $\gamma_{PCE}$ ) and naphthalene ( $\gamma_{NAP}$ ). The activity coefficient of naphthalene in the DPN mixture was much greater than 1. Since the nonideal behavior of PCE and naphthalene could be reasonably estimated by the UNIFAC model, this method was used to derive relationships for the activity coefficients of PCE and naphthalene that can be used in the dissolution models described above. These relationships are:

$$\gamma_{PCE} = 1.31 - 0.34X_{PCE} - 1.35X_{NAP} + 1.00X_{PCE}X_{NAP} \quad (2-25a)$$

$$\gamma_{NAP} = 2.35 - 2.45X_{PCE} - 2.41X_{NAP} + 4.57X_{PCE}X_{NAP} \quad (2-25b)$$

where  $X_{PCE}$ , and  $X_{NAP}$  are the mole fractions of PCE and naphthalene in the organic mixture, respectively. Note that  $X_{DEC} + X_{PCE} + X_{NAP} = 1$ . Equations 2-25 were used to modify the one-dimensional transport model for nonideal conditions.

Table 2-1 summarizes the data used to simulate the column experiment. Figure 2-2 shows simulated elution profiles for PCE and naphthalene under equilibrium conditions and for ideal and nonideal behavior. In these simulations, decane was considered as an insoluble pitch. In Figure 2-2, several characteristic features for elution from a multi-component OIL can be observed. Under equilibrium conditions, the constituent concentrations in the effluent remain constant

Table 2-1 Composition of DPN mixture and column parameters used for model simulation.

	mass (mg/cm <sup>3</sup> )	MW (g/mole)	S <sub>l</sub> (μg/mL)	S <sub>s</sub> (μg/mL)
PCE	20.0	165.8	244	-
naphthalene	4.92	128.2	114	30
Pitch	35.9	142.3		
Volumetric water content $\theta$ : 0.44 cm <sup>3</sup> /cm <sup>3</sup>				
Peclet number: 24				

Table 2-2 Composition of coal tar and column parameters used for model simulation.

	mass (μg/cm <sup>3</sup> )	MW (g/mole)	S <sub>l</sub> (μg/mL)	S <sub>s</sub> (μg/mL)
Naphthalene	103	128.2	114	32.0
1-Methylnaphthalene	57.3	142.2	27.1	27.0
2-Methylnaphthalene	100	142.2	34.1	26.0
Acenaphthylene	33.4	152.2	14.5	3.93
Acenaphthene	2.39	154.2	16.1	3.42
Fluorene	18.4	166.2	15.5	1.90
Phenanthrene	45.3	178.2	5.64	1.00
Anthracene	14.6	178.2	5.77	0.07
Fluoranthene	12.6	202	1.30	0.27
Pyrene	18.6	202	2.85	0.16
Chrysene	6.44	228.2	1.17	0.006
Benzo(a)anthracene	6.20	228.2	0.12	0.0057
Benzo(a)pyrene	4.06	252	0.13	0.0038
Pitch	1960	260		
Volumetric water content $\theta$ : 0.41 cm <sup>3</sup> /cm <sup>3</sup>				
Peclet number: 100				

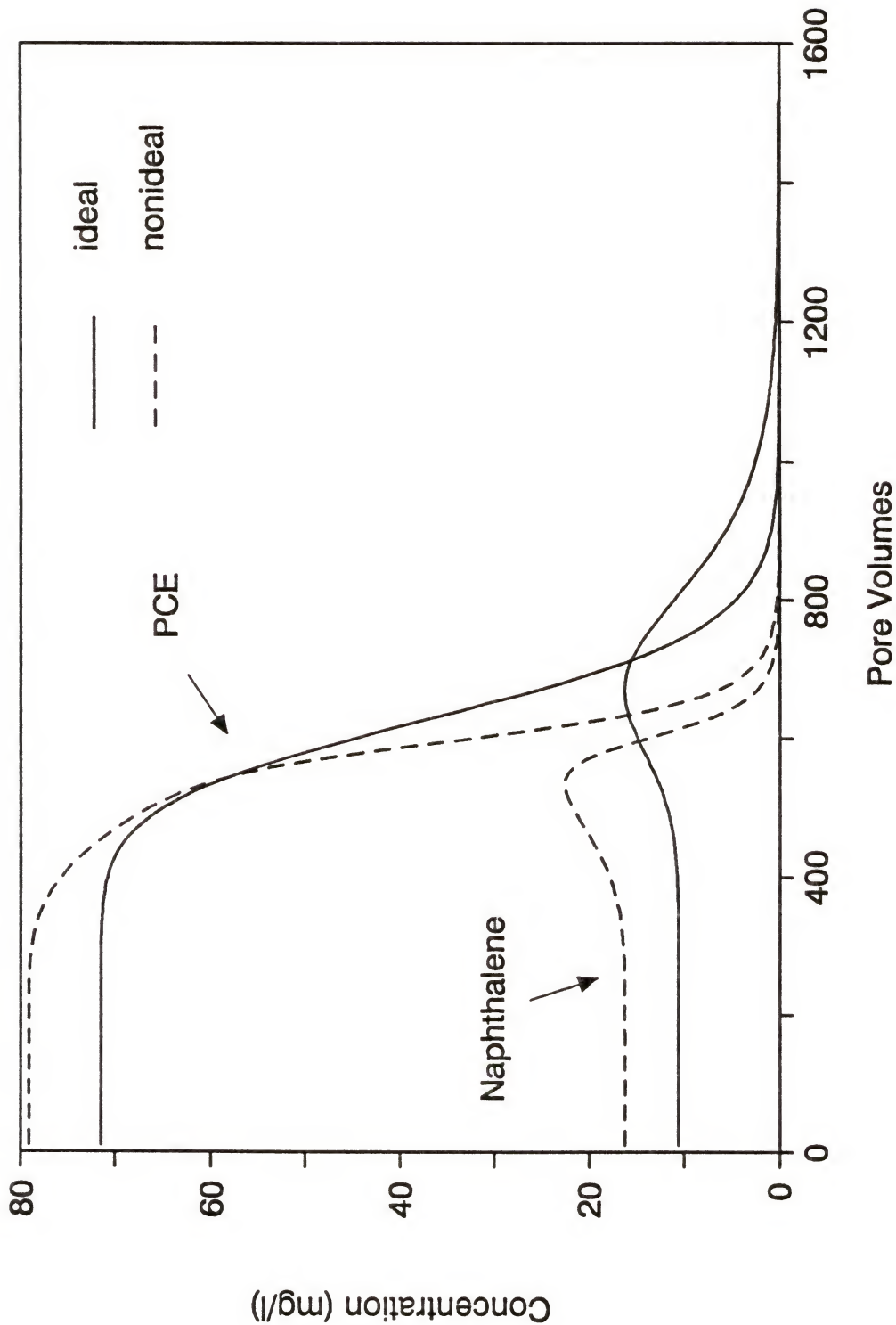


Figure 2-2 Simulated elution profiles for PCE and naphthalene from a decane/PCE/naphthalene mixture for ideal and nonideal behavior under equilibrium conditions.

until one of the components is depleted. When the concentration of the depleted component decreases, the concentrations of all other components increase, due to changing mole fractions. This effect can also be described by an increase in the partition coefficient (Mackay et al., 1991). Which component is depleted first depends on the solubility of the compounds and mass in the OIL phase. Under nonideal conditions, the activity coefficients of the components are larger than 1, and enhance the partitioning of the constituents into the aqueous phase. The results in higher solute concentrations in the effluent, and faster depletion of the components.

The experimental data collected for the elution experiment of the DPN mixture are shown in Figure 2-3. It is evident from the shape of these elution profiles that nonequilibrium conditions existed. A nonlinear least-square fitting program was developed for the nonequilibrium model (Equations 2-21 and 2-22), modified for nonideal behavior. The optimized fit to the experimental data resulted in first-order mass-transfer coefficients of 1.23 and 0.42  $\text{hr}^{-1}$  for PCE and naphthalene, respectively. These numbers indicate that the mass-transfer constraints for naphthalene were greater than for PCE, which was expected based on the size of the molecules. The model assumes that the OIL phase is initially in equilibrium with the solution phase, and hence the concentrations of PCE and naphthalene in the first column effluent are equal to the equilibrium concentrations predicted in Figure 2-2. After one pore volume, however, the equilibrated solution phase was displaced and the concentration decreased significantly due to nonequilibrium conditions. This initial drop in concentration was also simulated by the nonequilibrium model fitted to the data, but is not evident in Figure 2-3 because of the scale of the graph.



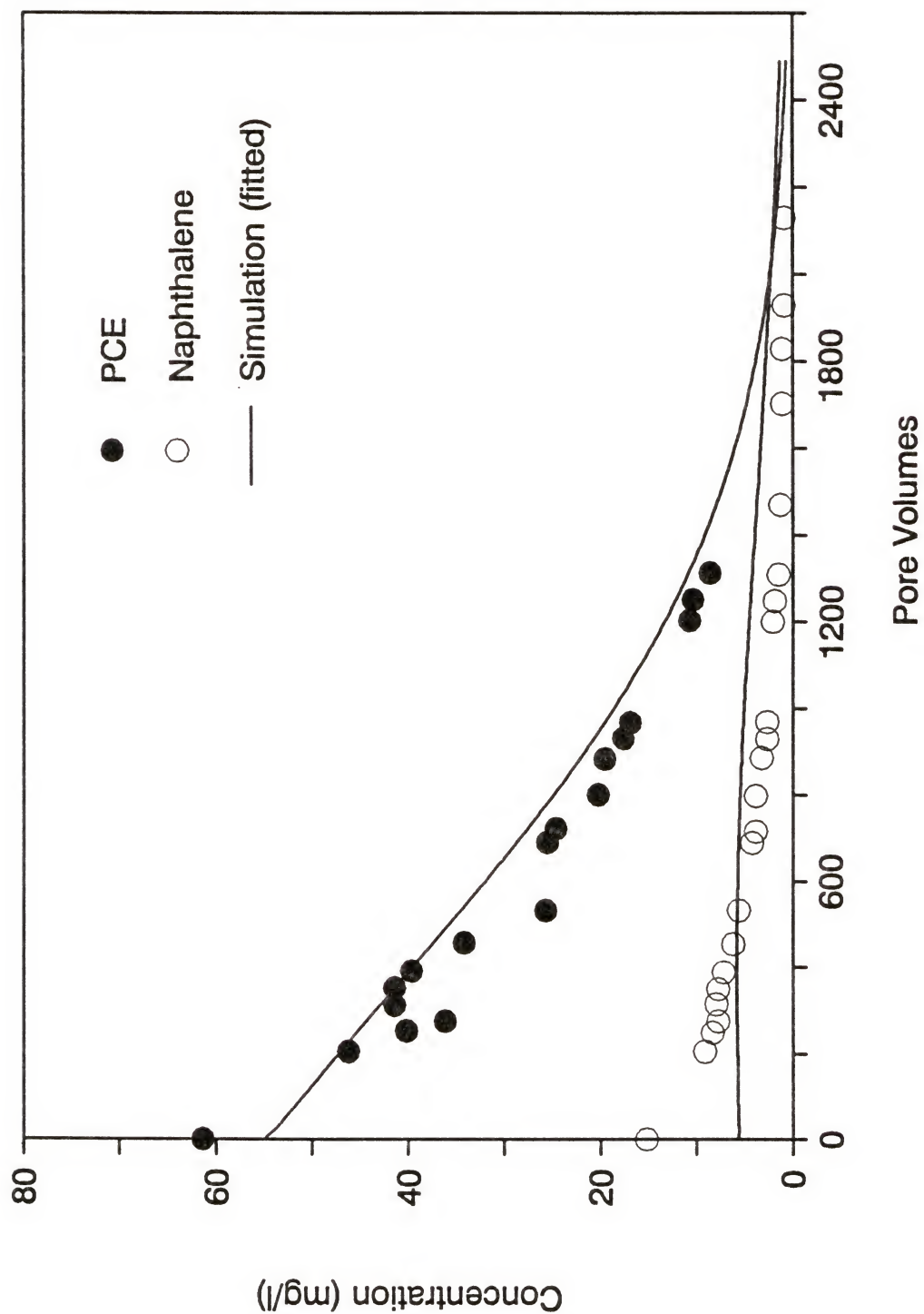


Figure 2-3 Simulated (fitted) and experimental elution profiles for PCE and naphthalene from a decane/PCE/naphthalene mixture.

For the results shown in Figure 2-3, only the two mass-transfer rate coefficients were varied to optimize the model fit to the experimental data; all other parameters were determined independently. For more complex mixtures, more parameters will likely be unknown, and the fitting procedure becomes less reliable when parameters are allowed to vary. Independent estimations may be obtained from relations as proposed by Powers et al. (1991). When diffusion through the pitch is rate-limiting, sphere- or film-diffusion models can be used. When the dissolution process becomes mechanistically close to desorption, sorption nonequilibrium models could be used. Some of these models will be discussed in more detail in the following chapter.

### Coal Tar

The input parameters used to simulate the elution profiles of the tar constituents are summarized in Table 2-3. The composition of the coal tar was obtained from EPRI (EPRI, 1993). The coal tar was assumed to consist of only 10 soluble compounds. The remainder of the tar (80% on mass basis) was considered as pitch. The experimental data and independent model predictions for 6 different constituents are shown in Figure 2-4. Considering the high level of uncertainty in the input data and model assumptions, the simulations and experimental data showed good agreement. The assumption of equilibrium dissolution of PAHs from the coal tar appeared to be reasonable. This was expected because the contact area between the tar and solution phase was large, because the coal tar was coated as a thin film over the mineral surfaces. Given the density of  $1.06 \text{ g/cm}^3$  for the tar, and assuming

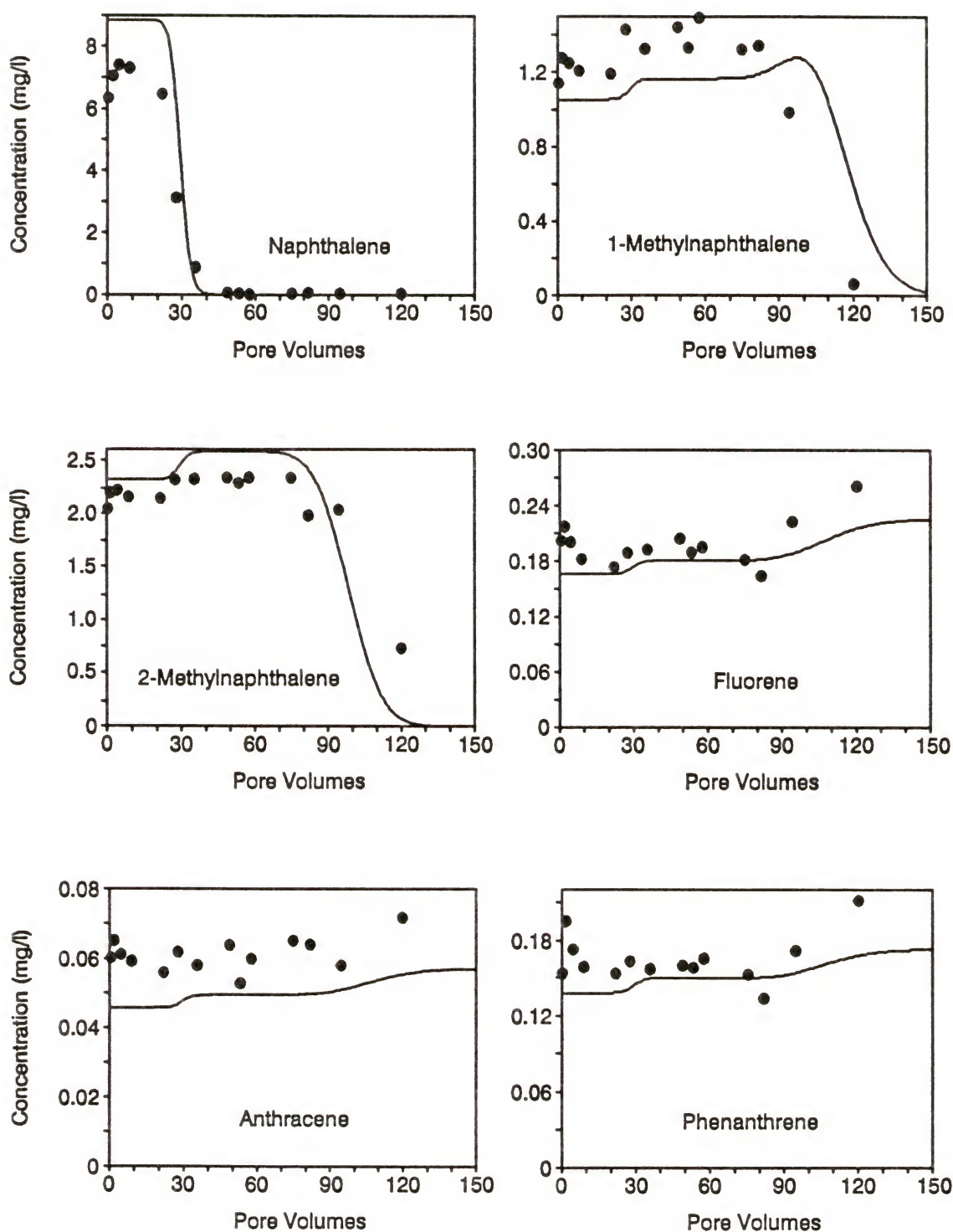


Figure 2-4 Elution profiles for six different tar-constituents from a column packed with a tar-treated sand.

that the sand grains can be approximated by spheres with an average diameter of 0.4 mm and a density of  $2.65 \text{ g/cm}^3$ , the average thickness of the tar film was estimated to be approximately 250 nm. A film thickness several hundred times more than the diameter of the soluble constituents caused apparently no significant mass-transfer constraints.

In Figure 2-5, the initial effluent concentration for each compound is plotted against the predicted aqueous-phase concentration, along with the equilibrium partitioning data collected by Lee et al. (1992b) in a batch equilibration study with the same coal tar. This plot suggests that, although the composition of coal tar is very complex, the behavior of the constituents in the tar phase is nearly ideal, i.e., the activity coefficient for each constituent approaches 1. Similar observations have been reported for gasoline (Cline et al., 1991), diesel fuel (Lee et al., 1992a), and motor oil (Chen, 1993).

### Conclusions

An accurate description of the multi-component dissolution process is essential when trying to predict the release of organic contaminants from complex waste mixtures. When more-soluble constituents dissolve from the OIL phase, the mole fraction of the remaining constituents increases, enhancing their partitioning into the solution phase. This effect has generally been ignored in existing multi-component dissolution models, but may have important consequences for the contamination and remediation of soils and aquifer media. For contamination, an increase in



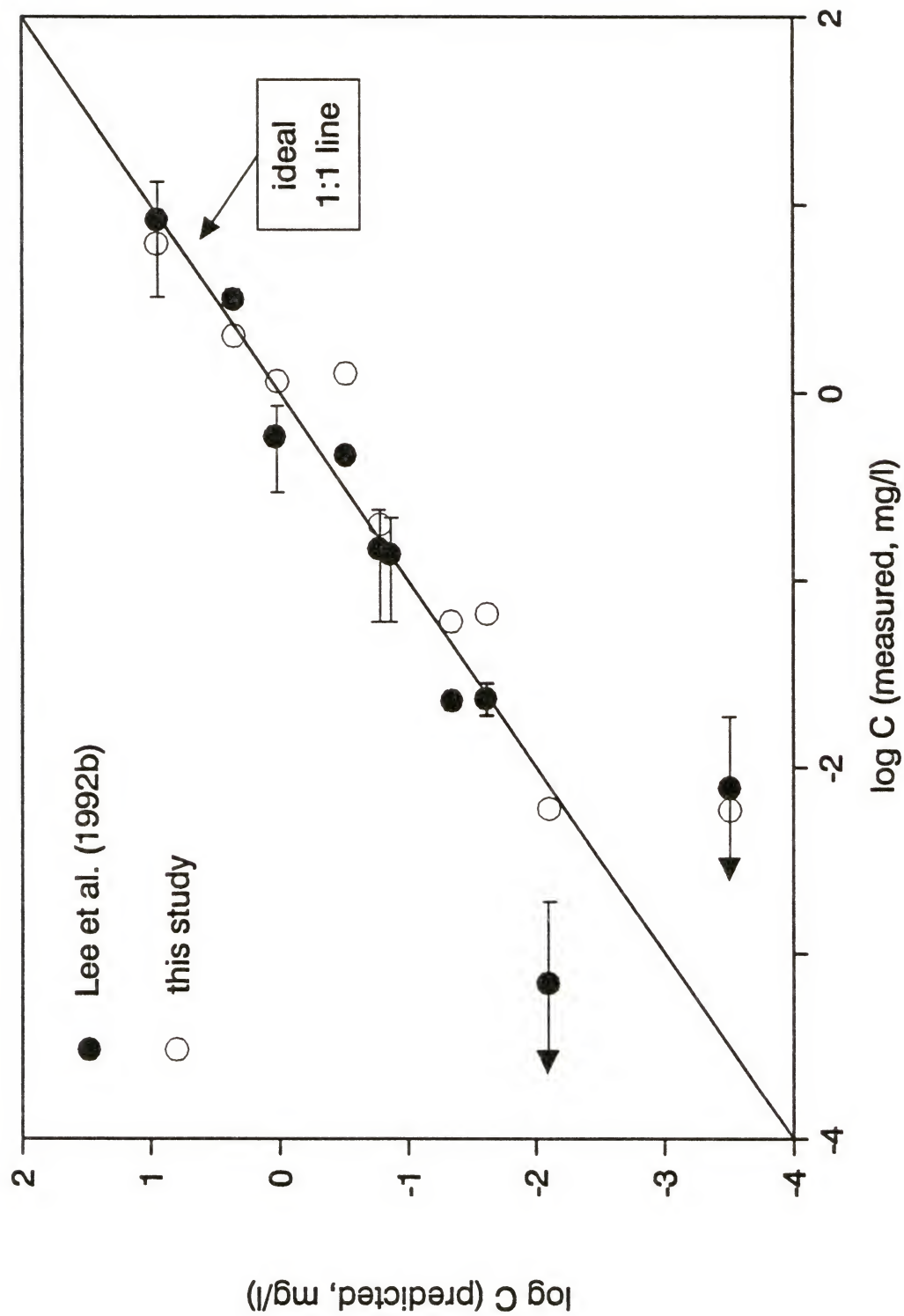


Figure 2-5 Measured versus predicted equilibrium solute concentrations for water in contact with coal tar ID#4.

concentration over time for the less-soluble constituents is unfavorable. On the other hand, for remediation, an increase in concentration leads to a more efficient removal of the contaminants.

Nonideal conditions will also increase the equilibrium concentration of OIL constituents in the solution phase, and has therefore a similar effect on contamination and remediation as changes in mole fraction. In field situations, however, the composition of the complex mixtures is never exactly known, and activity coefficients may be difficult to determine. In these cases, Raoult's law can be used as a first estimate to describe the dissolution of multi-component OILs.

## CHAPTER 3

### SORPTION DYNAMICS IN CONTAMINATED SOILS: MECHANISMS, MODELS, AND PREDICTIVE APPROACHES

#### Introduction

In previous chapter, the dissolution of complex waste mixtures was discussed. It was pointed out that when a large fraction of the OIL is composed of essentially insoluble compounds (i.e., the pitch), the mechanisms of dissolution and desorption are very close. In both processes, the solutes diffuse through an organic phase before they are released into the solution phase. For sorption, it is generally assumed that intra-sorbent diffusion is the rate-limiting mechanism. For most dissolution processes, the mass transfer across the OIL-water interface is assumed to be the rate-limiting mechanism. However, for viscous organic mixtures, such as coal tar, the diffusion within the OIL phase may become more rate-limiting. In addition, when an OIL phase is introduced into the subsurface, it will interact with the natural organic matter present in the soil. These interactions make it very difficult to distinguish between desorption from the sorbed phase or dissolution from the OIL phase. Based on these similarities, desorption and dissolution from a pitch may be described by the same models.

In this chapter, this hypothesis will be used to describe the release of organic contaminants from soils contaminated with complex waste mixtures with models

originally developed for sorption. First, the mechanisms of sorption will be reviewed, and different models will be discussed that describe these mechanisms. The bicontinuum first-order mass-transfer model is most commonly used to describe sorption and will here also be used to describe sorption by different contaminated matrices. It should be noted that the discussions in this chapter focus on single components. For soils contaminated with complex waste mixtures, the presence of high loadings of multiple components will affect the equilibrium concentrations over time due to changes in mole fraction. This effect can be simulated by reevaluating the mole fractions over time, as was done in previous chapter, or by adjusting the partition coefficient. As the more-soluble compounds dissolve or desorb, changes in the partition coefficient result from a reduction in the amount of organic carbon, and an increase in molecular weight of the organic phase (see Equation 2-9). The changes in composition will probably also alter the physical characteristics of the OIL phase, and therefore affect the mass-transfer through the organic phase.

### Sorption Mechanisms

Sorption is defined as the uptake of chemicals by the solid matrix of the soil, while desorption refers to the release of the sorbed chemical. There are two primary mechanisms by which sorption of organic chemicals can occur: (1) adsorption, which is the accumulation of matter at the interface between the solution phase and a solid phase; and (2) absorption, which is the uptake of a chemical species into a solid phase. Sorption of nonpolar organic chemicals is predominantly a solvent-driven



process, i.e., organic chemicals tend to escape the polar aqueous phase and accumulate at surfaces, or in more-hydrophobic regions such as soil organic matter. Many studies have shown that soil organic matter plays an important role in the sorption of hydrophobic organic chemicals; however, at low organic carbon contents, sorption on mineral surfaces may become more important (Schwarzenbach and Westall, 1981; Mingelgrin and Gerstl, 1983; Banerjee et al., 1985).

The importance of soil organic matter as a sorbent has led to the conceptualization of sorption as a partition process between the aqueous solution and soil organic matter. This mechanism would favor the term absorption to describe the sorption process. However, adsorption due to more specific interactions by Van der Waals forces, or weak electrostatic forces, should not be excluded. Thus, the term sorption continues to be a popular choice to describe organic contaminant uptake without specifying which of the two primary mechanisms is operative.

Soil organic matter may be viewed as a relatively open and flexible three-dimensional structure of cross-linked polymers (Schnitzer, 1978). Although organic matter has an overall hydrophobic character for neutral organic compounds, the molecules of which organic matter is composed have different moieties that range from extremely polar, like carboxyl and phenol groups, to nonpolar, like alkanes and lipids. The physical and chemical structure of organic matter is very complex, and has an important impact on the sorption capacity and rate of sorption as will be discussed later. Soil organic matter may be present as (a) separate particulates (not associated with minerals), (b) coatings on mineral surfaces, and (c) coatings in the

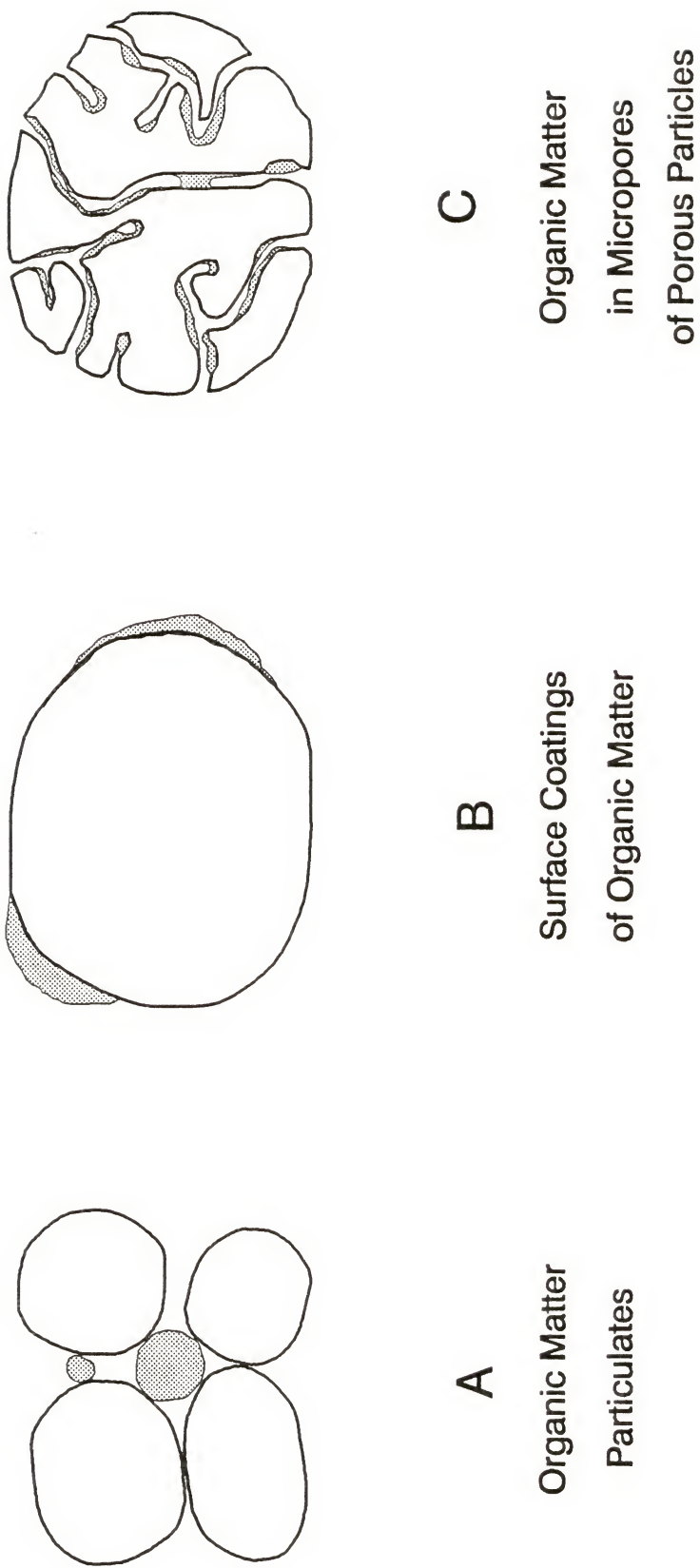


Figure 3-1 Schematic representation of the three possible forms of organic matter in soils.

internal pores of microporous particles (Figure 3-1). In most soils, organic matter is present in each of these three forms, but one of them may be the most abundant and controls the sorption process. The impact of these three forms of organic matter on the sorption of organic chemicals will be discussed next. The sorption mechanisms for discrete organic particles and surface coatings of organic matter are very similar and will therefore be discussed together.

#### Particulate organic matter and organic matter associated with mineral surfaces

Adsorption of humic substances on mineral surfaces occurs by electrostatic interactions, hydrogen-bonding, and Van der Waal's forces (Schnitzer, 1978). Thus, most of the organic matter is likely associated with the more-reactive minerals that are part of the smaller particle size fraction of the soil (Karickhoff and Morris, 1985; Ball et al., 1991; Barber et al., 1992). The accumulation of organic matter on mineral surfaces probably does not occur uniformly but in small patches, because of the heterogeneous energy distribution on mineral surfaces (Leenheer, 1991), and due to the hydrophobic nature of organic matter that tends to create a minimum surface area between organic matter and the aqueous phase.

When a nonpolar organic chemical is introduced into ground water, it tends to escape the polar aqueous phase and accumulates at the various interfaces present in the soil matrix. When organic molecules accumulate at the interface between water and soil organic matter, they may diffuse through the organic matrix towards inner regions under influence of a concentration gradient. This process is known as intra-organic matter diffusion (IOMD), and has been proposed as a possible

mechanism for rate limited sorption by several authors (Karickhoff and Morris, 1985; Brusseau and Rao, 1989a). The diffusion of the organic molecules takes place through the voids between the molecules of organic matter. These empty spaces are commonly referred to as the "free volume", which is continuously redistributed by thermal fluctuations. Only a portion of this free volume is available for molecular transport. This part is denoted the "hole-free volume" and the remainder as the "interstitial-free volume" (Zielinski and Duda, 1992). In this hole-free volume, the diffusing organic molecules have to compete with the solvent molecules.

Figure 3-2a shows a schematic diagram of a small portion of the structure of organic matter. This figure was inspired by the chemical structures of humic substances presented by Stevenson (1985), and the computer simulations of kerogen structure published by Rullkotter and Michaelis (1990). The structure of organic matter presented in Figure 3-2a may be chemically not correct, but gives a general idea of the compositional and geometric complexity of organic matter.

According to Wershaw (1986), more of the polar moieties will likely be found on the external regions of organic matter (those in contact with the polar solvent, water) and on the mineral/organic matter interface, where the polar groups provide chemical bonding with the mineral surfaces. Similarly, soil organic matter particulates can be considered as micelles with the polar regions facing externally, interlocking the hydrophobic domains. Figure 3-2b shows the distribution of polar and hydrophobic regions in the hypothetical structure of organic matter depicted in Figure 3-2a. Nonpolar organic molecules will have an affinity for the more-



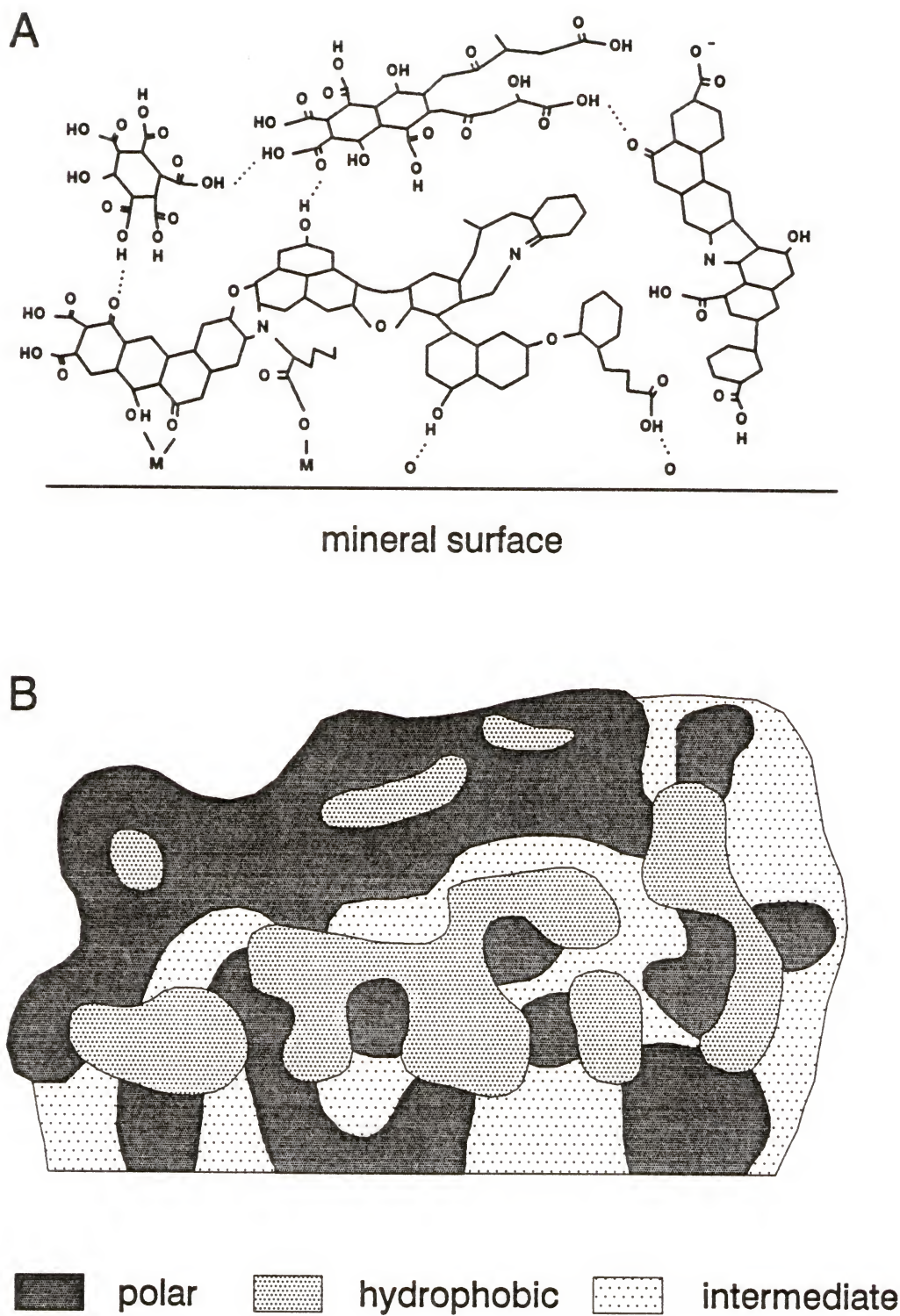


Figure 3-2 Schematic representation of the chemical structure of soil organic matter (a) and the distribution of polar and hydrophobic domains in this hypothetical structure (b).

hydrophobic regions in organic matter, and may even undergo specific interactions as a result of Van der Waal's forces. It is therefore likely that the molecules will have varying residence times in each of these different regions. In addition to different residence times in different regions of the sorbent, the diffusion of the molecules is subjected to tortuosity and entanglement within the sorbent matrix. Thus, molecular conformation as well as hydrophobicity can play major roles in determining sorbate diffusion within the organic matter matrix.

IOMD may cause significant constraints to sorption rates when the organic matter is sufficiently thick. The observed nonequilibrium for low  $f_{oc}$  aquifer materials indicates that the organic matter is thick enough, and supports the idea that organic matter is not equally spread over the mineral surfaces but is rather concentrated in small patches (Lion et al., 1990).

#### Organic matter in micropores of porous particles

Some minerals have micropores in which organic matter may have accumulated. Organic chemical in the solution phase will diffuse into this porous network and sorb onto the organic matter that is attached to the pore walls. This process is known as retarded intra-particle diffusion (RIPD) and has also been proposed as a possible mechanism for rate-limited sorption by several authors (Wu and Gschwend, 1986; Weber and Miller, 1988; Ball and Roberts, 1991). In contrast to the flexible pore network in soil organic matter visualized for the IOMD approach, the micropores are rigid and permanent. When a solute diffuses through the micropores, it may be constrained by the sinuous and tortuous path ways. Sorption

by the organic matter in the micropores is considered to be instantaneous. This may be justified by the narrow diameters of the micropores which do not allow for many molecular layers of organic matter. When the pores are partially filled or blocked by organic matter, the solutes have to diffuse through the organic matter, and the sorption process becomes a combination of RIPD and IOMD.

The distinction between IOMD and RIPD has been a subject for debate in the literature (cf., Ball et al., 1991, and Brusseau et al., 1991c). Both theories are somewhat speculative based on indirect evidence. Microscopic or spectroscopic data, providing direct evidence of the distribution and structure of organic matter on a grain scale is necessary to get a better understanding of the actual sorption process. Table 3-1 compares the microporous volume and the volume of soil organic matter for three different materials. Micropore analyses by  $N_2$  adsorption for the Eustis and Tampa soil were performed by the Advanced Material Research laboratory of the University of Florida. The same method was used by Ball et al. (1990) for the Borden aquifer material. The Borden aquifer material was used by Ball and Roberts (1991) to argue for RIPD as the principal mechanism responsible for rate-limited sorption. The Eustis and Tampa soil were used by Brusseau and coworkers (Brusseau et al., 1990; Brusseau and Rao, 1991) to illustrate rate-limited sorption by IOMD. It is evident from Table 3-1 that for Borden aquifer material most, or all of the organic matter could be located in the micropores; however, for the Eustis and Tampa soil, the volume of organic matter exceeds the volume in the micropores. This has consequences for the location of the organic matter, but does not necessarily

Table 3-1 Comparison of the volume of micropores and soil organic matter (SOM).

Material	$f_{oc}$	Microporosity	Volume of SOM <sup>a</sup>
Borden <sup>b</sup>	0.021%	4.9 cm <sup>3</sup> /kg	0.26 m <sup>3</sup> /kg
Eustis	0.39%	1.2 cm <sup>3</sup> /kg	4.8 m <sup>3</sup> /kg
Tampa	0.13%	0.75 cm <sup>3</sup> /kg	1.6 m <sup>3</sup> /kg

<sup>a</sup> based on an average density for dry soil organic matter of 1.4 g/cm<sup>3</sup> (Koorevaar et al., 1983), and a conversion factor of 1.72 to convert from organic carbon to organic matter. <sup>b</sup> data from Ball et al. (1990).



clarify which process dominates the sorption rates. The average pore diameter for the Eustis and Tampa soil were 5.4 and 3.7 nm, respectively. Note that the size of a small organic molecule like benzene is approximately 0.54 nm. These numbers indicate that large molecules like humic acids, a basic "building block" of organic matter (Schnitzer, 1978), are not able to occupy a large portion of the pores, making IOMD a more plausible mechanism for sorption nonequilibrium in Eustis and Tampa soils.

### The Fractal Nature of Soil Organic Matter

As discussed in previous sections, the rate of sorption is determined by the physical and chemical structure of the sorbent. In an attempt to describe irregular objects, Mandelbrot (1982) introduced the concept of fractals, that allows us to assign a non-integer dimension to a physical object. The basic principle of a fractal is that the irregularities of the object are repeated at different scales (self-similarity). In Euclidian space, integer dimensions of 0, 1, 2, and 3 represent a point, a line, a surface, and a volume, respectively. Fractals have non-integer dimensions between 0 and 3. An example of an object with a fractal dimension between 0 and 1 is the Cantor dust; between 1 and 2 the Koch curve; and between 2 and 3 the Menger sponge (Figure 3-3). For these objects, the fractal dimension can be calculated by dividing the logarithm of the number of units in the basic structure, by the logarithm of the number of units that make up the length.

All objects have three components, mass (solid material), surfaces, and the pores (voids). Pfeifer (1987) divided fractal objects into four different categories: (1)

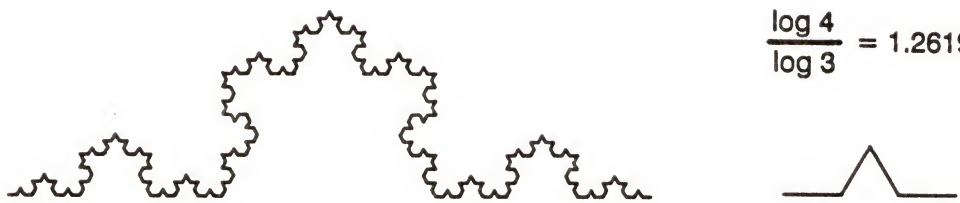
Cantor dust

$$\frac{\log 2}{\log 3} = 0.6309$$



Koch curve

$$\frac{\log 4}{\log 3} = 1.2619$$



Menger sponge

$$\frac{\log 20}{\log 3} = 2.7268$$

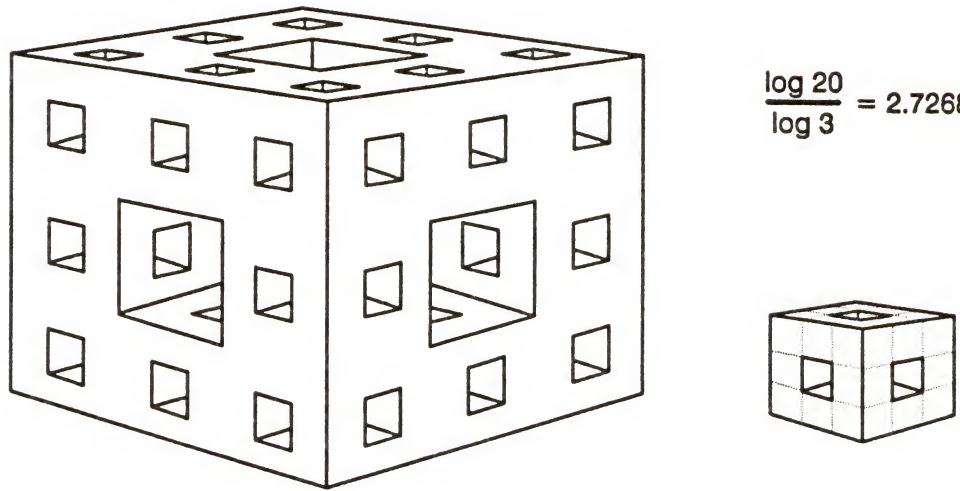


Figure 3-3 Three examples of fractal objects and the calculation of the fractal dimension from their basic structure.

Surface fractals, objects of which only the surface has a fractal dimension; (2) Mass fractals, where the mass and surfaces have the same fractal dimension; (3) Pore fractals, where the pores and surfaces have the same fractal dimension; and (4) Subfractal surfaces, for which neither mass, nor surfaces, nor pores have a fractal dimension, but the edges on the surfaces have an irregular distribution that can be described by a fractal dimension. Note that mass fractals have an infinitesimally small mass and pore fractals an infinitesimally small pore volume.

Since the introduction of the fractal theory, many patterns, objects, and materials have been described by fractal dimensions. In relation to sorption, Avnir et al. (1983), for example, determined the fractal dimension of various sorbents such as graphite, zeolites, and charcoal by vapor adsorption. Since soil organic matter is a very complex, and heterogeneous material, it is possible that the physical structure can be described by a fractal dimension. Recently, Rice and Lin (1993) determined the fractal dimension of various humic materials by X-ray scattering. They found fractal dimensions ranging from 1.6 for aquatic humus to 2.8 for lignite fulvic acid. Based on their data, they also concluded that dissolved humic materials are mass fractals and solid state humic materials surface fractals. If the fractal dimension of natural sorbents could be determined from existing sorption data, it could help to differentiate between IOMD and RIPD. Since soil organic matter can be viewed as a mass or surface fractal (Rice and Lin, 1993), the voids in the organic matrix are still three dimensional. Partitioning of organic chemicals into these voids should result in a traditional Euclidian dimension of 3. Porous particles are more likely

pore fractals, since the volume of the micropores approaches an infinitesimally small value. Diffusion of organic chemicals into the micropores and sorption onto the walls, should therefore result in a fractal dimension between 2 and 3.

The dimension (D) of an object can be calculated from the following equation:

$$N(r) = A r^{-D} \quad (3-1)$$

where  $N(r)$  is the number of probes that cover a surface or fill a volume;  $A$  a proportionality constant; and  $r$  the radius of the probe. Equation 3-1 can be linearized by taking logarithms:

$$\log N(r) = \log A - D \log r \quad (3-2)$$

If a surface is covered, or a volume is filled, by increasingly bigger probes, a smaller number of probes are necessary to cover the same surface, or fill the same volume. In the case of a fractal object, larger probes will also be excluded from certain areas or volumes which leads to non-integer dimensions. If soil organic matter or a porous particle is viewed as a fractal object (e.g., a Menger sponge), the molecules can be attached to the internal surfaces of the Menger sponge, indicating a surface mechanism as proposed for RIPD, or the molecules can fill up the pores of the Menger sponge as proposed for IOMD.

A simple calculation was performed in which balls (probe molecules) of different sizes are either paved on the surface or used to fill the holes in the porous structure of the Menger sponge. In Figure 3-4, the logarithm of the number of balls



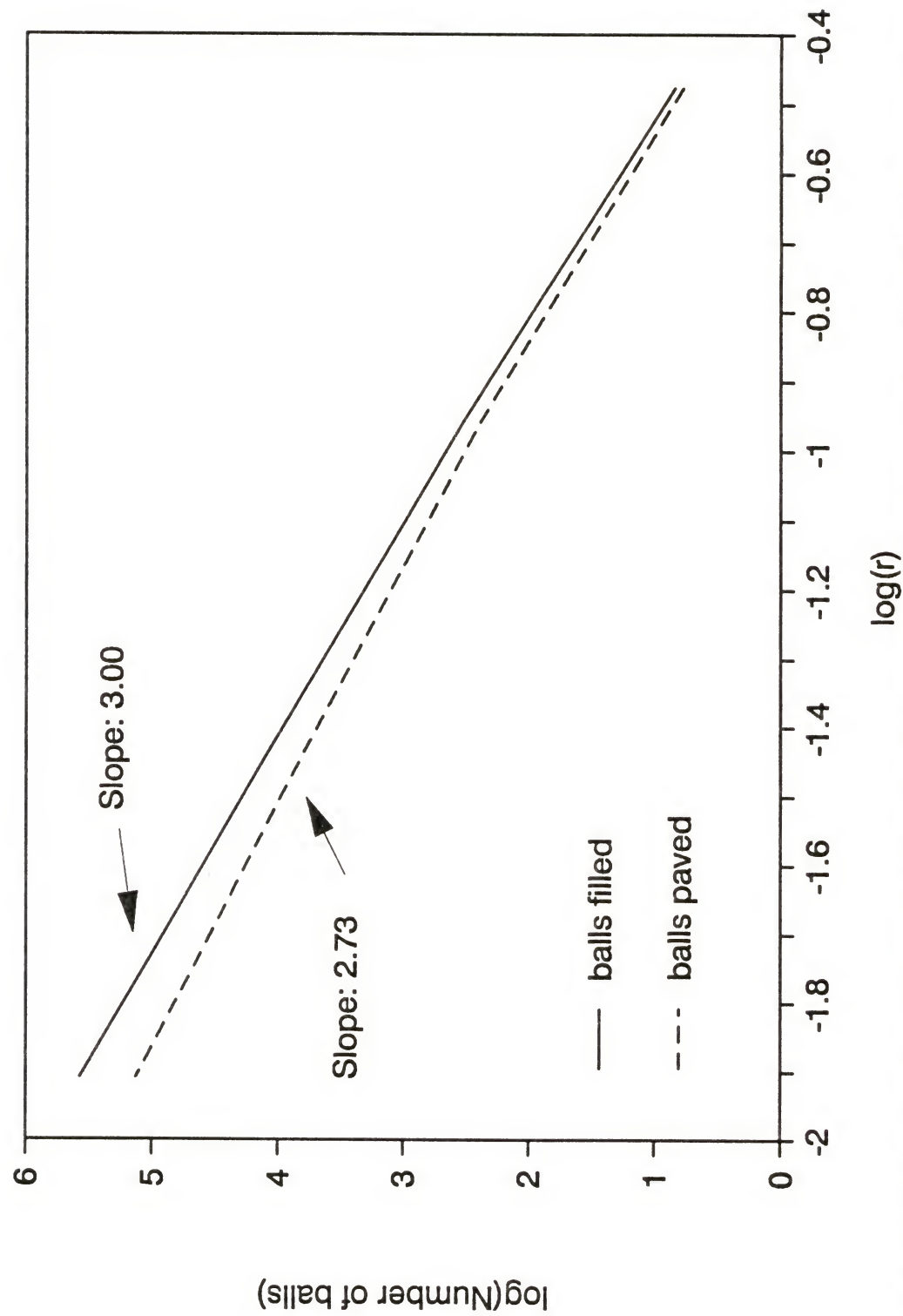


Figure 3-4 Plot for determination of the fractal dimension of the Menger sponge by filling the pores spaces or paving the internal surfaces with a sequence of balls with increasing different radii.

is plotted versus the radius of the balls in order to determine the fractal dimension of the Menger sponge according to Equation 3-2. This plot shows that filling the holes results in a dimension of exactly 3, whereas paving the balls on the surface resulted in a fractal dimension of 2.73 (i.e., the fractal dimension of the Menger sponge). This is typical for a mass fractal for which the mass and surfaces exhibit a fractal dimension, while the pore space is still three-dimensional.

An attempt was made to explore the fractal geometry of a natural sorbent by using existing sorption data.  $N(r)$  in Equation 3-1 represents the maximum loading of probes. The maximum loading of an organic chemical in soil organic matter would be the equilibrium sorbed concentration at the aqueous solubility limit of the compound (Chiou, 1989):

$$S^{om} = K S^w \quad (3-3)$$

This assumes that the partition process is linear up to the aqueous solubility of the compound. To calculate the actual loading in molecules per gram organic carbon, Equation 3-3 needs to be corrected by the mass fraction of organic carbon and multiplied by Avogadro's number ( $N_a = 6.02 \times 10^{23}$  molecules/mole):

$$N(r) = K_{oc} S^w N_a \quad (3-4)$$

Note that  $S^w$  is expressed here in mole/ml. The size of a molecule can be estimated from its molar volume. In Table 3-2 sorption data are compiled for Eustis fine sand and Tampa subsurface soil. The sorption data were obtained from Brusseau et al. (1990) for the Eustis soil, and Brusseau and Rao (1991) for the Tampa soil. The

Table 3-2 Data for determination of a fractal dimension for two different soils.

Soil	Compound	K (ml/g)	K <sub>oc</sub> (ml/g)	S <sup>w a</sup> (mg/l)	MW <sup>b</sup> (g/mol)	MV <sup>c</sup> (ml/mol)	d <sup>d</sup> (nm)
Eustis <sup>e</sup>	Benzene	0.08	21	1780	87.1	49	0.54
	Chlorobenzene	0.30	77	488	112.6	58	0.57
	1,2-Dichlorobenzene	0.94	241	100	147.0	67	0.60
	1,2,4-Trichlorobenzene	3.03	777	25	181.5	76	0.62
	Trichloroethene	0.23	59	1100	131.5	49	0.54
	Tetrachloroethene	0.74	190	165	165.8	58	0.57
	Naphthalene <sup>f</sup>	0.94	241	32	128.2	75	0.62
Tampa <sup>g</sup>	Toluene	0.05	38	535	92.1	59	0.57
	p-Xylene	0.14	108	198 <sup>h</sup>	106.2	67	0.60
	Chlorobenzene	0.09	69	488	112.6	58	0.57
	1,3-Dichlorobenzene	0.38	292	123	147.0	67	0.60
	1,2,4-Trichlorobenzene	0.73	562	25	181.5	76	0.62
	Trichloroethene	0.09	69	1100	131.5	49	0.54
	Tetrachloroethene	0.35	269	165	165.8	58	0.57
	1,1,1-Trichloroethane	0.03	23	720	133.4	52	0.55
	Naphthalene	0.22	169	32	128.2	75	0.62

<sup>a</sup> Aqueous solubility of the pure substance (mg/l) from Little (1981) unless stated otherwise. <sup>b</sup> Molecular weight from Verschueren (1983). <sup>c</sup> Molar volume (ml/mol) from Abernethy et al. (1988). <sup>d</sup> Diameter (nm) calculated from the molar volume. <sup>e</sup> K from Brusseau et al. (1990),  $f_{oc}=0.0039$ . <sup>f</sup> K from Brusseau et al. (1991b). <sup>g</sup> K from Brusseau and Rao (1991),  $f_{oc}=0.0013$ . <sup>h</sup> from Verschueren (1983).

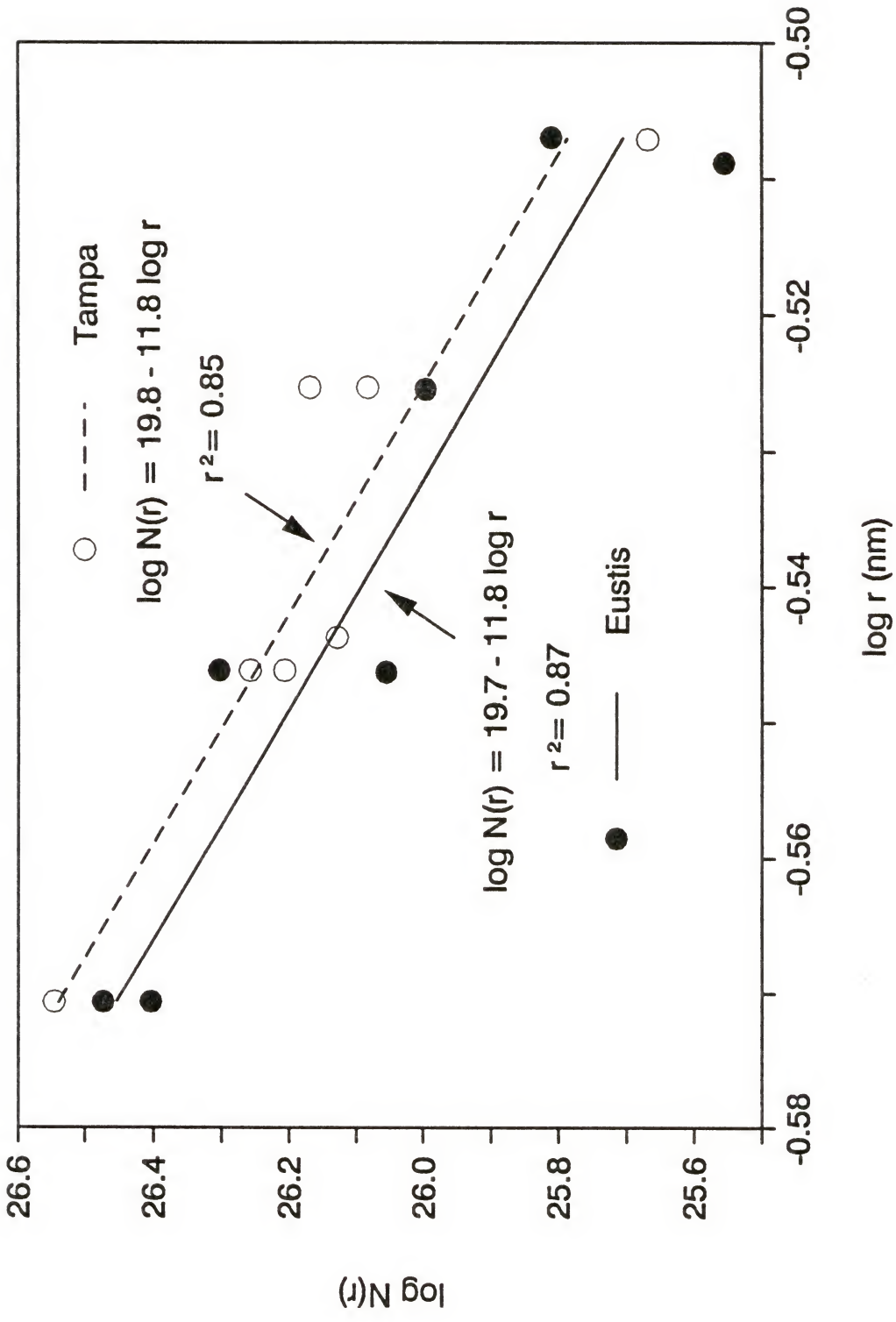


Figure 3-5 Plot of sorption data for determining the fractal dimension of Tampa and Eustis soils.



diameter of the organic chemicals listed in Table 3-2 were calculated from the intrinsic or Van der Waals molar volume (Abernethy et al., 1988), and the assumption that the shape of the molecules can be approximated by spheres.

The data in Table 3-2 are plotted in Figure 3-5. The slope of both regression lines in this plot is 11.8. This number is too high to assign a fractal dimension to the sorption process on Eustis or Tampa soil. One could speculate, however, on the possible reasons for this high number. First, perhaps the network of voids or pores explored by the organic chemicals is not fractal, i.e., irregularities are not repeated at scales covered by the probes. Second, the sorption data used in this study does not provide a good estimation for the fractal dimension. The first reason is unlikely since the data by Rice and Lin (1993) showed that organic matter could be characterized by fractal dimensions. The inadequacy of the sorption data from aqueous solutions used here to describe the fractal geometry of organic matter, is probably a more acceptable explanation for the large slopes of the regression lines in Figure 3-5. The structure of organic matter itself may be fractal, but the manner in which the sorbent is explored by the solutes may not sense the fractality. The manner in which the sorbent is explored depends on both the physical and chemical structure of the sorbent. The distribution of polar and hydrophobic regions in organic matter (Figure 3-2b), for example, may exclude more hydrophobic molecules from isolated pockets of hydrophobic regions located in a zone of predominantly polar regions. This phenomenon prevents the probe molecules from exploring the maximum possible volume or area, which is essential for the determination of a

fractal dimension. In addition, the assumptions made to calculate the loading, and size and shape of the molecules, may also introduce errors in the determination of the fractal dimension.

Figure 3-5 shows that the loading decreases faster than would be expected based on a realistic fractal dimension. This suggests that with increasing molecular size, less of the available volume is explored due to steric hindrance, molecular entanglement, or chemical exclusion. In conclusion, the concept of fractals with sorption data from aqueous solutions cannot be used to distinguish between sorption mechanisms, but confirms the complexity of sorption phenomena.

### Sorption Nonequilibrium Models

The most common way to describe sorption of nonpolar organic chemicals by soils from an aqueous solution under equilibrium condition is by the linear sorption isotherm:

$$S = K C \quad (3-5)$$

where  $S$  is the sorbed concentration (g/g);  $K$  the equilibrium sorption coefficient (ml/g); and  $C$  the solution concentration (g/ml). It has been recognized that sorption is initially rapid followed by a slower uptake (Selim et al., 1976; Cameron and Klute, 1977; Karickhoff, 1980; Brusseau and Rao, 1989a; Ball and Roberts, 1991). This has led to the development of a bicontinuum model in which the sorbent is divided into two domains:  $S_1$ , the rapid or instantaneous sorption domains, usually associated with the external regions of the sorbent; and  $S_2$ , the rate-limited

sorption domains which are located in regions of the sorbent less accessible for the sorbate. The sum of the sorbed concentration in each phase adds up to the total sorbed concentration,  $S$ :

$$S = S_1 + S_2 \quad (3-6)$$

As discussed in previous section, sorption into the rate-limited domains is usually conceptualized as a diffusion-limited process. Three models will be discussed that describe sorption under nonequilibrium conditions using the conceptual ideas presented above.

#### Film-Diffusion Model

The first model is a film-diffusion model, which is most representative for IOMD. In this model organic matter is represented as a film coating the soil particles, in which the organic solutes diffuse. The instantaneous sorption domains are in constant equilibrium with the solution phase, which is described by:

$$S_1 = F K C \quad (3-7)$$

where  $F$  is the fraction of instantaneous sorption domains, and all other parameters are as defined before.

The change of mass in the rate-limited sorption domains is proportional to the change in average concentration in these domains ( $\bar{C}_{om}$ ), or equal to the mass flux across the interface between  $S_1$  and  $S_2$ , which can be described by Fick's first law of diffusion:

$$\frac{\partial S_2}{\partial t} = (1 - F) \frac{f_{om}}{\rho_{om}} \frac{\partial \bar{C}_{om}}{\partial t} = - \frac{A D_f}{M_s} \left( \frac{\partial C_{om}}{\partial y} \right)_{y=0} \quad (3-8)$$

where  $f_{om}$  is the mass fraction of organic matter in the soil (g/g);  $\rho_{om}$  the density of organic matter (g/cm<sup>3</sup>);  $A$  the interfacial area through which the chemicals enter the rate-limited sorption domains (cm<sup>2</sup>);  $D_f$  the effective diffusion coefficient in the organic film (cm<sup>2</sup>/hr);  $M_s$  is the mass of soil (g);  $C_{om}$  the solute concentration in the rate-limited sorption domains of organic matter (g/cm<sup>3</sup>);  $y$  the distance within the rate-limited sorption domains (cm); and subscript  $y=0^+$  indicates that the flux depends on the concentration gradient just inside the rate-limited sorption domains.

The average concentration ( $\bar{C}_{om}$ ) and concentration gradient ( $\partial C_{om}/\partial y$ ) can be calculated from the concentration profile in the rate-limited domains of the sorbent, which is described by Fick's second law of diffusion:

$$\frac{\partial C_{om}}{\partial t} = D_f \frac{\partial^2 C_{om}}{\partial y^2} \quad (3-9)$$

The effective diffusion coefficient ( $D_f$ ) is a function of the tortuosity of the diffusion path for the organic chemical, and the residence time of the chemical in different regions of the organic phase (pseudo-retardation effect).

The boundary condition at the interface between  $S_1$  and  $S_2$  is given by:

$$C_{om} = K' C \quad (3-10)$$

and at the mineral surface:

$$\frac{\partial C_{om}}{\partial y} = 0 \quad (3-11)$$



which is a no-flux or reflection boundary.  $K'$  in Equation 3-10 is a dimensionless equilibrium sorption coefficient, which relates to  $K$  by the following equation:

$$K = \frac{f_{om}}{\rho_{om}} K' \quad (3-12)$$

These equations can be substituted into the one-dimensional solute transport equation discussed in Chapter 1 (Equation 1-8):

$$(\theta + F\rho K) \frac{\partial C}{\partial t} - \rho \frac{AD_f}{M_s} \left( \frac{\partial C_{om}}{\partial y} \right)_{y=0+} - \theta D_h \frac{\partial^2 C}{\partial x^2} - q \frac{\partial C}{\partial x} \quad (3-13)$$

The gradient  $(\partial C_{om}/\partial y)_{y=0+}$  is calculated from Equation 3-9, with boundary conditions 3-10 and 3-11.

### Pore-Diffusion Model

The second model is the radial pore-diffusion model which is most representative for RIPD. Ball and Roberts (1991) recognized the need of adding a fraction of instantaneous sorption in order to describe the sorption process more accurately. Sorption by the instantaneous fraction is described by Equation 3-7 regardless of the model for rate-limited sorption.

At any given time, the mass in the rate-limited sorption domains is the sum of the mass in the micropore solution, and the mass sorbed onto the pore walls:

$$\rho S_2 = (\theta_p + (1-F)\rho K) \bar{C}_p \quad (3-14)$$

where  $\theta_p$  is the volumetric water content residing in the micropores of the particles (ml/cm<sup>3</sup> soil); and  $\bar{C}_p$  is the average pore-water concentration in the micropores (g/ml). For spherical particles with radius  $a$  (cm), the average concentration is calculated by:

$$\bar{C}_p = \frac{3}{4\pi a^3} \int_0^a 4\pi r^2 C_p dr \quad (3-15)$$

where  $r$  is the radial distance in the particle (cm).

To be able to calculate the average concentration, the concentration profile needs to be known for the entire particle and is calculated from Fick's second law of diffusion in radial coordinates:

$$\frac{\partial C_p}{\partial t} = \frac{D_p}{r^2} \frac{\partial}{\partial r} \left( r^2 \frac{\partial C_p}{\partial r} \right) \quad (3-16)$$

where  $D_p$  is the apparent diffusion coefficient in the micropores (cm<sup>2</sup>/hr). It is assumed here, that diffusion only takes place in the solution phase of pores (pore diffusion), and not in the sorbed phase (surface diffusion). The boundary condition between the solution phase and the water in the micropores is:

$$C_p = C \quad (3-17)$$

The apparent diffusion coefficient is defined as (Ball and Roberts, 1991):

$$D_p = \frac{\lambda D_o}{R_p} \quad (3-18)$$

where

$$R_p = 1 + (1 - F) \frac{\rho}{\theta_p} K \quad (3-19)$$

and  $\lambda$  is a complexity factor that accounts for the sinuous and tortuous nature of the micropores, dead-end pores, variability in pore diameter, pore constrictivity in very small pores, and steric hindrances. In addition, the shape of the particles may affect the apparent diffusion coefficient. Note that for different shapes the formula for the average concentration (Equation 3-15) also changes. The assumption of spherical particles for minerals may be crude, especially for phyllosilicate minerals in the clay fraction, but work by Rao et al. (1982) and Van Genuchten and Dalton (1986) suggests that the uptake of solutes by objects of different geometries can be approximated by equivalent spherical objects.

Substitution of these equations into the general one-dimensional solute-transport equation gives:

$$(\theta + F \rho K) \frac{\partial C}{\partial t} - \theta_p R_p \frac{\partial \bar{C}_p}{\partial t} - \theta D_h \frac{\partial^2 C}{\partial x^2} - q \frac{\partial C}{\partial x} \quad (3-20)$$

The average pore-water concentration is calculated from Equations 3-15 and 3-16.

The pore-diffusion model is mathematically identical to the sphere-diffusion models used to describe physical nonequilibrium due to diffusion within spherical aggregates (Rao et al., 1980; 1982; Nkedi-Kizza et al., 1982; Rappoldt, 1990). The conceptual difference is a matter of scale: intra-particle diffusion versus intra-aggregate diffusion. The practical difference is that the amount of water residing in

the micropores is much smaller than the immobile water contents considered in physical nonequilibrium models, and that the effective pore-diffusion coefficient in the RIPD model is probably much smaller because of the expected higher tortuosity.

### First-Order Mass-Transfer Models

The bicontinuum first-order mass-transfer model is probably one of the most popular models used to describe nonequilibrium conditions for sorption. This model does not describe any physical process specifically, but approximates either of the two diffusion models, by assuming an average concentration in the rate-limited sorption domains. In the case of IOMD, the change of mass in the rate-limited sorption domains is described by the following first-order rate process:

$$\frac{\partial S_2}{\partial t} = k_f \left( \frac{S_1}{F} - \frac{S_2}{1-F} \right) \quad (3-21)$$

For RIPD, the first-order rate process is described by:

$$\rho \frac{\partial S_2}{\partial t} = \theta k_p (C - \bar{C}_p) \quad (3-22)$$

The general one-dimensional solute-transport equation for the mass-transfer models is given by:

$$(\theta + F\rho K) \frac{\partial C}{\partial t} + \rho \frac{\partial S_2}{\partial t} = \theta D_h \frac{\partial^2 C}{\partial x^2} - q \frac{\partial C}{\partial x} \quad (3-23)$$



where  $\partial S_2/\partial t$  is described by Equation 3-21 for IOMD, and Equation 3-22 for RIPD, respectively.

It is often convenient to express the transport equations in a nondimensional form. This facilitates easy comparison of experimental results obtained from different systems. The nondimensional equations for all three models are summarized in Table 3-3.

#### Other Sorption Nonequilibrium Models

Four different models that describe sorption nonequilibrium have been presented thus far. There are numerous other models of which a few will be reviewed below. When  $F$  is set to zero in the bicontinuum mass-transfer model, it reduces to a single-domain, first-order rate model (Cameron and Klute, 1977; Schwarzenbach and Westall, 1981). Although the applications of this model may be limited, the mathematics are much simpler, and therefore sometimes more convenient. What is considered to be the instantaneous sorption domain in the bicontinuum mass-transfer model, may actually require some time to reach equilibrium. Although this time may be relatively short (in the order of minutes to hours) compared to sorption into the rate-limited domains (days to months), it can be described by another rate coefficient (Karickhoff, 1980; Wu and Gschwend, 1986). The model, however, contains now three parameters that cannot be determined independently: the fraction of fast domains, and two rate coefficients that describe the mass transfer in each domain. More than two fitting parameters are usually not preferred, and is one of the reasons why this model is not widely used.

Table 3-3 Nondimensional solute transport equations for four different sorption nonequilibrium models

Film-Diffusion Model			
$\beta R \frac{\partial C^*}{\partial p} + (1 - \beta) R \frac{\partial \bar{C}_f^*}{\partial p} = \frac{1}{P} \frac{\partial^2 C^*}{\partial X^2} - \frac{\partial C^*}{\partial X}$	$\bar{C}_f^* = \int_0^1 C_f^* dY$	$\frac{\partial C_f^*}{\partial p} = \gamma \frac{\partial^2 C_f^*}{\partial Y^2}$	
$C^* = \frac{C}{C_o}$	$\beta = \frac{1 + \rho K / \theta}{R}$	$R = 1 + \frac{\rho K}{\theta}$	$p = \frac{vt}{L}$
$p = \frac{vt}{L}$	$X = \frac{x}{L}$	$Y = \frac{y}{d}$	
Pore-Diffusion Model			
$\beta R \frac{\partial C^*}{\partial p} + (1 - \beta) R \frac{\partial \bar{C}_p^*}{\partial p} = \frac{1}{P} \frac{\partial^2 C^*}{\partial X^2} - \frac{\partial C^*}{\partial X}$	$\bar{C}_p^* = 3 \int_0^1 C_p^* \eta^2 d\eta$	$\frac{\partial C_p^*}{\partial p} = \frac{\gamma}{\eta} \frac{\partial}{\partial \eta} \left( \eta^2 \frac{\partial C_p^*}{\partial \eta} \right)$	
$C^* = \frac{C}{C_o}$	$C_p^* = \frac{C_p}{C_o}$	$R = 1 + \frac{\rho K}{\theta}$	$p = \frac{vt}{L}$
$p = \frac{vt}{L}$	$X = \frac{x}{L}$	$\eta = \frac{r}{a}$	$\theta = \theta_m + \theta_p \sim \theta_m$
	$\gamma = \frac{D_p L}{va^2}$	$\phi = \frac{\theta_m}{\theta}$	

Table 4-3 Continued

Mass-Transfer Model 1 (IOMD)			
$\beta R \frac{\partial C^*}{\partial p} + (1-\beta)R \frac{\partial S^*}{\partial p} - \frac{1}{P} \frac{\partial^2 C^*}{\partial X^2} - \frac{\partial C^*}{\partial X}$	$(1-\beta)R \frac{\partial S^*}{\partial p} - \omega(C^* - S^*)$		
$C^* - \frac{C}{C_o}$	$\beta - \frac{1+F\rho K/\theta}{R}$	$R - 1 + \frac{\rho}{\theta} K$	
$p - \frac{\nu t}{L}$	$X - \frac{x}{L}$	$\omega - \frac{k_f(R-1)L}{\nu}$	
Mass-Transfer Model 2 (RIPD)			
$\beta R \frac{\partial C^*}{\partial p} + (1-\beta)R \frac{\partial C_p^*}{\partial p} - \frac{1}{P} \frac{\partial^2 C^*}{\partial X^2} - \frac{\partial C^*}{\partial X}$	$(1-\beta)R \frac{\partial C_p^*}{\partial p} - \omega(C^* - C_p^*)$		
$C^* - \frac{C}{C_o}$	$C_p^* - \frac{C_p}{C_o}$	$R - 1 + \frac{\rho}{\theta} K$	$p - \frac{\nu t}{L}$
$\beta - \phi \frac{R_m}{R}$	$R_m - 1 + F \frac{\rho}{\theta} K$		
$p - \frac{\nu t}{L}$	$X - \frac{x}{L}$	$\phi - \frac{\theta_m}{\theta}$	$\omega - \frac{k_p L}{\nu \theta}$
		$\theta - \theta_m + \theta_p \sim \theta_m$	

The distinction of two sorption domains was developed from experimental observations and mathematical convenience. One can argue that there must be a continuum of domains with different mass-transfer coefficients. A specific model that describes the continuous distribution of domains and associated rates is the Elovich equation in which the change in sorbed concentration is represented by an exponential function (Travis and Etnier, 1981). The same effect could be created with the diffusion models by making the diffusion coefficient a function of the distance within the sorption domains. Second-order rate models have been developed to describe sorption nonequilibrium for chemical compounds that exhibit nonlinear isotherms (Weber and Miller, 1988).

An effective dispersion coefficient (or Peclet number) can be used to describe weak nonequilibrium conditions. The idea of this approach is that the additional spreading of the breakthrough curve due to nonequilibrium conditions can be described by a larger dispersion coefficient. This model, however, is not useful when the breakthrough curve shows severe asymmetry. The effective dispersion model has been proposed by several authors for physical nonequilibrium (Passioura, 1971; Rao et al., 1980; De Smedt and Wierenga, 1984; Parker and Valocchi, 1986), but could as well be applied to sorption nonequilibrium.

It is not always easy to make a selection between models, especially because most models describe the same process. No standardized protocols exist yet to determine sorption rate coefficients, and therefore, factors such as the objective of the study, and the judgement and experience of the researcher, should lead to the selection of a model.



## Predicting Sorption Rate Coefficients

### Log $k_2$ - Log K Relationship Revisited

Brusseau and Rao (1989b) published an empirical relationship between the logarithms of the reverse first-order mass-transfer rate coefficient ( $k_2$ ) and the equilibrium sorption coefficient (K), based on nonequilibrium sorption data collected from the literature. This relationship provides a useful estimation for the mass-transfer rate coefficient when the equilibrium sorption coefficient is known. In Appendix B nonequilibrium sorption parameters are compiled that include most of the data collected by Brusseau and Rao (1989b), together with data published more recently. Data obtained in cosolvents, or parameters obtained from models other than the bicontinuum model described above, were omitted. The data compiled in Appendix B were obtained from two different experimental techniques: gas-purge and miscible displacement. In comparing the results, it was assumed that both techniques give essentially the same rate parameters, which is supported by the work of Brusseau et al. (1990).

The data in Appendix B are plotted in Figure 3-6, and a log-log inverse linear relation between  $k_2$  and K is evident. A separation was made between high- and low-velocity experiments. The boundary between high- and low-velocities was taken at an arbitrary pore-water velocity of 20 cm/hr. This separation was made because the sorption data for velocities below 20 cm/hr appeared to have significant lower mass-transfer rate coefficients. The regression line and 95% confidence interval shown in Figure 3-6 include the gas-purge and high-velocity data. The data cover a

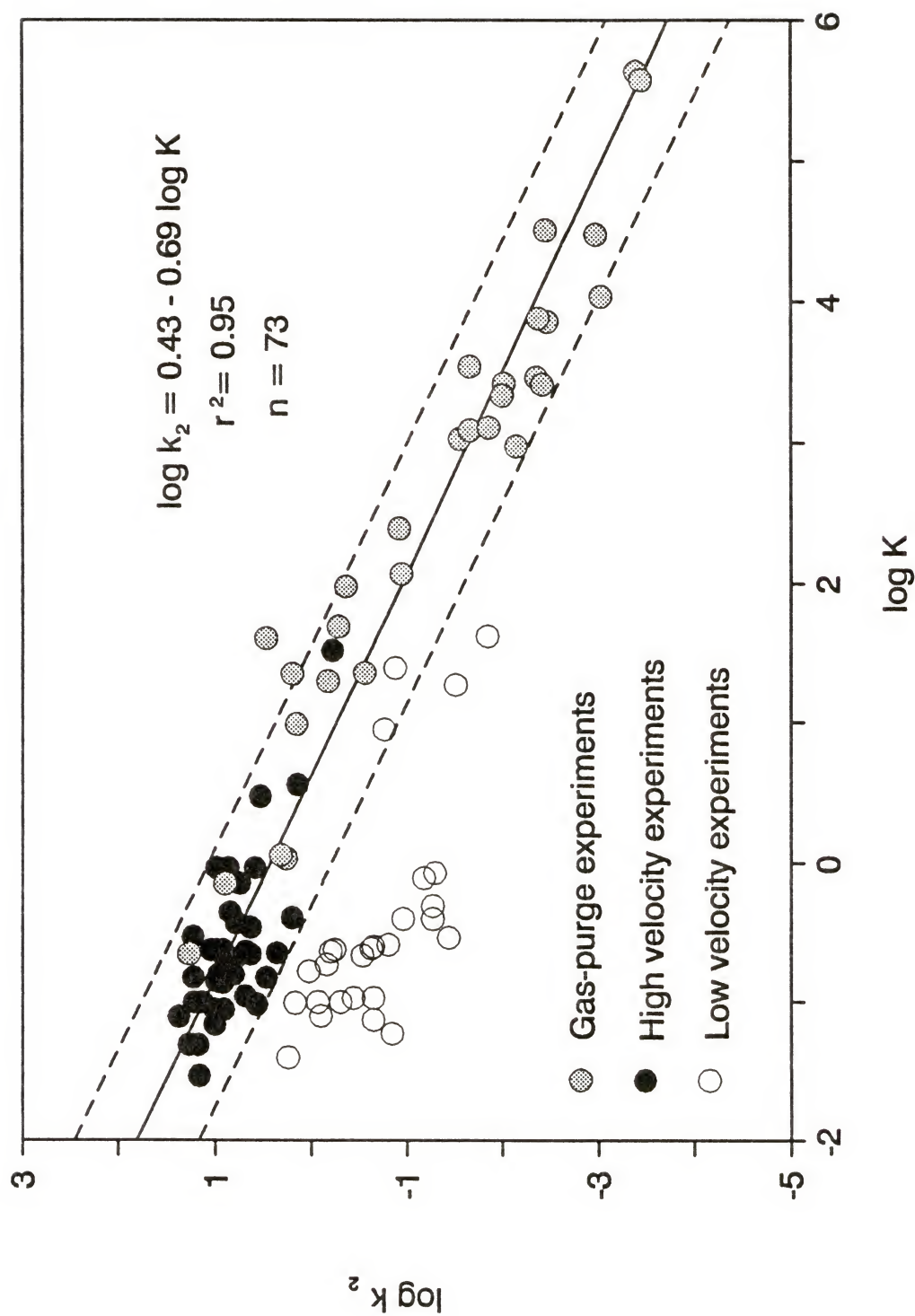


Figure 3-6 Correlation between the reverse first-order, mass-transfer rate coefficient ( $k_2$ ) and equilibrium sorption coefficient ( $K$ ).

variety of chemicals and a number of different soils and sediments ranging in organic carbon fraction.

First-order mass transfer is a simplification of diffusion, by assuming that the concentration in the organic phase is spatially constant. Based on this assumption, and setting Equations 3-8 and 3-21 equal, the following expression can be derived for  $k$ :

$$k = \frac{D_f}{(1-F)d^2} \quad (3-24)$$

From this relationship it is evident that  $k$ , and thus  $k_2$ , is proportional to the diffusion coefficient of the solute in the organic film ( $D_f$ ), and inversely related to the thickness of the organic film ( $d$ ). Note that  $(1-F)d$  represents the characteristic diffusion length through the rate-limited sorption domains. Brusseau et al. (1991a) and Brusseau and Rao (1991) used this formulation to explain the inverse relationship between  $K$  and  $k_2$  for a group of different chemicals in a given soil. They hypothesized that the increasing size of the molecules with increasing  $K$  causes more diffusion constraints and higher potential for molecular entanglement within the matrix of organic matter. The increase in molecular size, however, is very small (see Table 3-2), and considering the flexible nature of organic matter, a dramatic increase in diffusion constraints for a range of compounds is unlikely. An additional explanation for reduced diffusion rates with increasing hydrophobicity of the chemical is the heterogeneous distribution of polar and nonpolar regions in the organic matrix (see Figure 3-2). Hydrophobic organic compounds prefer to stay in the nonpolar

regions. Specific hydrophobic attractions between the organic solute and organic matter may also occur. This results in a pseudo-retardation of the organic compound within the matrix of organic matter. These effects become increasingly important for more-hydrophobic chemicals (i.e., larger  $K$ ), and results in slower diffusion of the solute in the rate-limited domains of organic matter (i.e., smaller  $k_2$ ).

For a single chemical and a range of different soils,  $K$  increases when the amount of organic matter increases. Equation 2-23 showed that  $K$  is directly proportional to the fraction of organic matter. The regression line in Figure 3-6 indicates that  $\log k_2$  decreases 0.6 units for each order-of- magnitude increase in  $K$ . This suggests that, based on Equation 3-24 and constant  $F$ , with a ten-fold increase in the amount of organic matter, the thickness, on the average, increases with a factor of 2. It is surprising that changes in  $K$  due to increased hydrophobicity of the chemical, and increasing amount of organic matter have essentially the same effect on the first-order mass-transfer rate coefficient. There is not yet enough data available to differentiate between the effect of chemicals and soils on the  $\log k_2$  -  $\log K$  plot.

Although the  $\log k_2$  -  $\log K$  relationship has been proven to be useful in predicting mass-transfer rate coefficients, several problems exist with this relationship.

(1) The reverse, first-order, mass-transfer rate coefficient ( $k_2$ ) is not a good representation of the actual mass-transfer rate, since  $k_2$  is also a function of  $F$ . A more appropriate coefficient to describe the mass-transfer process is  $k$ .

(2) The equilibrium sorption coefficient ( $K$ ) is a function of both chemical and soil. To eliminate the effect of different soils,  $K_{oc}$  could be used instead of  $K$ . There



are, of course, problems associated with the concept of  $K_{oc}$  (see Chapter 2), but these are mainly caused by the difficulties in the determination of  $K$ ; hence, the use of  $K_{oc}$  would not introduce much more uncertainty. Another advantage of using  $K_{oc}$  over  $K$  appears when a similar relationship is derived for contaminated soils that contain large amounts of essentially water-insoluble compounds, such as coal tar pitch. The rate at which the thickness increases with the amount of organic matter is determined by the genesis of natural soils. This rate seems to be fairly constant as was shown before. For contaminated soils, however, the distribution of contaminants may be extremely heterogeneous, which could make the  $\log k_2 - \log K$  relationship very different for a chemical or soil. Normalizing to the fraction of organic carbon, eliminates the dependence of soil or organic carbon distribution and makes it easier to compare data for different soils.

(3) From the low-velocity data included in Figure 3-6, it is evident that  $k_2$  values decrease with decreasing flow velocities. This phenomenon was observed by Brusseau (1992) whose data are also included in Figure 3-6. A theoretical evaluation of the dependency of  $k_2$  on the flow rate will be given below.

(4) A decrease in  $k_2$  with increasing  $K$  should not be interpreted as an increase in nonequilibrium conditions for stronger sorbed chemicals. The mass-transfer coefficient  $k_2$ , or better  $k$ , represents the rate of diffusion through the rate-limited domains of organic matter, not the rate of uptake from the solution phase. This will also be discussed below in more detail.

Based on the suggestions made in (1) and (2), Figure 3-7 shows a plot of  $\log K_{oc}$  versus  $\log k$  for the data in Appendix B. Since sorption nonequilibrium in the

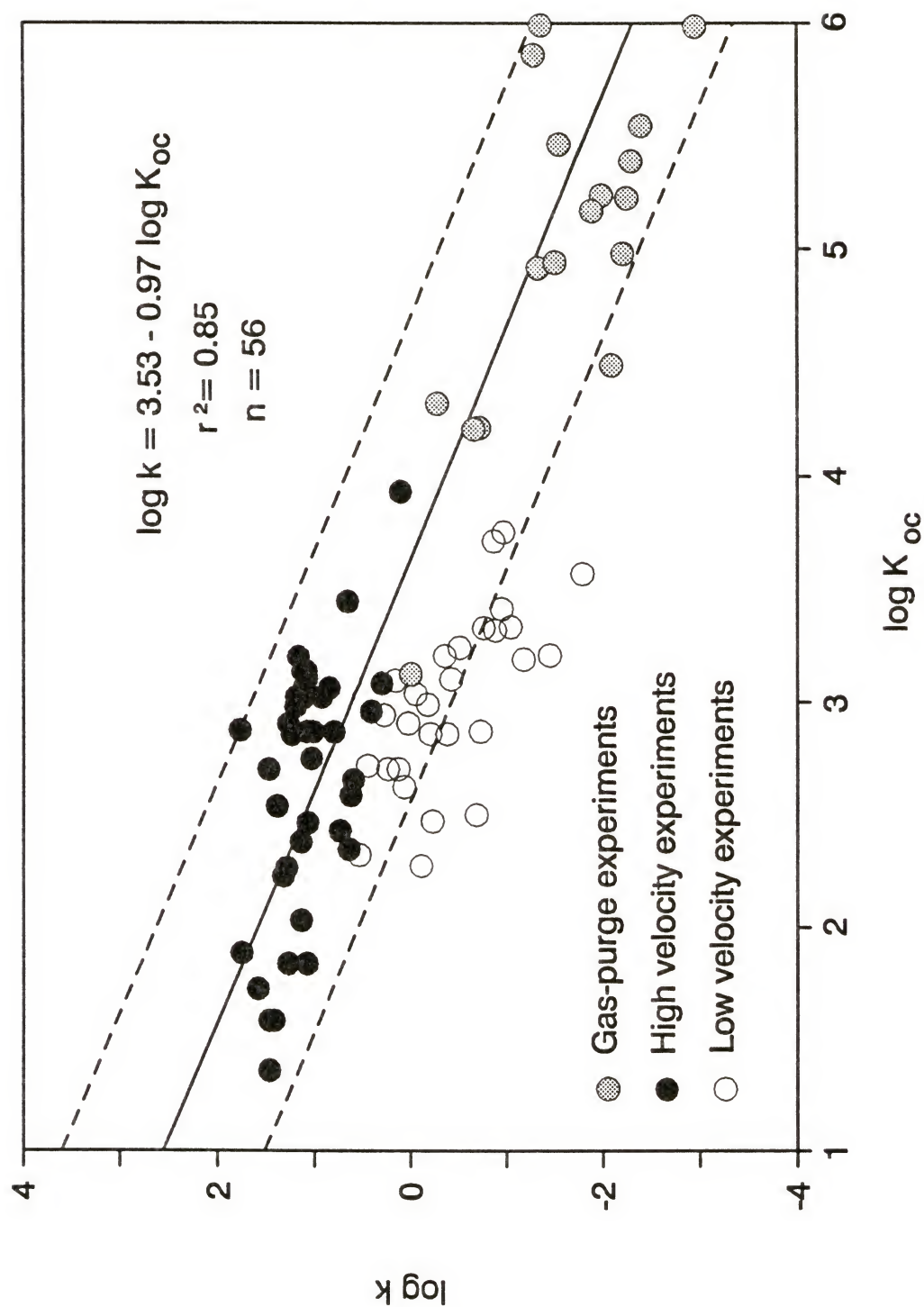


Figure 3-7 Correlation between the first-order, mass-transfer rate coefficient ( $k$ ) and the equilibrium sorption coefficient normalized to the organic carbon fraction ( $K_{oc}$ ).

bicontinuum model is described by the two parameters  $k$  and  $F$ , it is also interesting to know how  $F$  varies with  $K_{oc}$ . Note that  $F$  is defined as the volume fraction of instantaneous sorption domains, or:

$$F = \frac{V_1}{V_1 + V_2} \quad (3-25)$$

where  $V_1$  and  $V_2$  are the volume of instantaneous and rate-limited domains in the sorbent, respectively.

Brusseau et al. (1991a) found an increase in  $F$  with increasing sorption, and hypothesized that for larger molecules (more sorptive) the rate-limited domains are less accessible, causing a decrease in  $V_2$  and therefore an increase in  $F$ . They assumed that  $V_1$  remains essentially constant over a range of different chemicals. Other data sets, however, show an inverse relationship between  $F$  and  $K_{oc}$ . This could be explained by assuming that the total volume in the sorbed phase ( $V_1 + V_2$ ) is constant, but that the volume of instantaneous sorption domains ( $V_1$ ) becomes smaller for larger molecules due to increasing diffusion constraints. Figure 3-8 is a compilation of  $F$  values for different chemicals and soils, and shows no apparent relationship. Values for  $F$  varied between 0 (only rate-limited domains) and 0.77. Historically, a value of 0.5 was considered to be a reasonable first estimation for  $F$ . The average value for  $F$  for the data presented in Figure 3-8 was 0.40 with a standard deviation of 0.18. This supports the assumption that a value of 0.5 is a reasonable first approximation for  $F$ , when no specific data are available.

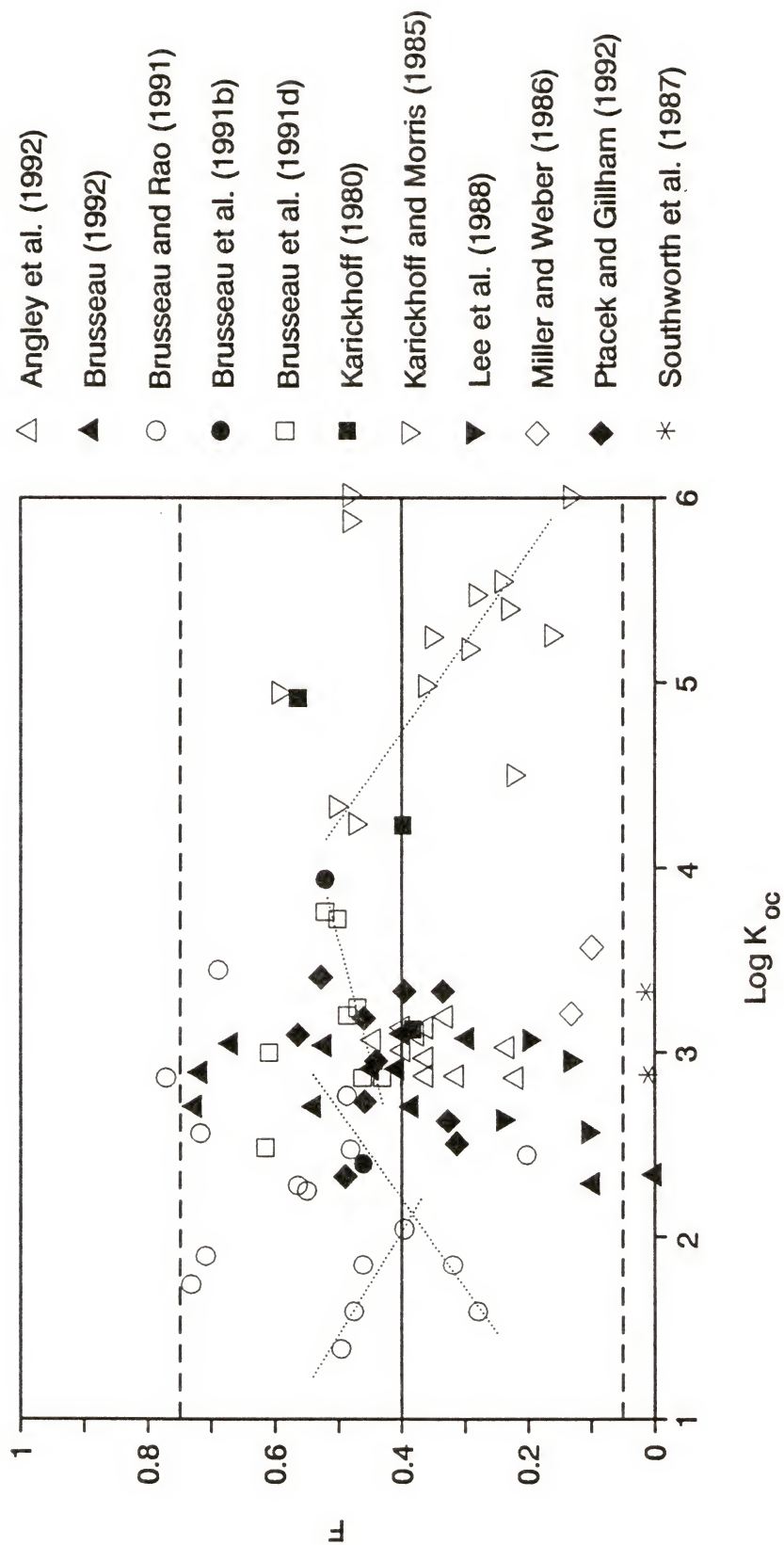


Figure 3-8 Correlation between the fraction of instantaneous sorption (F) and the equilibrium sorption coefficient normalized to the organic carbon fraction ( $K_{oc}$ ).



### Dependency of $k_2$ on Other Model Parameters

The velocity-dependence of the first-order, mass-transfer rate coefficient found by Brusseau (1992), is something commonly observed for mass-transfer models. A velocity-dependence of the first-order, mass-transfer rate coefficient ( $\alpha$ ) between mobile and immobile water was also observed by Van Genuchten and Wierenga (1977) and Nkedi-Kizza et al. (1984). From theoretical analyses for a batch system, Rao et al. (1980) found that  $\alpha$  decreased with contact time, and suggested that therefore  $\alpha$  is expected to decrease with decreasing pore-water velocities. Similar to the approach by Rao et al. (1980), the velocity dependence of  $k_2$  can be derived from comparing the film-diffusion model with the mass-transfer model.

By setting Equations 3-8 and 3-21 equal, the following expression for the first-order, mass-transfer rate coefficient can be derived:

$$k_2 = \frac{\partial \bar{C}_f / \partial t}{(K' C - \bar{C}_f)} \quad (3-26)$$

or, stated in nondimensional parameters:

$$k_2^* = \frac{\partial \bar{C}_f^* / \partial \tau}{(C^* - \bar{C}_f^*)} \quad (3-27)$$

where

$$k_2^* = \frac{k_2 d^2}{D_f} \quad (3-28)$$

$$\tau = \frac{D_f t}{d^2} \quad (3-29)$$

and all other parameters are as defined in Table 3-3.

A numerical model was developed for a continuous-stirred tank reactor (CSTR) in which sorption was described by the film-diffusion model. To test the model, the numerical solution for  $F=0$ , and no flow was compared with the analytical solution given by Crank (1975) and showed very good agreement. For every time step  $k_2^*$  was calculated from Equation 3-27. The results of the simulations are shown in Figure 3-9. These figures show the dependency of  $k_2^*$  on time, retardation factor ( $R$ ), dimensionless flow rate ( $T=qL^2/D_f V_w$ ; where  $q$  is the flow rate (ml/hr) and  $V_w$  is the volume of water in the CSTR (ml)), and fraction of instantaneous sorption domains ( $F$ ). Note that the solid line in each graph represents the same simulation. The end of each curve corresponds with the time at which equilibrium was reached. This shows that for a given diffusion coefficient ( $D_f$ ), and thickness of the film ( $d$ ), equilibrium is reached faster when the retardation factor is larger, and when the flow rate is higher.

For a given soil,  $D_f$  most likely decreases with increasing  $R$ , but for a given soil and chemical all parameters stay constant and the time to reach equilibrium conditions is truly shorter for higher flow velocities. This may have consequences for the remediation technology. When removing contaminants from a subsurface system, faster flow rates decrease the contaminant concentrations and reduces the actual time period required to remove the complete contaminant mass.

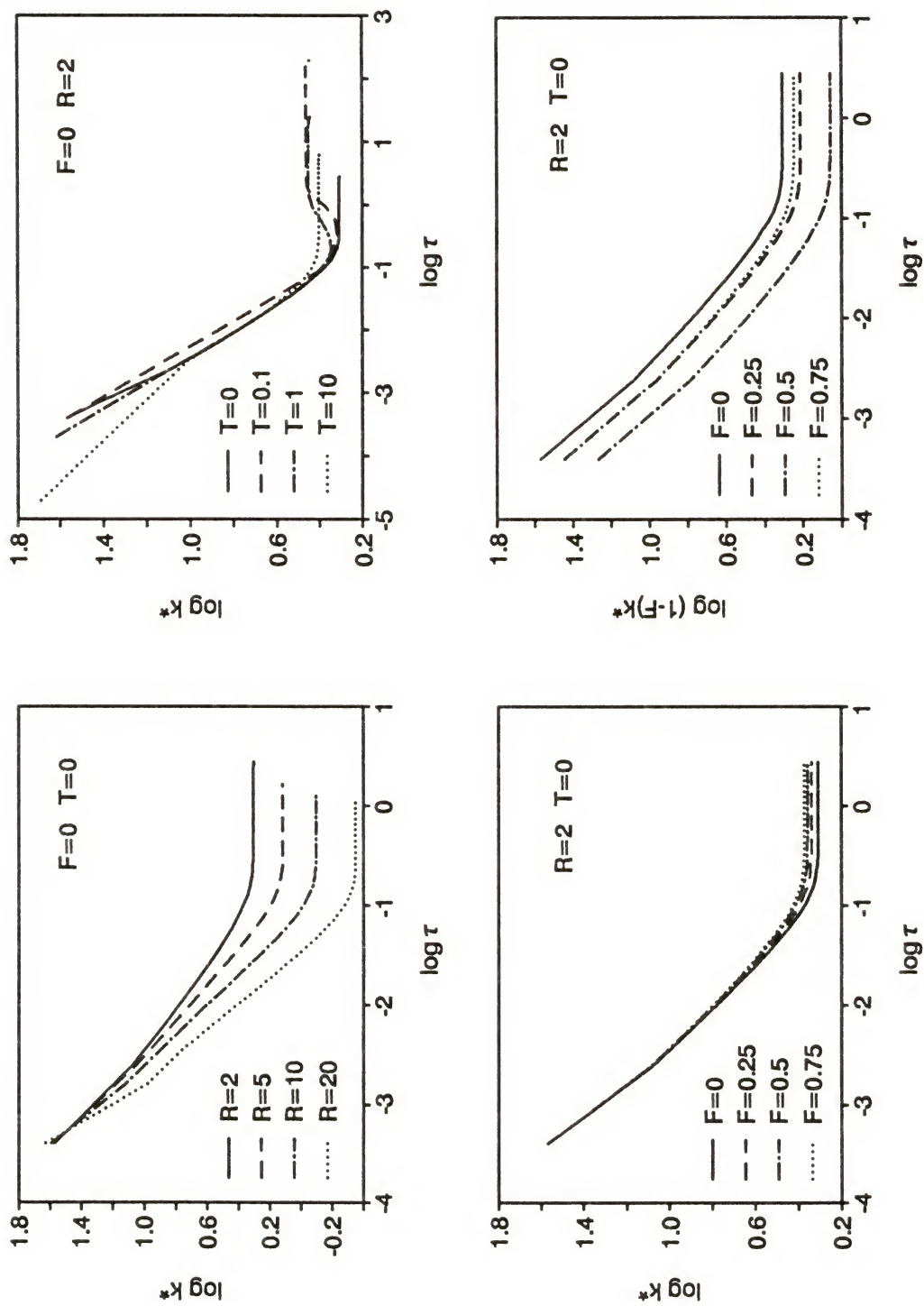


Figure 3-9 The dependence of the first-order mass transfer rate coefficient on the retardation factor ( $R$ ), flowrate ( $T$ ), and fraction of instantaneous sorption ( $F$ ).

The mass-transfer coefficient is best approached by a time-averaged value (Rao et al., 1980):

$$\bar{k}_2^* = \frac{1}{T} \int_0^T k_2^* d\tau \quad (3-30)$$

This time-averaged value for  $k_2^*$  decreases with increasing retardation factor, and decreasing fraction of instantaneous sorption domains. Since  $k_2^*$  itself is a function of  $F$ , Figure 3-9 also shows the dependence of  $k^*$  ( $= (1-F)k_2^*$ ) on  $F$ . This graph shows that  $\bar{k}^*$  first decreases with increasing  $F$  up to a minimum at  $F=0.5$ , and then increases with a further increase in  $F$ . The variation of  $k_2$  with velocity depends on the time scale over which the average of  $k_2$  is obtained. When, the entire time scale is taken, the average value for  $k_2^*$  increases slightly with decreasing flow rate. This is contradictory to the findings described before.

A possible explanations for the observed decrease in  $k_2$  with decreasing flow rates could be the increased importance of the stagnant boundary layer at lower velocities. The resistance of this boundary layer to diffusion of solute is less significant when the resistance associated with IOMD increases. This is consistent with the data in Figure 3-6, where the low-velocity data approaches the regression line at higher values of  $\log K$ . It also explains the fact that the gas-purge data, where presumably no stagnant boundary layer is present due to complete mixing, agreed well with the high-velocity data. However, normalizing the data to the fraction of organic carbon, eliminates much of the velocity effect (Figure 3-7), indicating that the small mass-transfer coefficients observed can partially be explained by the distribution of organic matter in these soils (i.e., thicker films or patches).



The dependency of  $k_2$  on various parameters is inherent to the assumption made in the mass-transfer model that the concentration profile in the rate-limited domains can be approximated by an average concentration. Although mass-transfer models are convenient in describing sorption nonequilibrium, one should be cautious when interpreting certain relationships between parameters, since they may be partially due to incorrect assumptions in the model. The film-diffusion may be considered as physically more correct, but it should be recognized that this model also is an approximation of a process that is not completely understood.

#### Degree of Nonequilibrium

Nonequilibrium conditions in column experiments are manifested in early breakthrough, asymmetry of the breakthrough curve, and extensive tailing. These features are more pronounced as the degree of nonequilibrium increases. The degree of nonequilibrium is described by the parameters  $\beta$  and  $\omega$  in the bicontinuum mass-transfer model (see Table 3-3). In this model,  $\beta$  represents the fractional retardation caused by the instantaneous sorption domains, and  $\omega$  is the Damkohler number. In general, lower values for  $\beta$  shift the breakthrough curve to the left, and lower values for  $\omega$  increase the asymmetry and tailing of the breakthrough curve. Note that the theoretical minimum value for  $\beta$  is  $1/R$ , and the maximum is 1, while  $\omega$  values range from 0 to  $\infty$ . Any given combination of  $\beta$  and  $\omega$  results in the same degree of nonequilibrium, independent of  $R$ .

The degree of nonequilibrium ( $\mu$ ) will be defined here as the ratio of the pore volumes required to reach  $C^* = 1$  (or  $C^* = 0$  for desorption) under nonequilibrium and

equilibrium conditions, respectively. If the degree of nonequilibrium is known, the total clean-up time in pore volumes required to remove the contaminant completely is equal to  $\mu R$ . Figure 3-10 shows the degree of nonequilibrium for different combinations of model parameters. All graphs give a perfect log-log inverse linear relationship between  $R$  and  $kL/v$ , and a nearly perfect log-log inverse linear relationship between  $(R-1)$  and  $kL/v$ . The slope for the relationship between  $\log(R-1)$  and  $\log kL/v$  for all lines is fairly constant, and has an average of approximately -0.75, which is close to the slope of the regression line in Figure 3-6. This indicates that all data in Figure 3-6 exhibits more or less the same degree of nonequilibrium. This is surprising because it suggests that there may be a unique degree of nonequilibrium associated with natural sorbents. The scatter in data is caused by differences in Peclet number, fractions of instantaneous sorption domains, and flow velocities. This is consistent with the data from Brusseau (1992), who found that the degree of nonequilibrium was almost the same for experiments performed at velocities that varied more than an order of magnitude. On the other hand, this conclusion seems very unrealistic, since it suggests that equilibrium conditions can never be reached. More research is necessary to resolve this issue.

The theoretical decrease in  $kL/v$  with increasing  $R$  results from defining the mass-transfer rate on a basis of sorbed-phase concentrations (Equation 3-21). The uptake of a strongly sorbed chemical by the solid phase is more rapid than for weakly sorbed chemicals (Crank, 1975), thus, to maintain the same degree of nonequilibrium the diffusion through the sorbed phase must be slower. The first-order, mass-transfer rate coefficient is therefore not a good representation of the sorption rate.

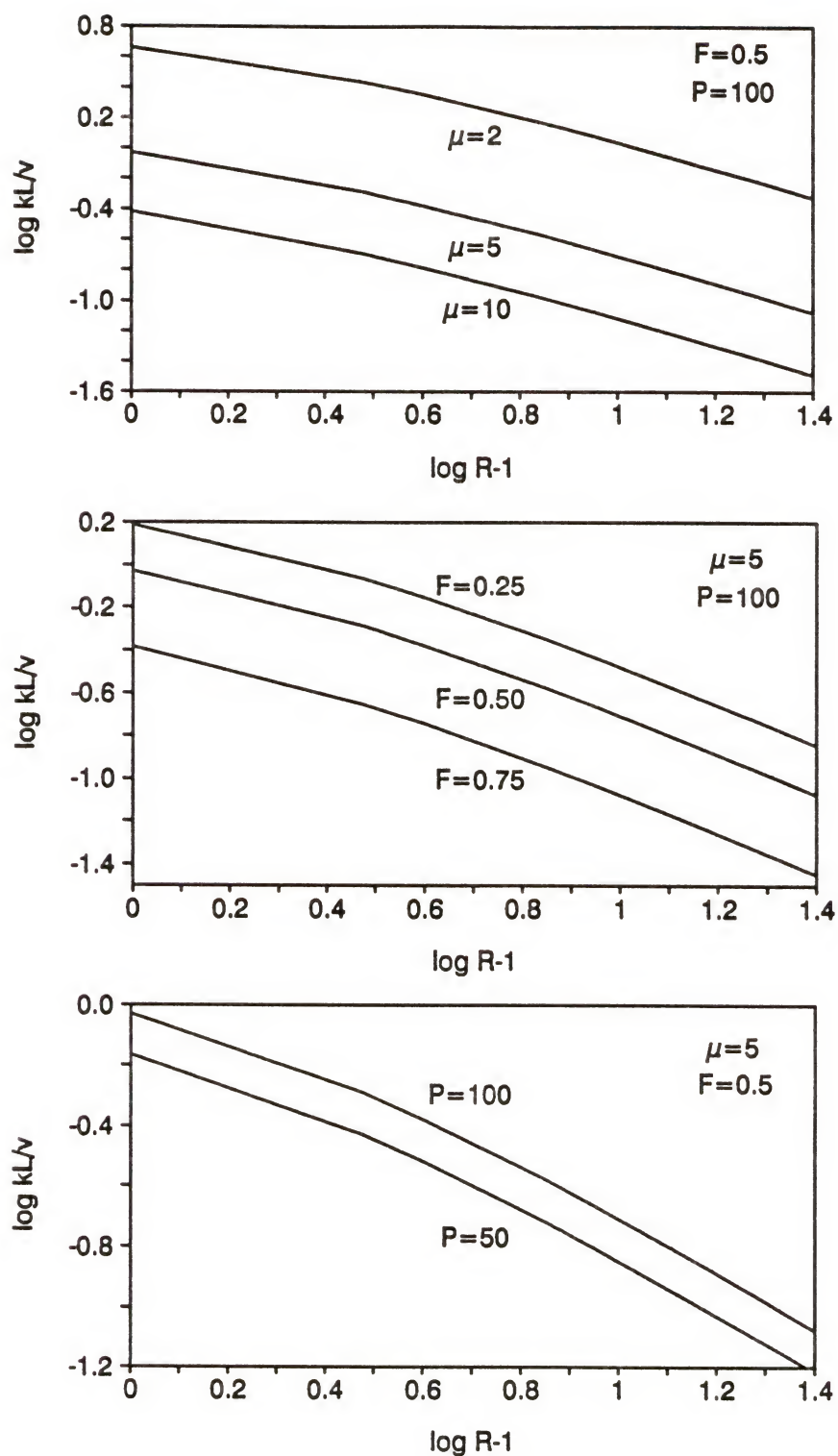


Figure 3-10 Representation of the degree of nonequilibrium ( $\mu$ ) as a function of the Damkohler number ( $kL/v$ ), retardation factor ( $R$ ), fraction of instantaneous sorption ( $F$ ), and Peclet number ( $P$ ).

Experiments for future study would be to investigate the  $k_2$ -K relationship for a single compound on a variety of different soils, varying over a wide range of organic matter contents. Furthermore, experiments should be designed to study the value of  $k_2$  for one compound on several different dilutions of the same soil. More experimental data should be collected for sorption nonequilibrium data under a standardized protocol, and investigate the degree of nonequilibrium as a function of different chemicals, soils, and velocities.

### Mass Transfer Rates in Contaminated Soils

#### Sorption onto Different Types of Sorbents

The data compiled in Figures 3-6 through 3-8, are for natural soils, sediments, and aquifer materials. In contaminated soils, sorption characteristics may be altered by the presence of an OIL phase or high concentrations of contaminants. The OIL may be absorbed by the soil matrix, and form an additional hydrophobic domain in which chemical can partition. Over time, interactions between the OIL and solid matrix, oxidation, and polymerization (ageing) may transform the residues of the OIL into a material that cannot be separated or distinguished from natural organic matter. The presence of an OIL creates a higher sorption capacity for the soil. Bouchard et al. (1989), for example, found that the equilibrium sorption constant had increased dramatically after gasoline was added to a soil. Sun and Boyd (1991) also observed an increase in K for soils that contained residues of polychlorobiphenyls. They found that the overall sorption capacity was proportional to the sorption onto



each phase. Desorption rates from soils containing aged residuals of OILs are important for the long term elution rates from these soils. As is discussed in Chapter 2, the difference between dissolution and desorption is rather vague when dealing with multicomponent systems; therefore, dissolution rates can be considered the same as desorption rates.

In this section sorption nonequilibrium will be studied on three different contaminated soils: (1) Eustis fine sand treated with decane (ED); (2) an aged contaminated soil with tar-derived constituents (KD-5); and (3) a tar-contaminated soil (UT#578).

### Experimental Procedure

The miscible displacement technique (Lee et al., 1988; Brusseau et al., 1990) was used for all experiments. This technique involves the displacement of a solution through a column packed with the material of interest. The columns used in this study were made of glass (Kontes) with a diameter of 2.5 cm and a length of 5.5 cm (total volume, 27 ml). The column had Teflon endplate fittings that were held in place by screw caps. The shafts in the fittings were funnel-shaped to obtain a smooth transition of flow from the narrow tubing to the larger column or vice versa. In the void space of the shaft, a Teflon mesh was placed to support a glass fiber filter (Gelman) that was secured with a Teflon O-ring. The inlet of the column was hooked up to a switching valve, and connected to two piston pumps (Gilson models 302 and 305) by Teflon tubing with an inner diameter of 1 mm. One of the pumps was used for the 0.01 N  $\text{CaCl}_2$  solution, and the other for the tracer. The outlet of

the column was connected to a flow-through UV detector (Gilson Holochrome), which was attached to a strip-chart recorder (Omniscribe D5000). All components of the column apparatus that came in contact with the solutions were glass, stainless steel or Teflon, in order to minimize sorption to materials other than the column packing.

When packing the columns, the soil was poured in the column in increments small enough to pack about 0.5 to 1 cm. For each increment the soil was stirred, to obtain a homogeneous mixture, tapped to settle the soil and tamped to compact the soil. Before a new increment of soil was added, the surface of the previous layer was disturbed to avoid layering, which could affect the hydrodynamic conditions of the packed material. After the soil was packed, the column was slowly saturated for at least 24 hours in a vertical position from bottom to top with a with helium degassed 0.01 N  $\text{CaCl}_2$  solution. After this period of slow saturation, the flow rate was increased for about 15 minutes to a rate presumably higher than the saturated hydraulic conductivity, in order to remove the final entrapped air. The weight of the column was recorded before and after saturation to obtain pore volume, dead volume, bulk density, and water content of the soil.

Once the soil was saturated, the column was placed in a horizontal position to avoid density-driven flow patterns. At time zero, the switching valve at the column inlet was switched from the background electrolyte solution to the solution containing the tracer. All solutions were made in the same electrolyte solution of 0.01 N  $\text{CaCl}_2$ . This electrolyte solution was used to prevent possible dispersion of clay.

The effluent concentration was continuously monitored by the UV detector and recorded on chart paper. The UV response of the tracer solution was established prior to the experiment by-passing the column. This response represented the input concentration ( $C_0$ ) and was later used to normalize the data. At some point in time, the influent solution was switched back to the 0.01 N  $\text{CaCl}_2$  to allow desorption of the tracer from the soil. This was usually done when the effluent concentration was equal to the influent concentration. For highly sorptive compounds or materials, the influent solution was switched back before this point was reached. Effluent samples were collected periodically to confirm the concentrations by analyses on the HPLC. In almost all cases, the UV response agreed reasonably well with measurements on the HPLC. In cases where a significant difference was observed between the two techniques, the HPLC data were judged to be more reliable, and used to calculate the final breakthrough curves. For the Eustis and decane-treated soil, the anion pentafluorobenzoic acid (PFBA) was used as a nonreactive tracer to determine the hydrodynamic dispersion. For the MGP soils, tritium ( $^3\text{H}_2\text{O}$ ) was used as the nonreactive tracer. For PFBA, the flow-through UV detector was used to monitor the breakthrough curve, and for tritium effluent samples were collected frequently and analyzed on the scintillation counter.

#### Preparation of the Soils

(1) For the decane-treated Eustis fine sand, 60 g of air-dried Eustis soil (fraction < 2 mm) was mixed with 0.37 g or approximately 0.5 ml of decane ( $\rho_{\text{dec}} = 0.72 \text{ g/cm}^3$ ). Decane was chosen as a model for an OIL with limited solubility



( $S^w = 0.009$  mg/l; Verschueren, 1983). Immediately after the decane was added the soil was mixed thoroughly to assure a homogeneous distribution of decane over the soil. Visually, the Eustis soil was able to absorb the decane completely, because after a few moments the soil appeared dry again, having a slightly darker color than the original soil. The soil was then quickly packed in a column as described before, and saturated, to avoid loss of decane by volatilization. No decane could be detected in the effluent. For comparison, experiments with untreated Eustis soil were also performed.

(2) The soil contaminated with tar-derived constituents was obtained from the Electric Power Research Institute (EPRI). This soil was one of total five samples collected along a transect covering a contaminant plume originating from a tar disposal area at a manufactured gas-plant (MGP) site. The first sample was low in organic carbon and represented uncontaminated aquifer material (KD-1). The last sample (KD-5) was collected near the source and was much higher in organic carbon content (1.4%). The enrichment in organic carbon was probably from tar-derived compounds that had aged for many years. The KD-5 soil would therefore be a good representation for an aged contaminated soil. Because of the relative high organic carbon content retardation factors, even for small compounds such as benzene, were expected to be high. Large retardation factors require long experimental times, and enhances the difficulties in resolving the tails of the breakthrough curves.

There are two ways to reduce the sorption capacity of a soil: (1) using cosolvents, and (2) by "dilution" of the soil with an inert material like builder's sand.



For the KD-5 soil was chosen to use a 33% methanol/ 66% water solution (by volume) to obtain nonequilibrium sorption data. Addition of a cosolvent, like methanol, reduces sorption and increases sorption rates, as will be discussed in more detail in Chapter 4, and is therefore a convenient method to obtain nonequilibrium sorption data for compounds or soils with large retardation factors. The data obtained from these experiments do not reflect the actual sorption parameters in aqueous systems, but according to Brusseau et al. (1991b) the use of cosolvents shifts the data in the upper-left direction along the regression line in Figure 3-6, indicating that the absolute values may be different, but that the mass-transfer rates are comparable to values obtained in aqueous systems. This is furthermore supported by the fact that Brusseau and Rao (1989b) also included nonequilibrium sorption data obtained with cosolvents in their compilation of data that was used to derive the empirical relationship between  $\log k_2$  and  $\log K$ .

(3) The soil contaminated with coal tar was obtained from the University of Texas, Austin and provided by EPRI. The soil was very dark (black) and had a strong smell. Oily films floated on top of the wet sample. Remnants of purifier box wastes were also found. The soil was wet-sieved through a 2.8 mm sieve. The extremely large retardation factors that would result from the high tar content, makes column experiments very impractical. To reduce the sorption capacity of the tar soil, 25 grams of the sieved material was mixed with 50 grams of a builder's sand ( $< 1$  mm) that was free of organic carbon. The fraction of organic carbon of the sand and tar soil mixture, determined by total combustion, was 14%.

The mixture was then packed in a column, and flushed with 100% methanol to remove the most soluble compounds from the tar. This was done to be able to study the sorption and desorption behavior of a single constituent in the tar soil, without interference of other eluting chemicals. Since 40 to 60% of coal tar consists of essentially insoluble compounds (EPRI, 1993), referred here to as the "pitch", it was assumed that diffusion through the pitch determined the overall release rate, and that the removal of other, more-soluble constituents had little effect on the release rates. While flushing the column with methanol, effluent samples were collected periodically and analyzed on the HPLC. After pumping more than 3 liters of methanol through the column, and several flow interruptions, no significant concentrations for any of the tar constituents could be detected in the effluent. The column was then saturated with an aqueous 0.01 N  $\text{CaCl}_2$  solution, and breakthrough curves for benzene and toluene were obtained. Preliminary experiments with this soil, showed very strong nonequilibrium conditions.

To enable better resolution of nonequilibrium, the flow interruption technique (Brusseau et al., 1989) was used. A flow interruption allows the solution to come in equilibrium with the soil matrix, resulting in a drop in concentration for the frontal portion of the breakthrough curve, and a rise in concentration at the distal portion. The drop or rise in concentration provides an additional degree of freedom when fitting the data, and provides a more unique fit under very strong nonequilibrium conditions.

Batch sorption isotherms and time studies were also performed. For these batch studies approximately 0.7 gram of the sand/tar soil mixture was weighted in 4.5

ml amber vials. The vials were then filled to the top with a 0.01 N  $\text{CaCl}_2$  solution containing approximately 120/40, 96/32, 60/30, or 30/10 mg/l benzene/toluene. The highest concentration for each compound was below 10% of the aqueous solubility. The vials were immediately capped after the solution was added to avoid losses by volatilization. It was assumed that no competitive or cooperative sorption between benzene and toluene occurred. All experiments were done in duplicate, and a blank containing no soil and receiving the same treatment, was used to calculate the initial concentration. The samples for the sorption isotherm were allowed to equilibrate for 170 hours ( $\approx$  1 week). After the equilibration period, the samples were centrifuged (approximately 2500 rpm) and directly analyzed by HPLC. For the kinetic study, only the 120/40 mg/L solution was used. The samples were subjected to various equilibration times, before they were centrifuged and analyzed.

### Data Analyses

The charts that recorded the response of UV detector, were digitized manually. In the order of 20 data points were used to describe the entire breakthrough curve. The breakthrough curves for the nonreactive tracers for each column was fitted with an equilibrium model and  $R=1$  to obtain a Peclet number. Fitting was done using the program CFITIM3, a predecessor of the CXTFIT model by Parker and Van Genuchten (1984). Retardation factors were obtained from the area above the frontal portion of the breakthrough curve (Nkedi-Kizza et al., 1987), or subtracting half the pulse size from the first moment of the breakthrough curve (Valocchi, 1985). The area above the curve can only be determined when the



relative concentration goes to 1. The technique of moment analyses can only be applied when the total mass is recovered. In cases where the experiment was terminated before the distal portion of the curve had reached the baseline, the tail could be extrapolated to account for the missing mass, and to be able to perform moment analyses. This manipulation, however, can be very erroneous, and should be used with caution. The retardation factor for benzene and toluene in the tar soil were calculated from the equilibrium sorption coefficient determined in the batch study.

The first-order bicontinuum model was used to fit all nonequilibrium data. The film-diffusion model was also used to fit the breakthrough curves for the tar-contaminated soil. Values for  $\beta$  and  $\omega$  were obtained by fitting the data with the CFITIM3 model. A separate model was developed by Brusseau et al. (1989) to fit the flow interruption data. When fitting the data, Values for P, R, and the pulse size were fixed, while only  $\beta$  and  $\omega$  were varied to obtain the minimum sum of squared differences between the model prediction and experimental data. Fitting two parameters simultaneously is considered the maximum to preserve the uniqueness of the fit. Fitting more than two parameters makes the data less reliable, i.e., other combinations of parameter values may give an equally good fit.

### Results and Discussion

The results of all experiments including the 95% confidence intervals are compiled in Table 3-4. The Peclet number for the decane-treated Eustis soil was lower than for the untreated Eustis soil. A lower Peclet number means a higher



Table 3-4 Summary of estimated transport parameter for the four different sorbents studied.

Sorbent	compound	P	R	K	K <sub>oc</sub>	$\beta$	$\omega$	F	k <sub>2</sub> (hr <sup>-1</sup> )	k (hr <sup>-1</sup> )
EUS	PFBA	84.2 (75.2-93.3)	1							
EUS	Benzene	84	1.22	0.04	11	0.94 (0.93-0.95)	0.16 (0.093-0.22)	0.65 (0.60-0.71)	27.3 (14.2-45.6)	78.3 (35.7-155)
EUS	Toluene	84	1.42	0.08	20	0.89 (0.88-0.90)	0.36 (0.25-0.47)	0.63 (0.58-0.67)	30.6 (18.9-45.5)	81.8 (45.1-139)
EUS	PCE	84	2.96	0.3	95	0.77 (0.75-0.79)	0.77 (0.62-0.93)	0.65 (0.62-0.69)	15.4 (11.3-20.3)	44.5 (30.1-64.7)
EUS	Naphthalene	84	5.69	0.88	227	0.70 (0.67-0.72)	1.32 (1.12-1.52)	0.63 (0.60-0.65)	10.2 (8.1-12.6)	27.6 (20.6-36.5)
ED	PFBA	39.4 (31.8-47.0)	1							
ED	Benzene	39	8.55	1.39	155	0.73 (0.71-0.74)	1.91 (1.70-2.12)	0.69 (0.67-0.71)	11.7 (9.9-13.7)	38.0 (30.4-46.8)
ED	TCE	39	16.8	2.92	324	0.91 (0.87-0.94)	0.91 (0.87-0.94)	0.90 (0.86-0.94)	8.4 (5.8-14.1)	85.1 (42.6-233)
KD5	<sup>3</sup> H <sub>2</sub> O	84.6 (78.7-90.5)	1							
KD5	Benzene	85	1.59	0.13	11	0.65 (0.62-0.68)	1.01 (0.76-1.27)	0.07 (-0.01-0.15)	10.7 (7.3-14.7)	11.5 (7.2-17.3)
KD5	Toluene	85	2.94	0.42	37	0.48 (0.42-0.54)	0.93 (0.60-1.27)	0.21 (0.11-0.30)	3.5 (2.0-5.4)	4.5 (2.3-7.7)
KD5	p-Xylene	85	6.44	1.17	103	0.36 (0.33-0.39)	0.66 (0.51-0.81)	0.24 (0.21-0.27)	0.93 (0.69-1.2)	1.2 (0.86-1.6)
KD5	Naphthalene	85	9.74	1.89	165	0.48 (0.45-0.51)	1.29 (1.10-1.47)	0.42 (0.39-0.46)	1.5 (1.2-1.8)	2.6 (2.0-3.3)
UTS78	<sup>3</sup> H <sub>2</sub> O	32.8 (28.6-37.0)	1							
UTS78	Benzene	33	11.6	2.9	21			0.12	0.015	0.02
UTS78	Toluene	33	19.9	5.2	37			0.16	0.015	0.02

dispersion coefficient. The decane-treated soil was slightly moist with decane when packed, this may have had impact on the packing. Not surprisingly, the most heterogeneous soil (UT#578), had the lowest Peclet number.

Figure 3-11 depicts the nonequilibrium sorption parameters for all soils on top of the  $\log k$ - $\log K_{oc}$  plot. The objective of this study was not to obtain specific sorption parameters for different type of sorbents, but to get a general impression of the mass-transfer limitations that can be expected in contaminated soils. From Figure 3-11 it is evident that the decane-treated soil behaved similar to natural sorbents, while the tar-contaminated soils exhibited much smaller mass-transfer rate coefficients.

Addition of the decane increased the total sorption capacity of the soil. When decane was added to the Eustis soil, the soil completely absorbed the decane. The decane was probably immediately incorporated in the organic matter of the soil. Most organic solvents cause a swelling of organic matter, making the organic matter more open. On the other hand, the relatively long molecules of decane may block some of these newly created voids. Increasing  $K$  by addition of decane would shift the data points in Figure 3-11 to the right. The fact that the data for the decane-treated Eustis soil still falls close to the regression line, suggests that the decane has reduced the net mass-transfer rate through the rate-limited domains of organic matter.

Both tar-related contaminated soils show mass-transfer rates lower than observed for natural sorbents. The mass-transfer rate coefficient for the tar soil is

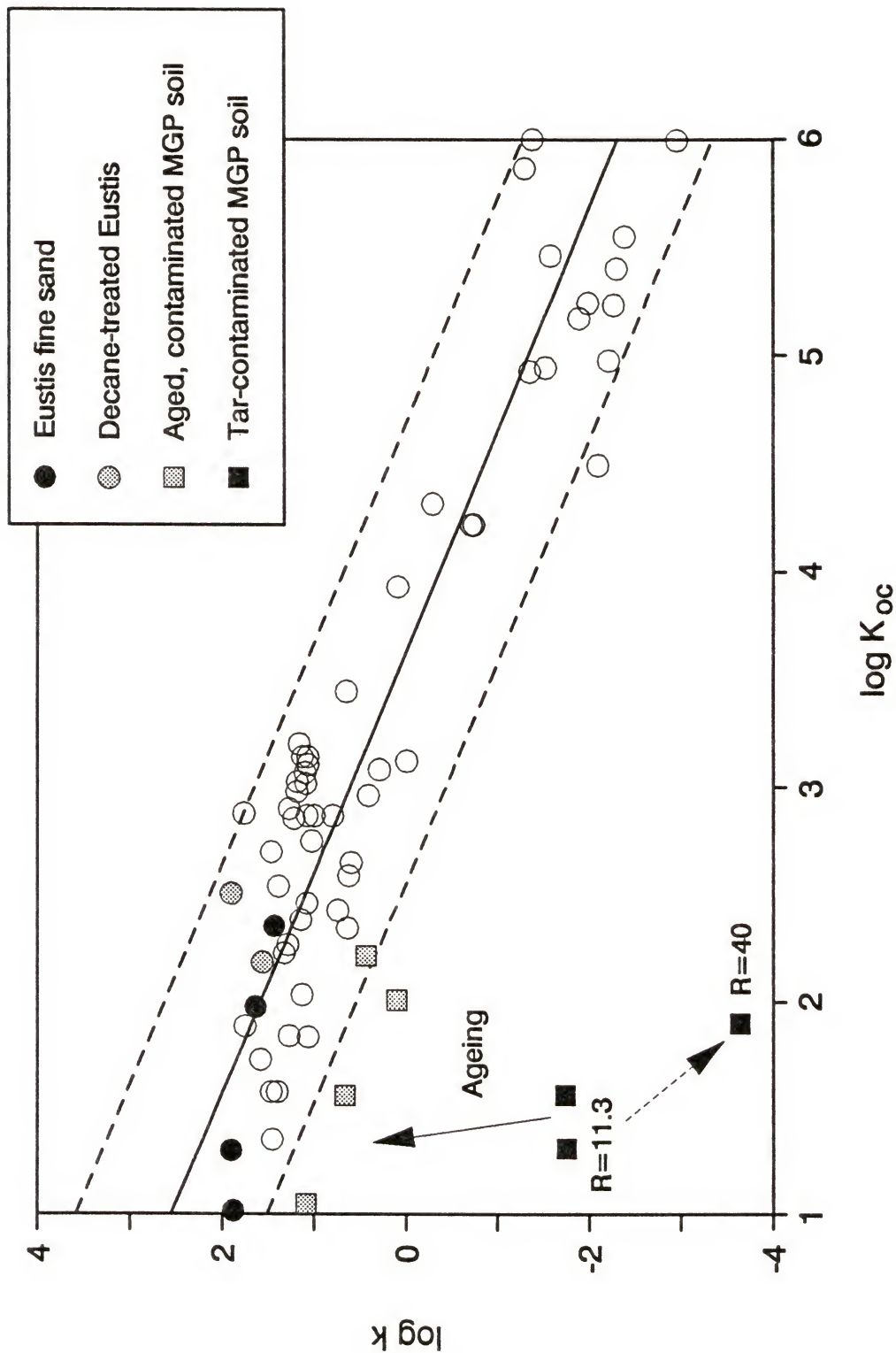


Figure 3-11 Comparison of the mass-transfer rates found for three types of contaminated soils with the rate coefficients reported for natural systems (see Figure 4-7).

approximately an order of magnitude lower than the regression line for natural sorbents. The rate coefficient for the aged soil (KD-5), however, is much closer to this regression line. It is hypothesized that with ageing the tar residues slowly degrade, oxidize and polymerize. This process reduces the amount of organic matter and makes the organic phase more open and polar. This results in a smaller  $K$  and larger rate coefficients, indicated by the solid arrow, and eventually the contaminated soils may approach a behavior similar to natural soils.

Figure 3-12 shows a breakthrough curve for benzene in the tar-contaminated soil/sand mixture. This breakthrough curve displays all features that point towards strong nonequilibrium conditions: an early breakthrough (after about one pore volume benzene already appears in the effluent); asymmetry; tailing (the breakthrough curve levels off at a plateau below  $C^* = 1$ ); and a significant drop in concentration after the flow was interrupted for approximately 12 hours. The bicontinuum mass-transfer model was not able to describe the breakthrough curve very accurately. The fit was not obtained by optimization (least squares method), but by manual trial and error to obtain an overall better agreement with the breakthrough curve. By fitting the breakthrough curve manually, focus was on fitting the plateau level and drop in concentration from the flow interruption more closely than the curvature of the frontal and distal portion of the curve. The film-diffusion model was also used to fit the experimental data, and showed much better agreement. Plotting the mass-transfer coefficients in Figure 3-11, shows that the mass-transfer through the pitch of the tar-contaminated soil was much slower than



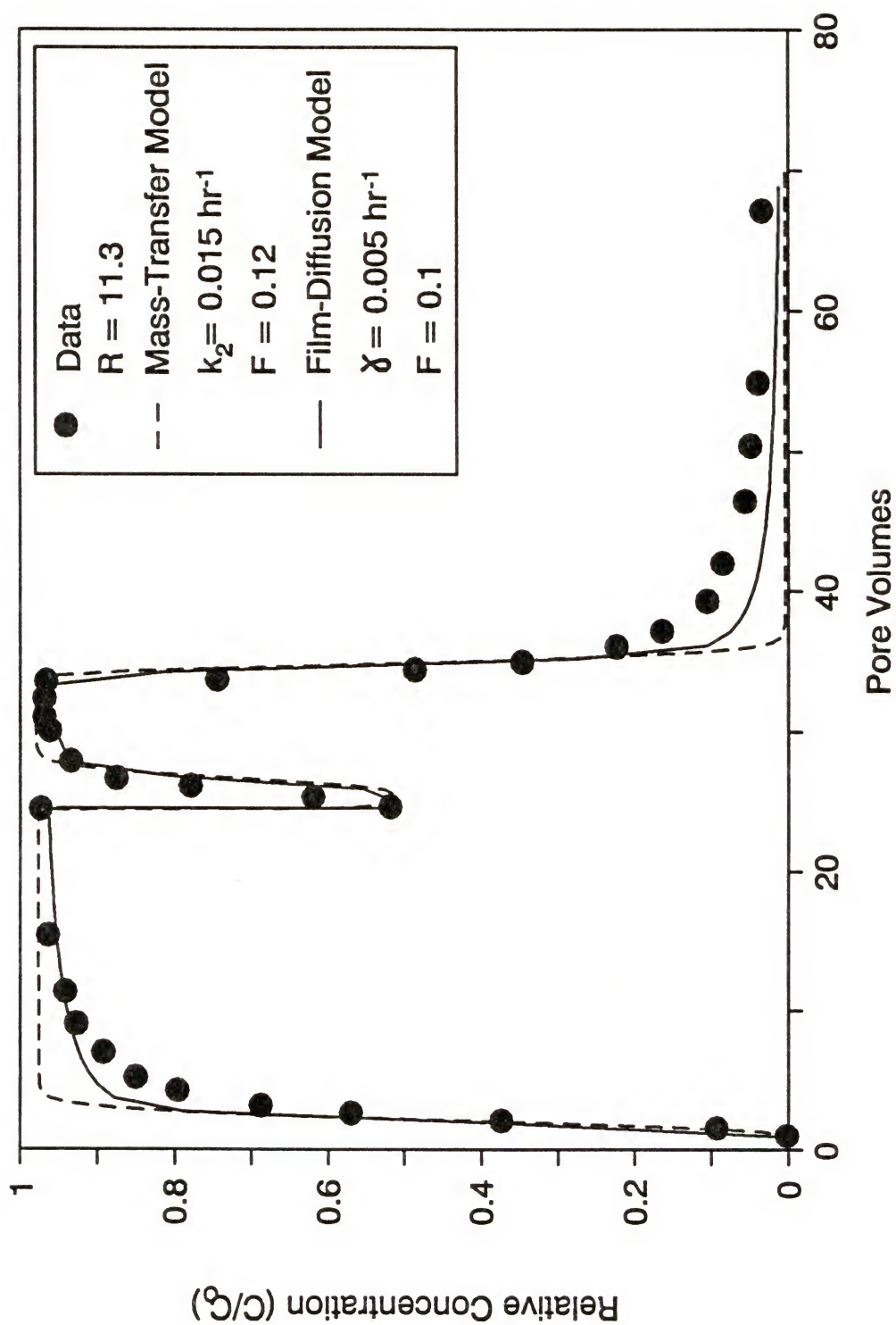


Figure 3-12 Experimental breakthrough curve for benzene through a column packed with the coal tar/sand mixture.

the mass-transfer through the matrix of soil organic matter. This suggests that the physical structure of the tar pitch is less open than that for organic matter. The pitch is probably also more hydrophobic in nature (i.e., it has a lower (O+N)/C ratio than organic matter), which forms a potential for more hydrophobic interactions or a larger pseudo-retardation factor in the pitch.

The values for the retardation factor used to fit the experimental data for benzene and toluene were calculated from the equilibrium sorption coefficient obtained from batch experiments. Figure 3-13 shows the results of the sorption time study. The solid line through the data points was calculated based on the parameters obtained from the best fit to the breakthrough curve. The last data points in this figure were obtained from the sorption isotherm, and shows that equilibrium may not have been reached after 170 hours. It is therefore questionable if the correct equilibrium sorption coefficient was used to fit the experimental breakthrough curve. Moreover, equilibrium sorption coefficients calculated from literature  $K_{oc}$  values, are much higher than the ones used (11.1 and 16.1 for benzene and toluene, respectively). If any different, the  $K$  values for the pitch are expected to be higher than the  $K$  values calculated from  $K_{oc}$  values that were determined for natural soils, because of the suspected more-hydrophobic nature of the pitch material. When a higher value for the retardation factor is used to fit the data for benzene ( $R=40$ , based on the  $K_{oc}$  value), the mass-transfer rate has to decrease to compensate for the larger retardation factor. This results in an even worse fit of the first-order, mass-transfer model to the experimental breakthrough curve, and a down-right shift of the

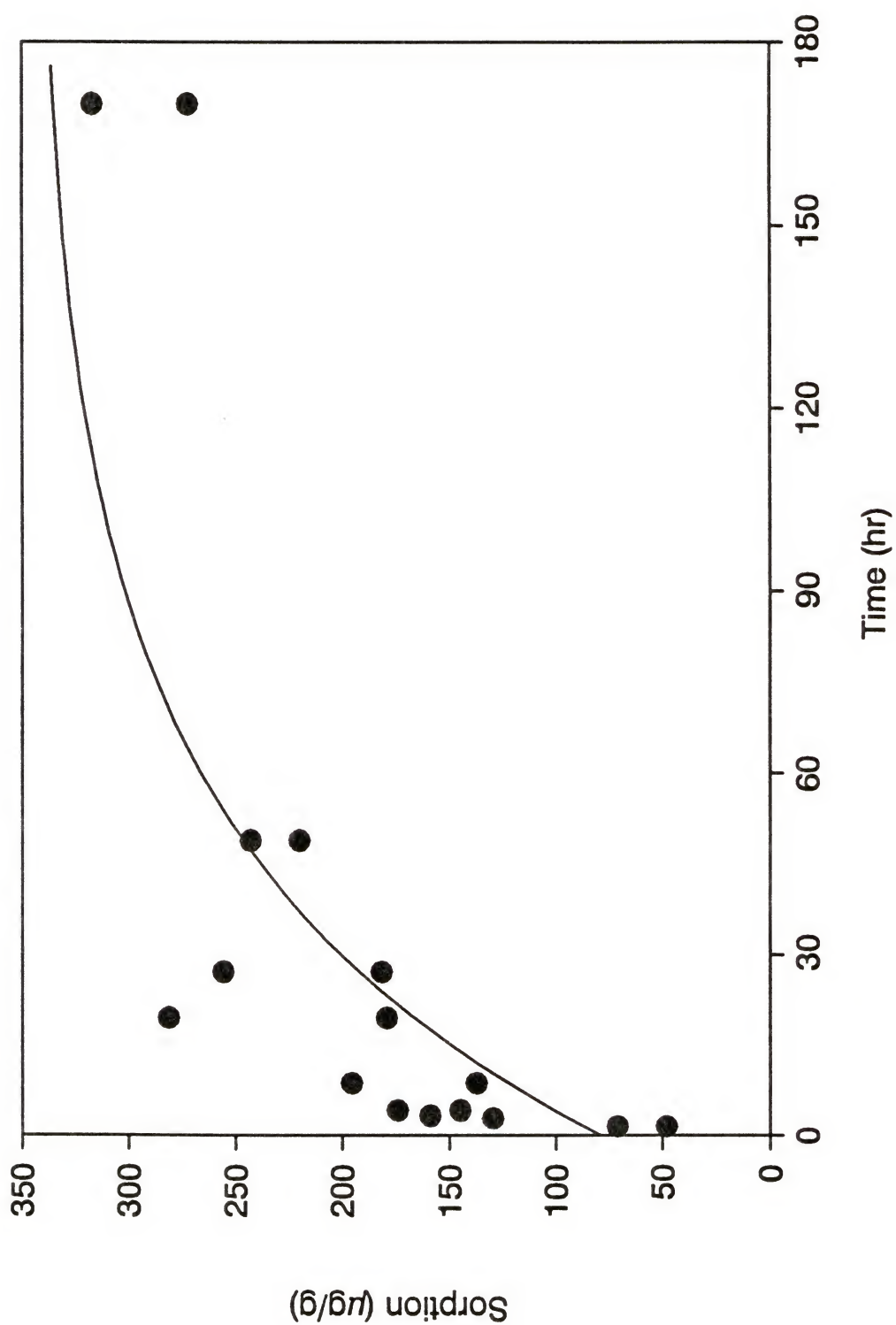


Figure 3-13 Results of the batch time-study for sorption of benzene by the coal tar/sand mixture.

data points in Figure 3-11, and hence remains far below the regression line for natural media.

The extreme degree of nonequilibrium observed for the tar-contaminated soil has consequences for the remediation of these soils. The rate at which contaminants are released from the pitch is at least one order of a magnitude lower than for natural soils. Recall that in this study the tar was first washed with methanol. This may have changed the conformation of the pitch material, although it was expected that this change is nominal. Then, the sorption and desorption of benzene and toluene were studied by introducing the chemicals into the column and monitoring the effluent concentrations. In the field, however, the contaminants have always been part of the coal tar. Several studies have shown that long term contact times between contaminants and soils result in much slower desorption rates, and even irreversible sorption of the chemical (Oliver, 1985; Pignatello, 1990). In the field, release of the contaminants could be even slower than observed in this study. Ageing of the tar, on the other hand, could reduce the amount of chemicals that is eventually released. Another point that is important to consider here is the fact that the soil used for this study contained purifier box waste. Small metallic granules, and pieces of coal were detected in the soil after drying. The presence of these materials may also have had an effect on the measured sorption rates. More studies are needed to confirm these preliminary results.

In addition to sorption nonequilibrium, in the field, nonequilibrium conditions caused by the heterogeneous distribution of the OILs should be considered. The



heterogeneous distribution can create zones of lower permeability to ground water (see Chapter 1). Mass transfer from these low permeable zones to the regions of higher permeability could create severe nonequilibrium conditions. Large ganglia reduce the contact area between water and OIL which could lead to nonequilibrium conditions because there is only a short contact time between OIL and water, or to apparent nonequilibrium conditions, due to mixing of fresh and contaminated water, because only a limited volume of water is contaminated. All these effects should be considered when evaluating the problems in the field.

## CHAPTER 4

### REMEDIATION OF SOILS CONTAMINATED WITH COMPLEX WASTE MIXTURES: SOLVENT FLUSHING

#### Overview of Remediation Techniques

Most environmental research is aimed at studying physical-chemical processes that give us a better understanding of the behavior of contaminants in the environment. Ultimately, some of this knowledge should help in developing more efficient techniques for remediation. Figure 4-1 gives an overview of possible remediation techniques that may be employed when remediating a soil or aquifer contaminated with OILs. There are three options: containment, removal, or transformation of the contaminants.

Containment does not always lead to restoration of the site, but is used to prevent the contaminant from spreading over a larger area, before another remediation technique is implemented. Containment of the contaminants can be done in several ways. Physical barriers like sheet piling or slurry walls can be installed around the source to exclude the source from contact with flowing water (Barcelona et al., 1990). Sorption barriers can be installed on the downstream edge of the plume. Sorption barriers consist of highly sorptive materials that retain the contaminants from the plume, concentrating the chemicals down to a smaller volume which makes it easier to excavate or treat.

# Remediation of Soils and Aquifers Contaminated with OILs

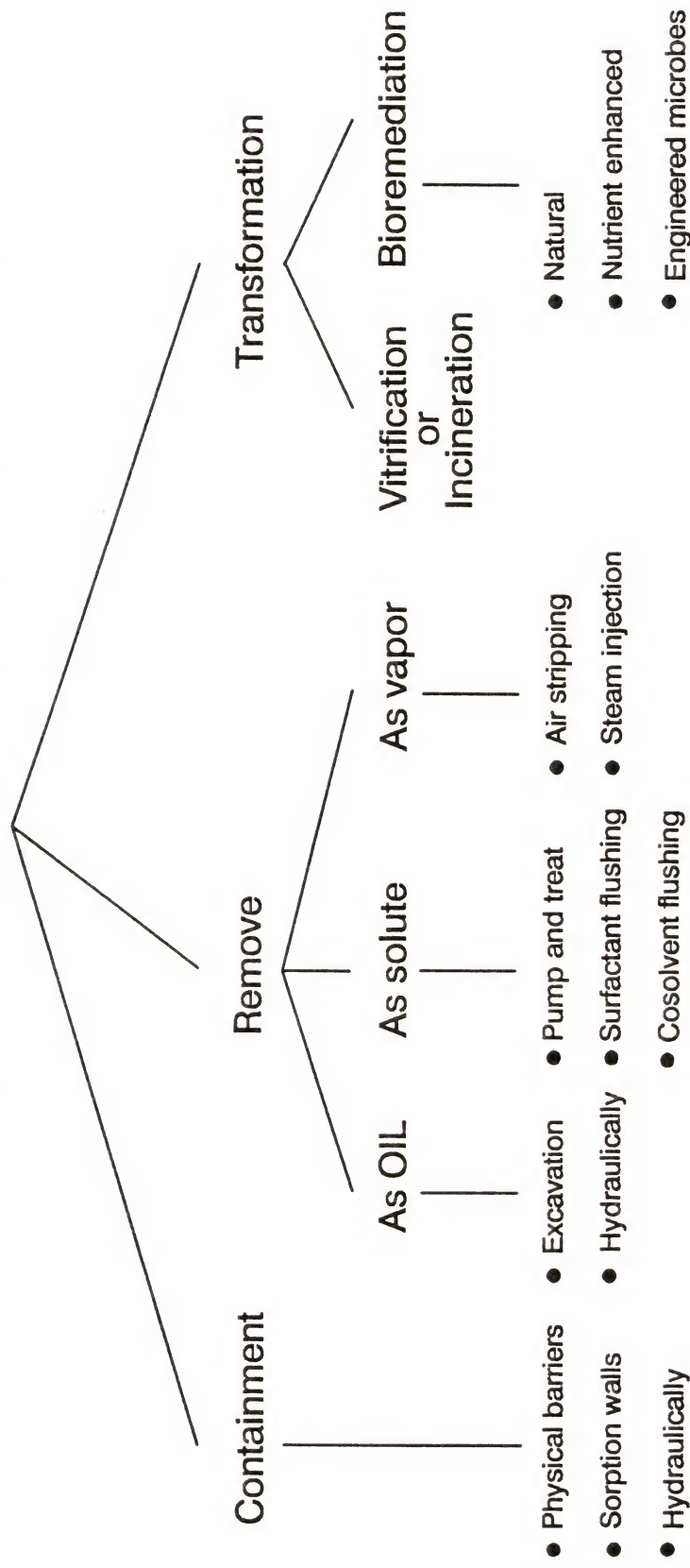


Figure 4-1 Schematic of the possible options for remediating soils and aquifers contaminated with organic immiscible liquids.

Removal of contaminants can also be done in different ways: as a pure OIL phase (recovery of free product), as a dissolved chemical in the solution phase, or as a vapor in the gas phase. Excavation of the contaminated soil is the most effective type of remediation, but may be very expensive when the contamination extends over a large volume, and may not even be possible when the site is located under permanent structures. The disposal or treatment of excavated material can be another problem. When possible, excavation is often done for the most heavily contaminated regions, while other techniques are used for the remainder of the contaminated soil. Hydraulic removal of the OIL is only possible when a free moving OIL is present on top of the water table or at the bottom of the aquifer. The location and amount of free moving OIL are very difficult to determine. In the most effective way, this method removes the OIL to residual saturations.

Removal of contaminants via the solution phase by pump-and-treat is probably the most common remediation technique for restoration of the saturated zone. For this technique, wells are installed and water is extracted from the contaminant plume. Recently, many researchers have pointed out the ineffectiveness of this technique; the most important reason being nonequilibrium conditions (Mackay and Cherry, 1989). The introduction of chemical additives to enhance the release and transport of organic chemicals is currently an active field of research (Palmer and Fish, 1992). In this chapter cosolvents will be discussed as potential additives to ground water to enhance the remediation of contaminated soils.

Removal of contaminants via the gas phase applies only to volatile compounds and is especially useful for remediation of the vadose zone. Vapor extraction is a



widely employed technique to remove volatile contaminants from the unsaturated zone. This technique is much more efficient than extraction of water by wells, because larger volumes of air can be removed faster than water, however, similar problems may occur due to nonequilibrium conditions. In some cases, aquifers are partially dewatered to be able to employ this technique. Release of chemicals in the gas phase may be enhanced by steam or hot-air injection (Hunt et al., 1988). For removal of volatile organic compounds from the saturated zone, air sparging can be used. This method is only effective at a small scale and possible only in media with high permeability.

A site can also be restored by transforming the contaminants into less harmful derivatives. In situ heat treatments can be used to burn the chemicals. Bioremediation is another field of active research. It involves the in situ biodegradation of chemicals by indigenous microorganism or microorganisms that are introduced to specifically degrade the target chemical. In most subsurface systems some degradation occurs naturally. In many cases, however, degradation needs to be stimulated to make it more efficient. The microorganisms are often limited by the supply of oxygen or nutrients. Oxygen can be introduced as ozone or by air sparging. If nutrients are the limiting factor, injection of nutrients may enhance the degradation. The injection of specific microbial consortia is not a common practice, because of the limited dispersion of these microbes in the subsurface. They tend to accumulate around the injection point by attachment to the surfaces. Another major problem of bioremediation is the availability of chemicals for degradation

(bioavailability). Most microorganism consume the chemicals from the dissolved phase; hence, dissolution and desorption must first take place before the contaminants are available for biodegradation. The rate of these processes may be limited at a local scale, as discussed in previous chapters.

Which technique is most efficient, in terms of contaminant removal and cost, should be evaluated individually for each site. In many cases, any one technique may not be sufficient, but a combination of techniques may be required to remediate the site most efficiently. In this chapter, the use of cosolvents will be discussed as a potential remediation technique. In situ solvent flushing involves the injection of a mixed solvent (water plus miscible organic cosolvents) at a site contaminated with organic chemicals. Cosolvents increase the solubility, and reduce sorption and mass-transfer limitations of organic chemicals, which all favor an enhanced release and transport of contaminants. Site remediation efforts may involve only the highly contaminated "source" area, or may focus on treating the "contaminant plume" emanating from the source.

Solvent flushing would be most logically applied for clean up of the source area, since removal of the source prevents further contamination of groundwater. In situ solvent flushing involves the following steps (U.S. EPA, 1991): (1) the solvent mixture is injected upstream of the contaminated zone; (2) the solvent with the dissolved contaminants is extracted downstream and treated above ground to recover the solvent; and (3) the recovered solvent may be reinjected. An impermeable layer as well as physical barriers (e.g., sheet piling, slurry walls) or hydraulic control

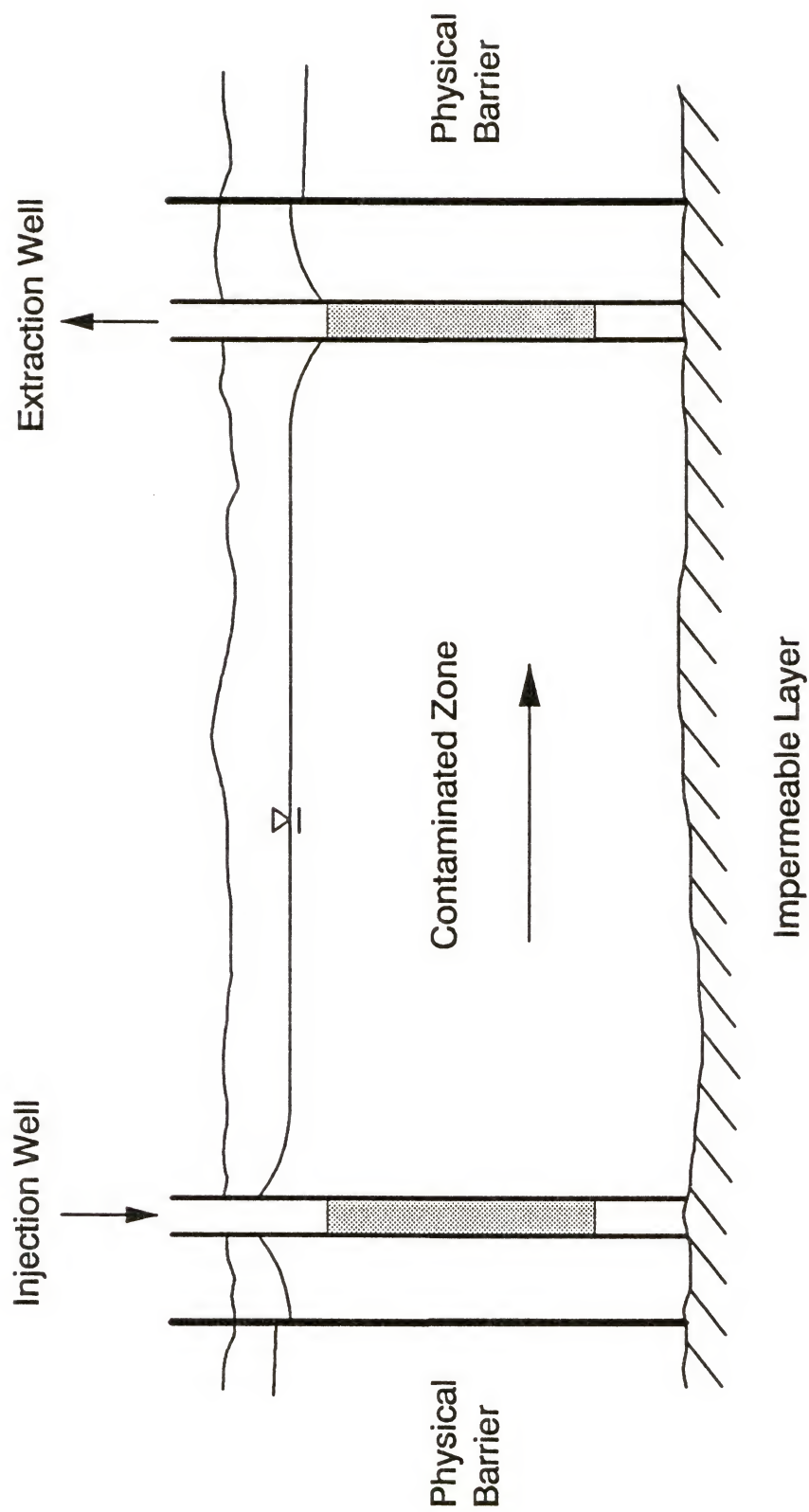


Figure 4-2 Schematic representation of the in situ solvent flushing technique.

measures may be required to prevent off-site transport of contaminants and solvents. A schematic representation of this technique is shown in Figure 4-2.

The study of the effect of cosolvents on the behavior of organic chemicals is not only of interest for remediation purposes, but cosolvents may also be present at sites as part of the OIL (e.g., as additive to gasoline; Mihelcic, 1990; Poulsen et al., 1992), or introduced by codisposal, and alter the behavior of other chemicals (Rao et al., 1989). To date, cosolvents have only been used to facilitate laboratory investigation of sorption and transport of low-solubility organic chemicals in soils (Rao et al., 1991), and for studying the behavior of complex organic wastes such as coal tar (Lane and Loehr, 1992). Information on commercial use of cosolvents for remediation of contaminated soils is very limited, although the use of cosolvents for extraction of some organic contaminants from various environmental matrices has been successfully demonstrated either at the pilot-scale or in full-scale commercial applications (U.S. EPA, 1990). The effects of cosolvents on the behavior of organic solutes, referred to as cosolvency, have now been well established based on considerable experimental data and theoretical analysis (Rao et al., 1991), and will be reviewed in next section.

### Cosolvency Theory

#### Cosolvent Effects on Solubility

The effect of cosolvents on the solubility is primarily important for dissolution processes. By adding an organic solvent to water, the polarity of the solvent mixture



decreases, resulting in an increased solubility of nonpolar organic chemicals. The solubility of a nonpolar organic solute in a binary solvent mixture ( $S_m$ ) increases in a log-linear manner with increasing volume fraction of cosolvent ( $f_c$ )<sup>1</sup> (Yalkowsky and Roseman, 1981; Fu and Luthy, 1986a; Morris et al., 1988):

$$\log S^m = \log S^w + \beta \sigma f_c \quad (4-1)$$

where

$$\sigma = \log \left( \frac{S^c}{S^w} \right) \quad (4-2)$$

$S^w$  is the solubility in water (g/ml);  $S^c$  is the solubility in a neat solvent (g/ml);  $\beta$  is an empirical coefficient that accounts for water-cosolvent interactions; and  $\sigma$  is the cosolvency power. When it is assumed that the cosolvent effects are additive, Equation 4-1 can be generalized as follows for a mixture of water and several cosolvents:

$$\log S^m = \log S^w + \sum \beta_i \sigma_i f_{c,i} \quad (4-3)$$

where the subscript  $i=1,2,\dots,n$  designates the values for the  $i^{\text{th}}$  cosolvent, and  $n$  is the number of cosolvents in the mixture.

The log-linear model stated in Equations 4-1 and 4-3 is adequate for describing the solubility profiles of a number of nonpolar organic chemicals in a

---

<sup>1</sup> Note that  $f_c$  is defined as a volume fraction prior to mixing. A volume fraction of 0.5, for example, is obtained by mixing equal volumes of cosolvent and water. Since the density of the mixture changes in a nonlinear fashion, the actual volume fraction will be slightly different.

variety of solvent-water mixtures (Rao et al., 1991). However, when water-cosolvent interactions are significant, deviations are found from the log-linear solubility profiles predicted by Equation 4-3. This can be accounted for by  $\beta$ . The degree of nonideality varies with cosolvent content, and therefore  $\beta$  is also expected to change. Usually, however,  $\beta$  can be considered as a constant larger than 1 up to a cosolvent fraction of 0.5, after which it normally decreases back to a value of 1.

Pinal et al. (1991) proposed a more elegant method to account for deviations due to nonideal behavior. They proposed the following modification to the log-linear model:

$$\log S^m = \sum f_{c,i} \log S_i^c + 2.303 \sum f_{c,i} \log \gamma_i \quad (4-4)$$

where  $\gamma_i$  is the activity coefficient of the compound in the  $i^{\text{th}}$  cosolvent. Pinal et al. (1991) estimated the activity coefficient from UNIFAC, and were able to predict deviations from the log-linear model reasonably well with Equation 4-4.

The equilibrium concentration of a solution in contact with a pure liquid compound is equal to the solubility of that compound in the particular solvent. Hence, the equilibrium concentration in various solvent mixtures is described by Equation 4-3. For multi-component OILs, the equilibrium concentration is described by Raoult's law (Equation 2-13). Substitution of Equation 4-3 into Raoult's law yields:

$$\log C_j = \log X_j + \log S_j^w + \sum \alpha_i \beta_i \sigma_i f_{c,i} \quad (4-5)$$

where  $C_j$  the equilibrium concentration of constituent  $j$  in a solvent mixture;  $X_j$  is the mole fraction of the same constituent in the OIL phase; and  $\alpha$  is a correction factor that accounts for nonideal behavior due to cosolvent-OIL interactions. All other parameters are as defined previously. Thus, cosolvent addition to a multi-component waste mixture can be expected to result in an exponential increase in solution-phase concentrations of organic constituents of the waste. This prediction is consistent with the data reported by Lane and Loehr (1992) for the dissolution of several aromatic hydrocarbons from tar-contaminated soils into binary mixed solvents.

Deviations from the log-linear model can be expected due to cosolvent-OIL and solvent-cosolvent interactions (accounted for by  $\alpha$  and  $\beta$ , respectively). Changes in mole fractions will also cause deviations from the log-linear model. A decrease in the mole fraction of all constituents occurs when cosolvents partition into the OIL phase. At high cosolvent fractions, the mole fraction can also change when significant amounts of the constituents are extracted from the OIL phase. For constituents that are solid in their reference state, the super-cooled liquid solubility can also be described by Equation 4-3, since none of the parameters in the correction in Equation 2-16 are a function of cosolvent fraction.

#### Cosolvent Effects on Sorption

The change in sorption of organic chemicals from mixed solvents is directly related to cosolvent effects on the solubility of the organic solute. Since sorption is inversely related to the solubility (Equation 2-23), an increase in solubility, upon addition of cosolvents, leads to a proportional decrease in sorption (Rao et al., 1985;

Nkedi-Kizza et al., 1985; Fu and Luthy, 1986b):

$$\log K^m - \log K^w - \sum \alpha_i \beta_i \sigma_i f_{c,i} \quad (4-6)$$

where  $\alpha$  is an empirical coefficient that accounts for cosolvent-sorbent interactions (Rao et al., 1991), the superscripts  $m$  and  $w$  denote mixed solvent and water, respectively. Although deviations from the log-linear model due to cosolvent-sorbent and cosolvent-OIL interactions (Equation 4-5) are indicated with the same coefficient ( $\alpha$ ), they may be different in magnitude.

For transport problems, equilibrium sorption is commonly expressed in terms of a retardation factor ( $R$ ) which represents the residence time of a chemical in pore volumes:

$$R = 1 + \frac{\rho}{\theta} K \quad (4-7)$$

where  $\theta$  is the volumetric water content (ml/cm<sup>3</sup>), and  $\rho$  the dry bulk density (g/cm<sup>3</sup>). Combination of Equations 4-6 and 4-7 gives (Nkedi-Kizza et al., 1987):

$$\log (R^m - 1) - \log (R^w - 1) - \sum \alpha_i \beta_i \sigma_i f_{c,i} \quad (4-8)$$

The validity of the log-linear model for describing the impact of cosolvents on the mobility of organic solutes is confirmed by column data (Nkedi-Kizza et al., 1987, 1989; Wood et al., 1990; Brusseau et al., 1991b).

### Cosolvent Effects on Nonequilibrium Conditions

Nonequilibrium conditions are an important limitation for many remediation techniques. Dissolution and desorption rates can be maximized by flushing, such that



solute concentrations are maintained and large concentration gradients are established at local scale (Seagren et al., 1993). Flushing techniques, like pump-and-treat, however, do not affect the rate coefficients. Several researchers have found that sorption-rate coefficients increase upon addition of a cosolvent (Nkedi-Kizza et al., 1989; Wood et al., 1990; Brusseau et al., 1991b). Brusseau et al. (1991b) attributed this to swelling of organic matter in the presence of an organic cosolvent, enhancing diffusion of the sorbate through the sorbent. In case of retarded intra-particle diffusion this phenomenon can be explained by reduced retardation.

An increase in the mass-transfer rate coefficient ( $k$ ) with increasing cosolvent content is also expected based on the log-log linear inverse relationship between  $k_2$  (or  $k$ ) and  $K$  (see Chapter 3), and the log-linear decrease of  $K$  with increasing cosolvent fraction (Equation 4-6). Combination of these two relationships gives:

$$\log k_2^m - \log k_2^w = a \sum \alpha_i \beta_i \sigma_i f_{c,i} \quad (4-9)$$

where  $a$  is the absolute value of the slope for the linear regression between  $\log K$  and  $\log k_2$ . This relationship suggests that the use of cosolvents will shift data points in the upper left direction along the regression line established for natural sorbents. This justifies the comparison of nonequilibrium sorption data obtained in solvent mixtures with data obtained from aqueous systems. Brusseau et al. (1991b) found Equation 4-9 to be useful up to a volume fraction of 70%.

Another parameter describing sorption nonequilibrium is the fraction of instantaneous sorption domains ( $F$ ). Brusseau et al. (1991b) found that  $F$  generally is unaffected up to 20% cosolvent and then decreases with increasing cosolvent

fraction. Based on this observation, Augustijn et al. (1993) expressed the functionality between  $F$  and  $f_c$  as follows:

$$\begin{aligned} F^m - F^w & & 0 \leq f_c < 0.2 \\ F^m - F^w - b(f_c - 0.2) & & 0.2 \leq f_c \leq 1 \end{aligned} \quad (4-10)$$

where  $b = (F^w - 0.01)/0.8$ . Equation 4-9 assumes an initial constant  $F$ , and a linear decrease beyond a cosolvent fraction of 0.2 to an arbitrary value of 0.01 for the neat organic solvent. General applicability of this relationship is uncertain (see also the discussion on  $F$  in Chapter 3), and more research is needed to develop a clear understanding of the cosolvent effects on  $F$ .

When a cosolvent is added to a soil contaminated with an OIL, the solubility will increase according to Equation 4-3, enhancing the dissolution rate. In addition, a decrease in surface tension upon addition of an organic cosolvent may emulsify, and possibly mobilize, the residual OIL. The enlarged contact area between the OIL and the solvent mixture will also enhance the dissolution process. In viscous, multi-component liquids like coal tar or crude oil, diffusive transport within the organic phase is most likely the mechanism controlling the dissolution kinetics. Similar to the cosolvent effects on sorption, the cosolvent may permeate into the OIL phase and change its conformation such that the release of constituents is enhanced. Since no experimental data are available on the effect of cosolvents on the actual mass-transfer rate coefficient for dissolution, and very little research has been done on the dissolution kinetics from complex mixtures, this process will not be considered in the following sections.

### Parameter Estimation

When evaluating a contaminated site for potential remediation techniques, it is convenient to be able to estimate the parameters needed to predict the release and transport rates of contaminants with a limited amount of (experimental) work. The following discussion focuses on methods for estimating several parameters needed in the use of the cosolvency model for soil clean up. All equations are summarized in Table 4-1. It should be noted that most of the approaches presented below were not derived from first principles, but are based on empirical correlations using measured data.

#### Cosolvency Power

The cosolvency power ( $\sigma$ ) is probably the most important parameter in the cosolvency theory. It determines the relative change in solubility, sorption and mass-transfer rates with increasing cosolvent fraction. The larger the value for  $\sigma$ , the more effective the removal of the contaminant will be. For this reason, the cosolvency power is sometimes also referred to as solubilization or extraction power. The cosolvency power is a function of the solute molecular surface area and the interfacial free energy of the cosolvent, and can be derived from thermodynamic principles (Rao et al., 1985). The solubility of a hydrophobic solute will increase with decreasing polarity of the solvent. For this reason,  $\sigma$  values can be estimated from polarity or hydrophobicity indices.

One hydrophobicity index for which a large data base has been established over the past several years is the octanol-water partition coefficient ( $K_{ow}$ ). Since the

Table 4-1 Summary of equations to estimate important parameters related to the cosolvency theory.

Parameter	Estimation	Reference
$S^m$	$\log S^m = \log S^w + \sum \beta_i \sigma_i f_{c,i}$	Yalkowsky and Roseman, 1981
$K^w$	$\log K^m = \log K^w - \sum \alpha_i \beta_i \sigma_i f_{c,i}$	Rao et al., 1985
$k_2^w$	$\log k_2^m = \log k_2^w + 0.668 \sum \alpha_i \beta_i \sigma_i f_{c,i}$	Brusseau et al., 1991
$\sigma$	$\sigma = A \log K_{ow} + B$	Morris et al. , 1988
$S_l$	$\log S_l = \log S_s + 2.95(T_m - T)/T$	Yalkowsky, 1979
$K^w$	$\log (K^w/f_{oc}) = \log K_{ow} - 0.21$	Karickhoff et al., 1979
$R^m$	$\log (R^m - 1) = \log (R^w - 1) - \sum \alpha_i \beta_i \sigma_i f_{c,i}$	Nkedi-Kizza et al., 1987
$k_2^w$	$\log k_2^w = 0.301 - 0.668 \log K^w$	Brusseau and Rao, 1989
As an initial estimate $F = 0.5$ , $\alpha = 1$ and $\beta = 1$		



solubility in a cosolvent is proportional to the solubility in octanol, the cosolvency power can be estimated from (Morris et al., 1988):

$$\sigma = A \log K_{ow} + B \quad (4-11)$$

where A and B are empirical constants, unique to each cosolvent, and represent the slope and intercept of the  $\sigma$  vs.  $\log K_{ow}$  plot. Ideally,  $A=1$ , and  $B=\log(S_c/S_o)$  where  $S_c$  is the solute solubility in the neat cosolvent and  $S_o$  its solubility in octanol. In general, the solubility in an organic solvent and octanol are of similar magnitude; hence, B is relatively small. As a first approximation, the cosolvency power can therefore be estimated as follows:

$$\sigma \approx \log K_{ow} \quad (4-12)$$

In reality, B is not a true constant because different compounds may have nonproportional solubilities in the solvent and octanol, depending on their structure. In addition, nonideal behavior may affect the values of A and B. Morris et al. (1988) performed regression analysis to estimate A and B values using data for solubility of several solutes measured in mixtures of water and organic solvents that are completely miscible in water.

### Solubility

Values for the aqueous solubility of various organic chemicals can be found in most chemical reference books (e.g., Verschueren, 1983). For solids dissolved in a multi-component OIL, the super-cooled liquid solubility ( $S_l$ ) can be calculated from Equation 2-3. When limited thermodynamic data is available, it is convenient to

replace the heat of fusion ( $\Delta H_f$ ) by the entropy of fusion ( $\Delta S_f = \Delta H_f/T_m$ ), since  $\Delta S_f$  has a nearly constant value of approximately 13.5 cal/mole K for all organic compounds (Yalkowsky, 1979). This substitution, and using 1.987 cal/mole K as value for the gas constant, Equation 2-3 reduces to:

$$\log S_l - \log S_s + \frac{2.95(T_m - T)}{T} \quad (4-13)$$

where  $T_m$  is the melting point ( $^{\circ}\text{K}$ ), and  $T$  the ambient temperature ( $^{\circ}\text{K}$ ).

### Equilibrium Sorption Coefficient

The equilibrium sorption coefficient normalized to the soil organic carbon content ( $K_{oc}$ ) has been correlated to several properties of the organic chemical. These correlations can be used to estimate  $K^w$ . The most popular correlation is perhaps the one between  $K_{oc}$  and the octanol-water partition coefficient ( $K_{ow}$ ; Karickhoff et al., 1979):

$$\log K_{oc} = 1.00 \log K_{ow} - 0.21 \quad (4-14)$$

Since this relationship was first published, similar relationships have been developed for specific groups of compounds (cf., Gerstl, 1990). It should be recognized that correlations like the one in Equation 4-14 have several limitations (Mingelgrin and Gerstl, 1983), nevertheless, they provide a reasonable first approximation for the equilibrium sorption coefficient when no specific data is available.

### Nonideality Coefficients

Significant cosolvent-water interactions and cosolvent-OIL/sorbent interactions, may cause deviations from the generally accepted log-linear model.

Cosolvent-water interactions generally lead to positive deviations from the log-linear model; thus,  $\beta$  values are expected to be  $\geq 1$ . Cosolvent-sorbent interactions may result in either positive deviations ( $\alpha > 1$ ) or negative deviations ( $\alpha < 1$ ). The product  $\alpha\beta$  accounts for deviations arising from both cosolvent-water and cosolvent-sorbent interactions. Values for  $\alpha$  and  $\beta$  vary with cosolvent, soil, and chemical. Since limited information is available for estimating  $\alpha$  or  $\beta$  values for specific cases, as a first approximation, the product  $\alpha\beta$  can be assumed equal to 1.

### Sorption Nonequilibrium Parameters

To be able to describe sorption nonequilibrium in various cosolvent mixtures, two parameters are needed:  $k_2^m$  (or  $k^m$ ), and  $F^m$ . Even though  $k$  was proposed as a better parameter to describe the mass-transfer process,  $k_2$  rather than  $k$  will be used in the following sections. This is done because more data are available on the correlation between  $f_c$  and  $k_2$ . The reversed first-order mass-transfer rate coefficient in the mixed solvent ( $k_2^m$ ) can be calculated from Equation 4-8. Values for  $k_2^w$  and  $a$  can be obtained from correlations between  $\log k_2$  and  $\log K$ , like the one presented by Brusseau and Rao (1989b;  $a=0.668$ ), or in Chapter 3 ( $a=0.69$ ).  $F^m$  can be calculated from Equation 4-10. In the absence of specific data, the best first guess would be  $F^w=0.5$  (see discussion in Chapter 3).

### Applications

It is evident from the discussion in the previous sections that addition of cosolvents can help in faster clean up of contaminated soils for three reasons: (1)

increased solubility due to reduced polarity of the solvent mixture; (2) decreased sorption or retardation due to enhanced solubility; and (3) decreased nonequilibrium conditions due to faster sorption/dissolution kinetics. Cosolvents could be used to clean up contaminated soils excavated from a site or for in situ remediation. The first technique is often referred to as solvent washing or solvent extraction, while the latter process is referred to as solvent flushing. Pilot-scale and commercial-scale applications of the solvent extraction technology have been documented (U.S. EPA, 1990) for treating organic contaminants from a wide range of matrices, and a spectrum of waste types. Information on commercial use of cosolvents for in situ remediation of contaminated soils, however, is very limited.

In this section, the use of the solvent flushing technique will be illustrated using model simulations, and some experimental data. For a field-scale application of solvent flushing, three-dimensional solute transport equations in a heterogeneous domain should be considered. The focus of the present investigation is to examine the efficiency of cosolvents on the removal of organic contaminants, not as much the impacts of heterogeneities. Therefore, for simplicity, the advective-dispersive transport of the cosolvent (assumed to be nonsorbed) and contaminants are assumed to occur in a homogeneous medium under steady, one-dimensional flow conditions.

Three hypothetical remediation scenarios are considered as case studies. Case 1 involves remediation of a soil with low-level contamination of highly-sorptive constituents (naphthalene and anthracene). Case 2 represents a contaminated soil containing excess of a single-component OIL (PCE). Case 3 was chosen to represent



dissolution from a multi-component OIL (coal tar). These three hypothetical cases cover a range of remediation scenarios that require the use of increasingly more complex models to describe the processes of contaminant release into the environment. Also, note that while Case 1 is typical for remediation of "far-field" regions, Cases 2 and 3 represent "near-field" regions.

The models described in previous chapters were modified to simulate the effect of solvent flushing on the removal of contaminants for each case. It was assumed that the system was initially in equilibrium with the contaminant, and that at  $t=0$  a "clean" solvent mixture was introduced. As the mixed solvent progresses through the soil, solubility, sorption and nonequilibrium parameters change as discussed in previous sections. Experiments were performed to validate the models for Case 1 and 3.

#### Case 1: Solvent Flushing of a Low-Level Contaminated Soil

This case represents the removal of a highly-sorptive compound (i.e., relative large  $\log K_{ow}$  values such as observed for naphthalene and anthracene) from soils or aquifer materials. The term "low-level" contamination indicates that the contaminant only resides in the solution and sorbed phase, and is not present in a separate phase. This is representative for the contaminant plume in the far-field region. Augustijn et al. (1993) developed a one-dimensional transport model, including sorption nonequilibrium, that may serve as a first approximation for the elution profiles as affected by in situ solvent flushing. This model was modified from the first-order bicontinuum model for intra-organic matter diffusion, discussed in Chapter 4. The

main differences are the initial condition and the fact that sorption parameters change as the cosolvent front progresses through the column. The initial mass in the system ( $M_0$ ) is given by the sum of the mass in the sorbed and solution phase:

$$M_0 = \theta C_0 + \rho S_0 \quad (4-15)$$

The system is assumed to be initially at equilibrium, thus, the linear sorption isotherm can be used to describe the relation between the sorbed concentration and solution concentration, and Equation 4-15 can be rewritten as:

$$M_0 = \theta RC_0 \quad (4-16)$$

where  $R$  is the retardation factor. For convenience, the concentration in this model is normalized to the initial mass in the system:

$$C^* = \frac{\theta C}{M_0} = \frac{C}{RC_0} \quad (4-17)$$

This means that the area under the elution curve ( $C^*$  versus pore volumes) is always equal to one when the contaminant is completely recovered. Since the soil is initially at equilibrium with the contaminant solution, the initial relative concentration in the solution phase equals the reciprocal value of the retardation factor in water. Hence, the relative concentration in the column effluent during the early stages of the elution serves as a convenient estimator of the aqueous retardation factor. Also, note that  $C^* = 1$  corresponds to the case when all of the initial sorbed mass in a volume element of the soil desorbes instantaneously into the solution phase. The transport equations were solved using a Crank-Nicolson, central finite-difference

method (Wang and Anderson, 1982). A numerical solution of the advective dispersive equation for a nonreactive solute was used to predict the cosolvent composition in the column. As the mixed solvent front progresses through the soil, cosolvent effects on sorption are reflected by the changing values of three model parameters: the retardation factor ( $R$ ); the fraction of instantaneous sorption ( $F$ ); and the first-order mass-transfer coefficient ( $k_2$ ).

In Figure 4-3, simulated curves for naphthalene elution by two methanol-water mixtures are shown for equilibrium and nonequilibrium conditions. Also shown is the normalized breakthrough curve for methanol, which is assumed to behave as a nonreactive tracer. The following general features of the contaminant elution curves are evident: (1) For the initial portion of the curve (up to one pore volume effluent) the naphthalene concentration is constant; this corresponds to a displacement of the resident aqueous solution by the incoming mixed solvent. The magnitude of the relative effluent concentration during this period is equal to  $1/R^w$ , as defined by the initial condition. (2) The area under the contaminant breakthrough curves at all cosolvent contents is the same, and equals unity. (3) Coincident with the breakthrough of the cosolvent, the contaminant concentration rises sharply, and then declines gradually to zero. (4) With increasing cosolvent fraction, the peak concentration is greater and the breakthrough curve is increasingly symmetrical and more compressed. (5) At higher cosolvent fractions (50% in this example) the relative effluent concentration ( $C^*$ ) exceeds 1, indicating that mass is compressed into a small liquid volume.

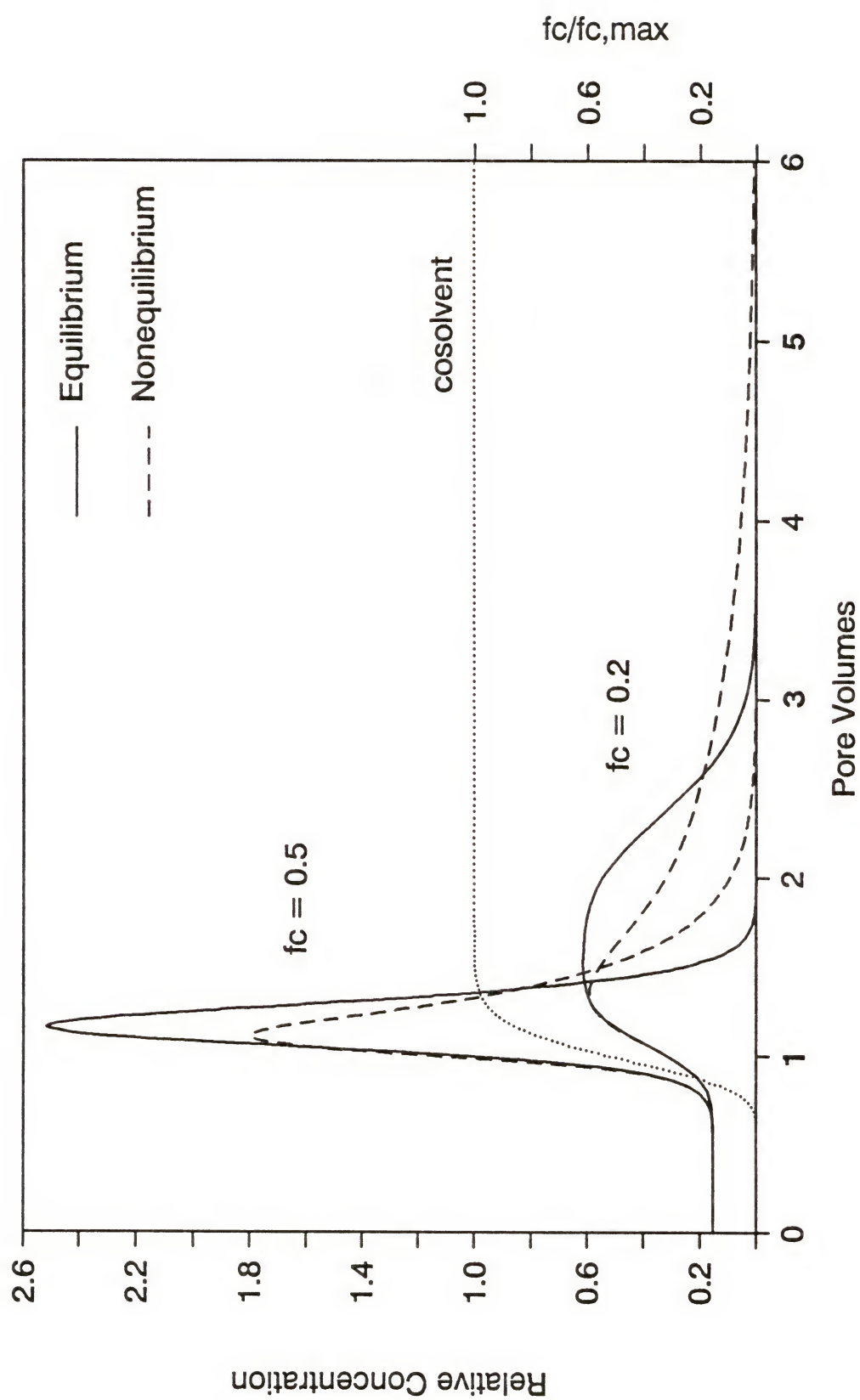


Figure 4-3 Simulated elution profiles of naphthalene for 20% and 50% methanol fractions.



Increasing peak height and narrowing band width is a well known effect of gradient elution in liquid chromatography (Snyder and Kirkland, 1979). A similar effect was reported in the cation exchange literature, and is referred to as the "snowplow" effect (Starr and Parlange, 1979). This effect can be attributed to a change in the sorption coefficient as the solvent composition changes during an elution experiment. The mixed solvent front passing through the column favors desorption so strongly that most of the sorbed mass desorbs immediately into solution and is transported along with the mixed solvent causing an accumulation of solute at the solvent front. The compression of contaminant mass in a small liquid volume is very convenient for remediation purposes since it reduces the number of pore volumes required to remove the contaminant from the soil. Figure 4-3, for example, shows that the naphthalene can be removed with only one injected pore volume of a 50% methanol fraction, assuming equilibrium conditions.

To further illustrate the effects of contaminant elution from soils, Figure 4-4 shows simulated concentration profiles of naphthalene within the column for the solution (Figure 4-4a) and sorbed phase (Figure 4-4b) at two different times and a methanol fraction of 0.2. The nonequilibrium curves shown in Figures 4-3 and 4-4 are very similar to those for equilibrium conditions for the initial portion of the elution profiles, while the peak concentration is lower and the distal portion of the elution curve exhibits more tailing for nonequilibrium conditions. As the high concentrations move forward in the column, sorption occurs along the mixed solvent front (sorbed concentrations at the solvent front are higher than the initial

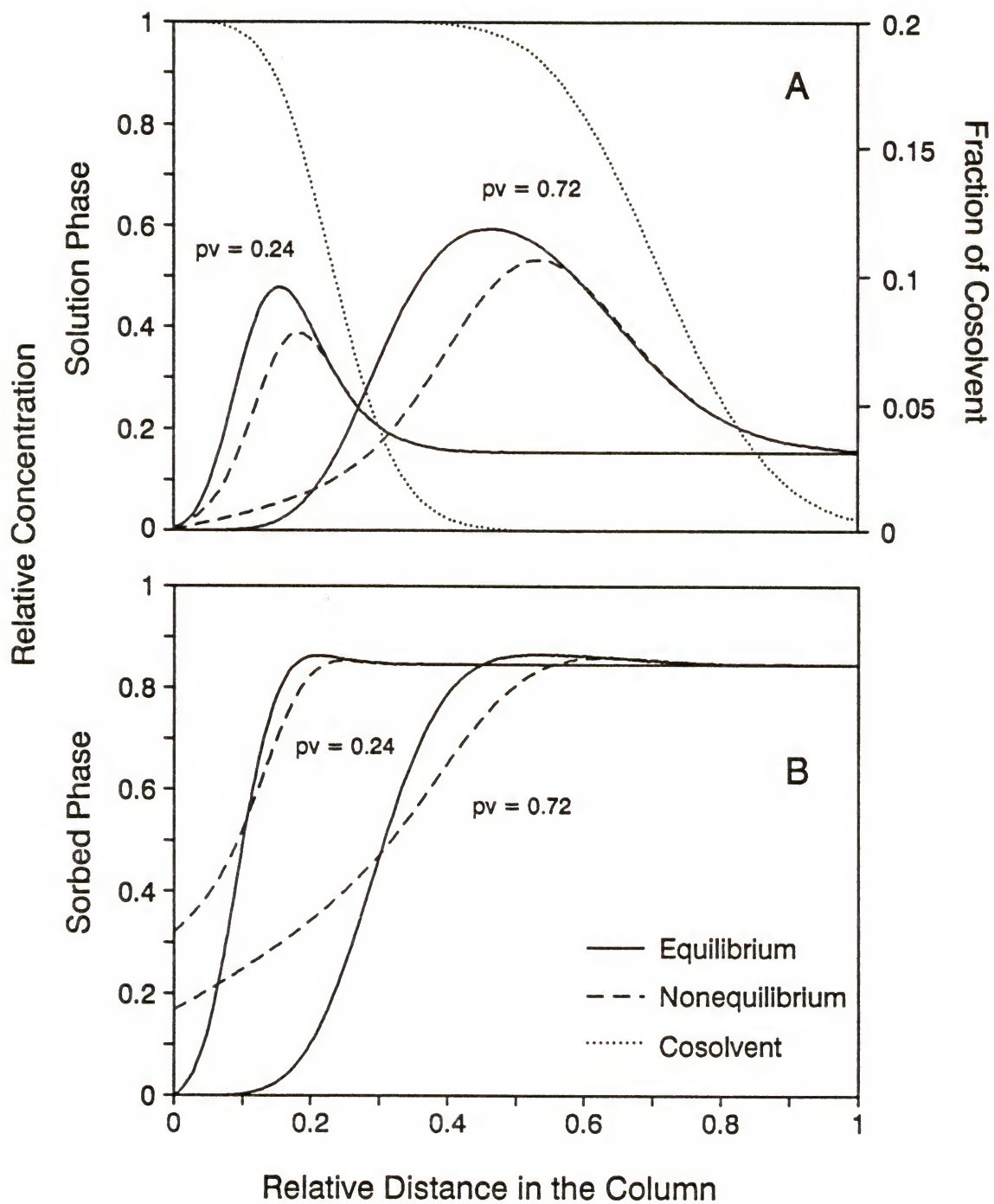


Figure 4-4 Simulated concentration profiles within the column for naphthalene at two different pore volumes (pv) in the solution (a) and sorbed phase (b) at a methanol fraction 20%

concentrations in the sorbed phase, see Figure 4-4b). Under equilibrium conditions sorption is instantaneous; however, under nonequilibrium conditions sorption occurs slower causing the contaminant to travel faster. For this reason, contaminant concentrations at the front of the elution profiles under nonequilibrium conditions are similar to, or even higher than, those for equilibrium conditions. As the front passes, the cosolvent fraction increases favoring desorption. Since desorption is rate-limited under nonequilibrium conditions, this results in tailing of the distal end of the elution curves. It is evident that nonequilibrium conditions reduce the efficiency of contaminant elution.

Experimental procedure. The experimental procedure used in this study is modified from the miscible displacement technique which is discussed in detail in Chapter 3. An air-dry sample of Eustis fine sand was packed in a glass column (diameter 2.5 cm, length 5.3 cm). The packed soil had a dry bulk density of  $1.75 \text{ g/cm}^3$  and a porosity of  $0.33 \text{ cm}^3/\text{cm}^3$ . The column was saturated overnight by flushing with an aqueous  $0.01 \text{ N CaCl}_2$  solution. Pentafluorobenzoic acid (PFBA) was used as a non-reactive tracer to determine the hydrodynamic dispersion characteristics of the water-saturated column. The breakthrough curve for a pulse of PFBA was used to estimate the Peclet number for the soil column ( $P=84$ ).

The soil column was then saturated with an aqueous naphthalene solution (approximately  $15 \text{ mg/L}$ ) in a  $0.01 \text{ N CaCl}_2$  matrix. Naphthalene concentration in the column effluent was tracked using a flow-through UV detector (Gilson Holochrome). The detector response was recorded on a strip chart recorder



(OmniScribe D5000). The naphthalene solution was applied until the signal from the detector reached a plateau equal to the signal of the input concentration. The flow was then interrupted for approximately 12 hours. When the flow was resumed a slight decrease was observed in the response of the detector, indicating that the concentration had decreased during the quiescent period. This indicates that equilibrium was not established before the flow was interrupted (Brusseau et al., 1989). The naphthalene solution was applied for at least another 3 hours at a flow rate of 1 ml/min ( $v = 37$  cm/hr). After this, it was assumed that equilibrium was established in the column, satisfying the initial condition assumed for the model.

The solvent flushing experiment was initiated by introducing a mixed solvent (methanol plus water) at the column inlet. The column effluent was collected in 4-ml amber vials for HPLC analysis for naphthalene (Acetonitrile/water 50/50 mobile phase; LCPAH column). At times when the naphthalene concentration in the effluent was expected to change rapidly, smaller volume fractions were collected in neat methanol to avoid volatilization losses of naphthalene; otherwise, all effluent samples were collected until the vials were filled and no headspace remained. All vials were immediately capped with screw caps fitted with Teflon septa. Naphthalene elution experiments were done with 0.01 N  $\text{CaCl}_2$  solutions containing 10, 20, and 30% (by volume) methanol at a pore water velocity of about 70 cm/hr. Between each experiment the soil was reequilibrated with an aqueous naphthalene solution for at least 12 hours. The same procedure was followed to conduct additional experiments where the soil was initially equilibrated with an aqueous solution of naphthalene and anthracene prior to elution with 30 and 70% methanol solutions.



The soil (Eustis fine sand), organic solutes (naphthalene and anthracene), and the cosolvent (methanol) used in this study were chosen primarily because the required data for sorption from mixed solvents were available from the literature (Brusseau et al., 1991b).

Experimental results. The experimental data for elution of naphthalene at three cosolvent fractions are shown in Figure 4-5. Independent predictions were performed for each curve using the solvent flushing model. The column parameters were obtained experimentally, values for the cosolvency powers were taken from Pinal et al. (1990), and all other transport and cosolvency parameters were obtained from regression analyses using the data of Brusseau et al. (1991b). A summary of the parameter values is given in Table 4-2. The Peclet number was assumed to be constant for all cosolvent fractions. This assumption was based on experiments by Wood et al. (1990) who showed that cosolvents had very little effect on the hydrodynamic parameters for the packed material. The experimental data show all characteristic features of typical elution curves as discussed before. Considering the independent estimation of parameter values, the simulations agree reasonably well with the experimental data, except that at 20 and 30% methanol fractions the model overpredicts the peak concentrations of the elution profiles. The model is most sensitive to the value for the retardation factor in the solvent mixture ( $R^m$ ). A small reduction in  $R^m$  results in lower peak concentrations and more dispersed elution curves. Given the large confidence intervals associated with  $R^m$  and  $\alpha\beta$  (Table 4-2), which determine  $R^m$  (Equation 4-7), the fit to the experimental data may be

Table 4-2 Parameter values for the elution of naphthalene and anthracene with methanol-water mixtures from Eustis fine sand.

---

Column Parameters:

$$\begin{aligned}v &= 70 \text{ cm/hr} \\L &= 5.3 \text{ cm} \\ \rho &= 1.75 \text{ g/cm}^3 \\ \theta &= 0.33 \\ P &= 84 \text{ (78-93)}\end{aligned}$$

Transport and Cosolvency Parameters (adapted from Brusseau et al., 1991b):

	Naphthalene	Anthracene
$R^w$	6.5 (3.2-14.6)	229 (58-922)
$\omega^w$	0.57 (0.50-0.65)	0.03 (0.005-0.2)
$F^w$	0.46 (0.42-0.50)	0.52 (0.34-0.70)
$\sigma$	3.42*	4.06*
$\alpha\beta$	0.87 (0.26-1.48)	1.00 (0.67-1.33)
$a$	0.59 (0.07-1.11)	0.87 (0.71-1.03)

---

Values in parentheses give 95% confidence intervals.

\* Values from Pinal et al. (1990).

Table 4-3 Parameter values used for the simulation of elution profiles from a soil contaminated with a single-component OIL.

---

$K^w = 0.2 \text{ ml/g}$	$S^w = 500 \text{ } \mu\text{g/mL}$
$f_{oc} = 0.001$	$M_o = 60 \text{ mg/cm}^3$
$\rho/\theta = 4 \text{ g/ml}$	$P = 50$
$\sigma = 2.5$	$\alpha = \beta = 1$

---

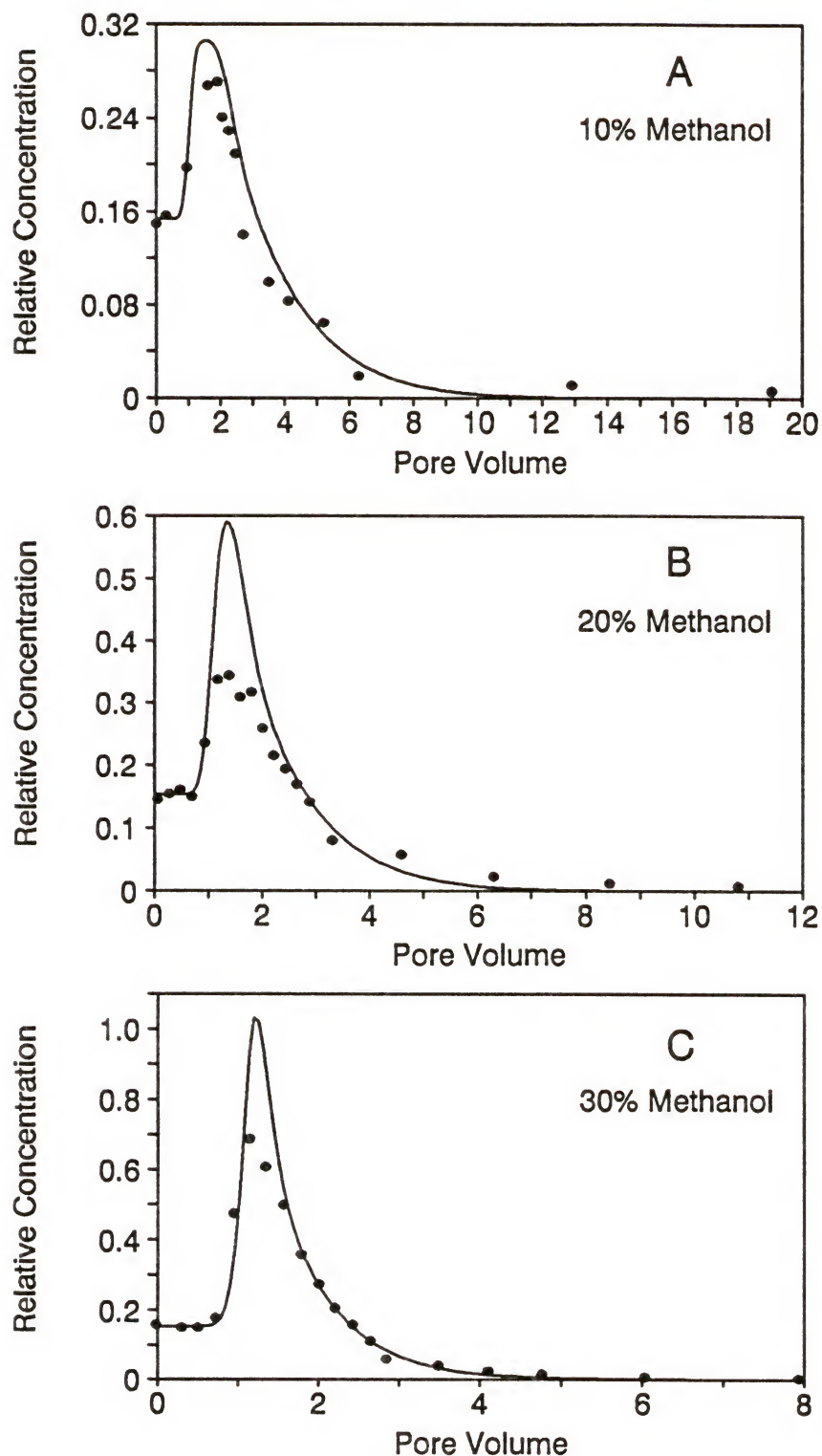


Figure 4-5 Experimental data (filled circles) and independent model predictions (solid lines) for naphthalene elution curves at three different cosolvent fractions.

considered reasonable. Another reason for the lower peak concentration at higher cosolvent fractions may be the so called relaxation time. This is the time needed by the system to adapt to the new solvent conditions. The swelling of soil organic matter may require some time, hence, the changes in mass-transfer coefficients are not instantaneous as the cosolvent passes by. This means that increase in  $k_2$  may be overestimated resulting in lower concentrations.

When solvent flushing is applied to sites contaminated with multiple components, the compounds may become separated at lower cosolvent fractions as a result of large differences between retardation factors and sorption nonequilibrium parameters (see Table 4-2). This behavior is illustrated in Figure 4-6a, where experimental data and predicted elution curves are shown for naphthalene and anthracene at a cosolvent fraction of 30%. At higher cosolvent fractions, however, such chromatographic separation is negligibly small as shown in Figure 4-6b. At 70% methanol, retardation factors for both naphthalene and anthracene are reduced to values close to 1, causing the compounds to co-elute at an earlier time. This behavior is well known in liquid chromatography where the mobile phase composition is chosen to optimize separation of compounds and minimize elution times (Snyder and Kirkland, 1979). The experimental data agree reasonably well with the simulated trends. It is therefore evident that higher cosolvent fractions are most efficient for remediation of a contaminated site. The data collected for naphthalene elution at 30% methanol (Figure 4-5c) are also included in Figure 4-6a as open circles. The agreement between the data collected from two separate experiments indicates a good reproducibility of the experimental data.



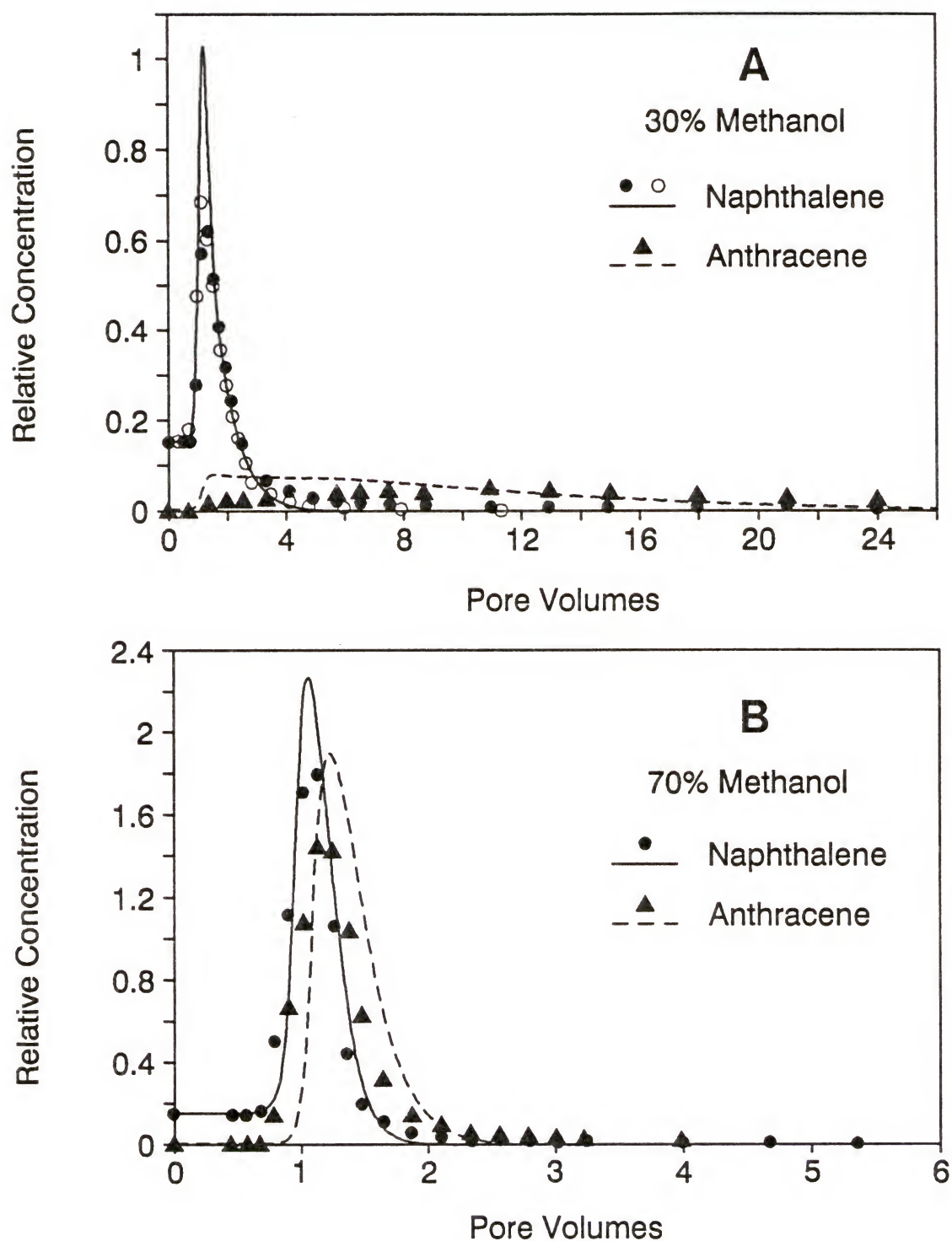


Figure 4-6 Experimental data (symbols) and independent model predictions (lines) for the binary solute elution experiments at two different cosolvent fractions.

## Case 2: Solvent Flushing of Soils Contaminated with Single-Component OILs

Dissolution processes control the concentration in the solution when the contaminant(s) are present in a separate phase. During dissolution, solutes may be sorbed onto the soil. Organic immiscible liquids (OILs) may also interact with the solid matrix of the soil, which may affect the dissolution kinetics as well as the sorption of solutes. In the following it is assumed that the interactions between the OIL and the soil have no effect on dissolution or sorption. Further, it is assumed that sorption of hydrophobic organic chemicals can be described by a linear isotherm over the entire concentration range, up to the solubility of the compound.

For dissolution of a single-component OILs or solid, the concentration in the solution will remain at the solubility limit until the separate phase is completely dissolved. Beyond this point, the contaminant is only present in the solution and sorbed phase and the concentration profiles behave the same as discussed in Case 1. Figure 4-7 shows the enhanced effect of cosolvents on the removal of a hypothetical compound. The parameter values of this hypothetical compound, given in Table 4-3, are in the same range as for TCE and PCE. The mass of OIL corresponds to a residual saturation of approximately 10% assuming a density for the OIL of 1.5 g/ml. When cosolvents are introduced in the soil, the ganglia of OIL will dissolve and decrease in size. The shrinking ganglia reduces the contact area between the solvent mixture and OIL, which reduces the rate of dissolution. On the other hand, a smaller volume of OIL in a pore makes the pore more accessible for flowing water, which means an increasing contact area between the OIL and mobile

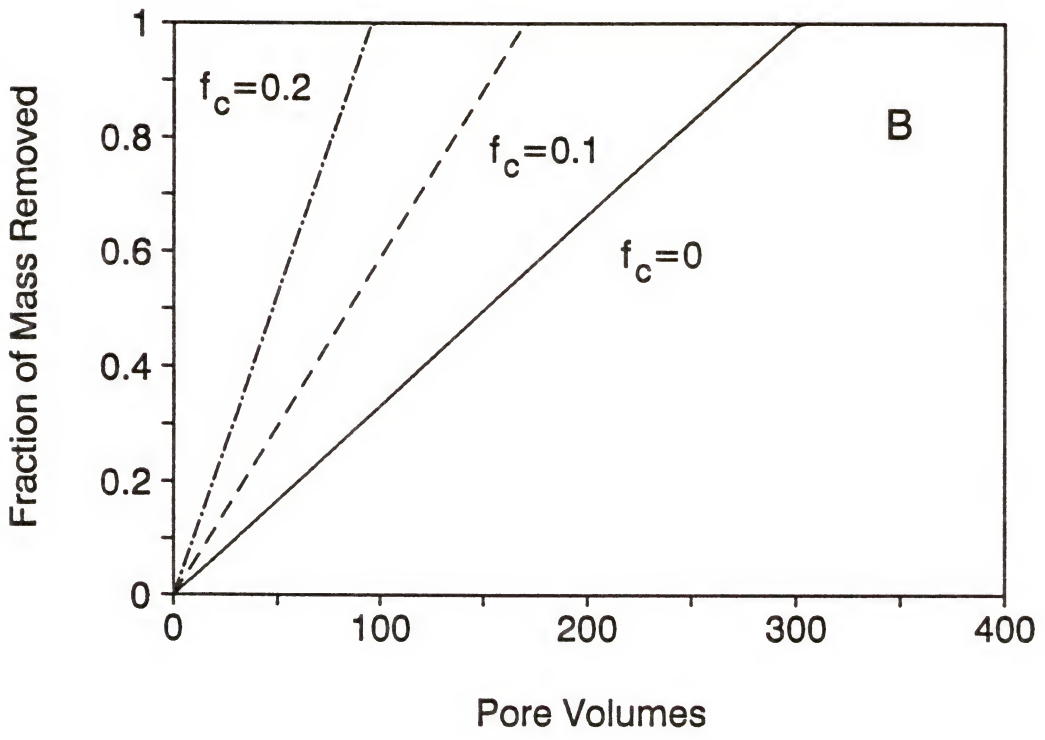
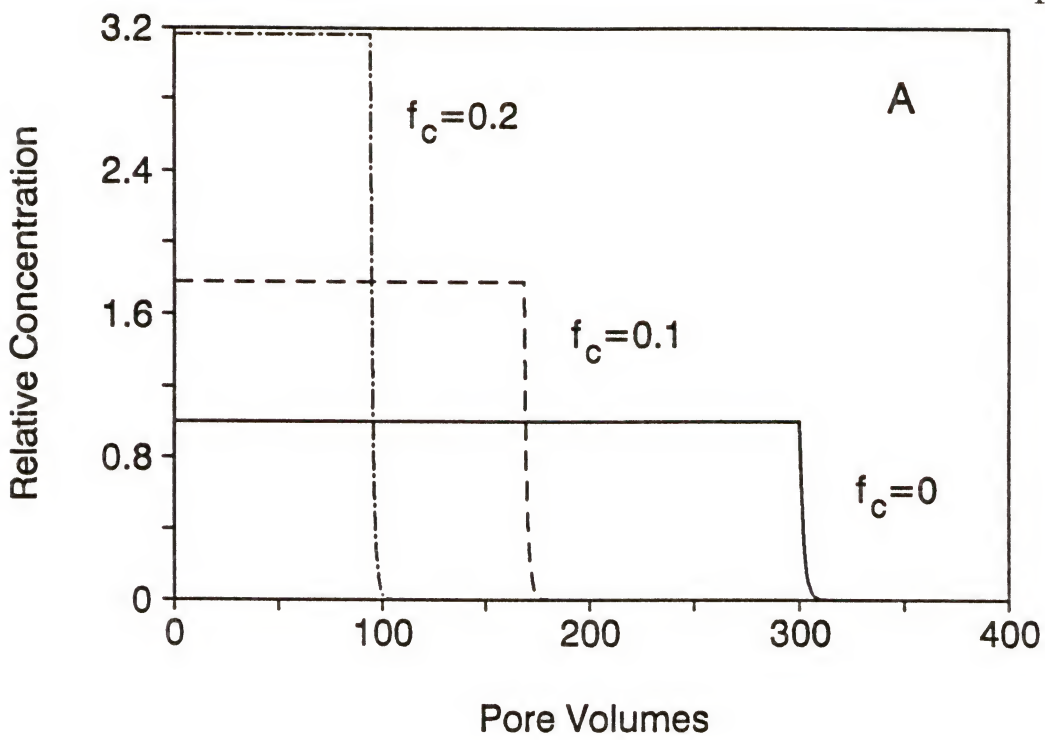


Figure 4-7     Simulated concentration and mass removal profiles for elution from a single-component OIL.

water. When the ganglia become smaller, the capillary pressure also decreases, which could mobilize the OIL and transport it as a blob to another location in the porous medium where it gets trapped or joins another ganglia of OIL. Addition of a cosolvent also reduces the surface tension between the OIL and solvent mixture. This also leads to a reduction of the capillary pressure, and facilitates mobilization of the OIL. These phenomena make the dissolution process very complex but generally lead to an enhanced recovery of the OIL.

In the model developed for this case, these processes are ignored for simplification. The change in volumetric water content ( $\theta$ ) is assumed to be small enough such that it can be treated as a constant. The Peclet number is also expected to change when the ganglia dissolve away. The blockage of pores by the OIL may initially cause more dispersion, while with decreasing amount of OIL the flow field becomes more homogeneous, reflected by a higher Peclet number. In the model, however, the Peclet number is assumed constant. Initially, the concentration equals the compound solubility in the respective solvent or solvent mixture. Once the residual phase is depleted, the solute concentration decreases very rapidly to zero, due to limited sorption, especially at higher cosolvents. For this same reason, the removal of mass may be approximated by a straight line with a slope equal to  $\theta S^m/M_o$ , where  $\theta$  is the volumetric water content;  $S^m$  the solubility in the solvent mixture (g/ml); and  $M_o$  the initial mass of OIL in the system. Note that this only holds for equilibrium conditions, and for situations where the time for desorption is negligible compared to the time for dissolution.



As evident from Figure 4-7, the plateau at which the concentration equals the solubility becomes shorter with increasing  $f_c$ . Depending on the solubility and total mass of OIL in the system, it is possible that at high cosolvent fractions all mass will instantaneously dissolve into the solution phase. This means that in some cases only one pore volume is required to clean up the soil by in situ solvent flushing.

### Case 3: Solvent Flushing of Soils Contaminated with Multi-Component OILs

To investigate the effect of solvent flushing on the elution of constituents from a complex mixture, similar experiments were conducted with coal tar as described in Chapter 3. The only difference was that in this case 0.01 N  $\text{CaCl}_2$  solutions containing 25 and 50 percent methanol were used. After the column was packed, the column was saturated with either of these two solutions. When the first effluent appeared at the end of the column, the column was sealed and allowed to equilibrate for several days. Since the system was initially equilibrated with the same solvent mixture as used for elution, the multi-component dissolution model described in Chapter 3, can be used directly by simply adjusting the solubilities for the particular solvent mixture. For a real solvent flushing experiment, the column would have been in equilibrium with water and then flushed with a solvent mixture. In this case, the solubility of each constituent would increase over the first pore volume as the cosolvent front progresses through the column. The results are shown in Figure 4-8 for 25% methanol, and 4-9 for 50% methanol. The independent model predictions were not as good as for the aqueous elution experiment. This may be attributed to several factors: (1) The cosolvent may partition into the tar phase, lowering the mole

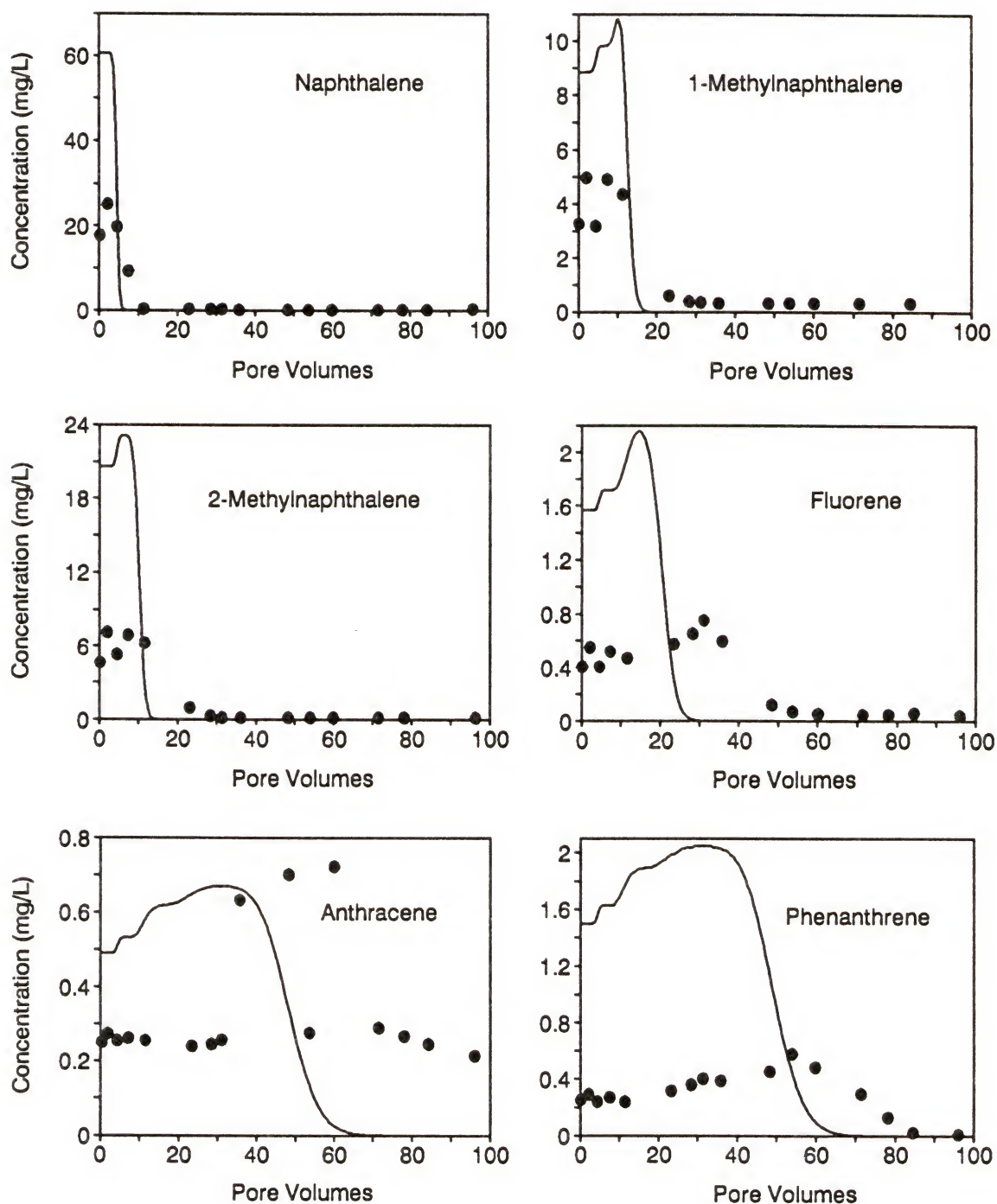


Figure 4-8 Experimental (filled circles) and predicted (lines) elution profiles for six different coal tar constituents and 25% methanol.

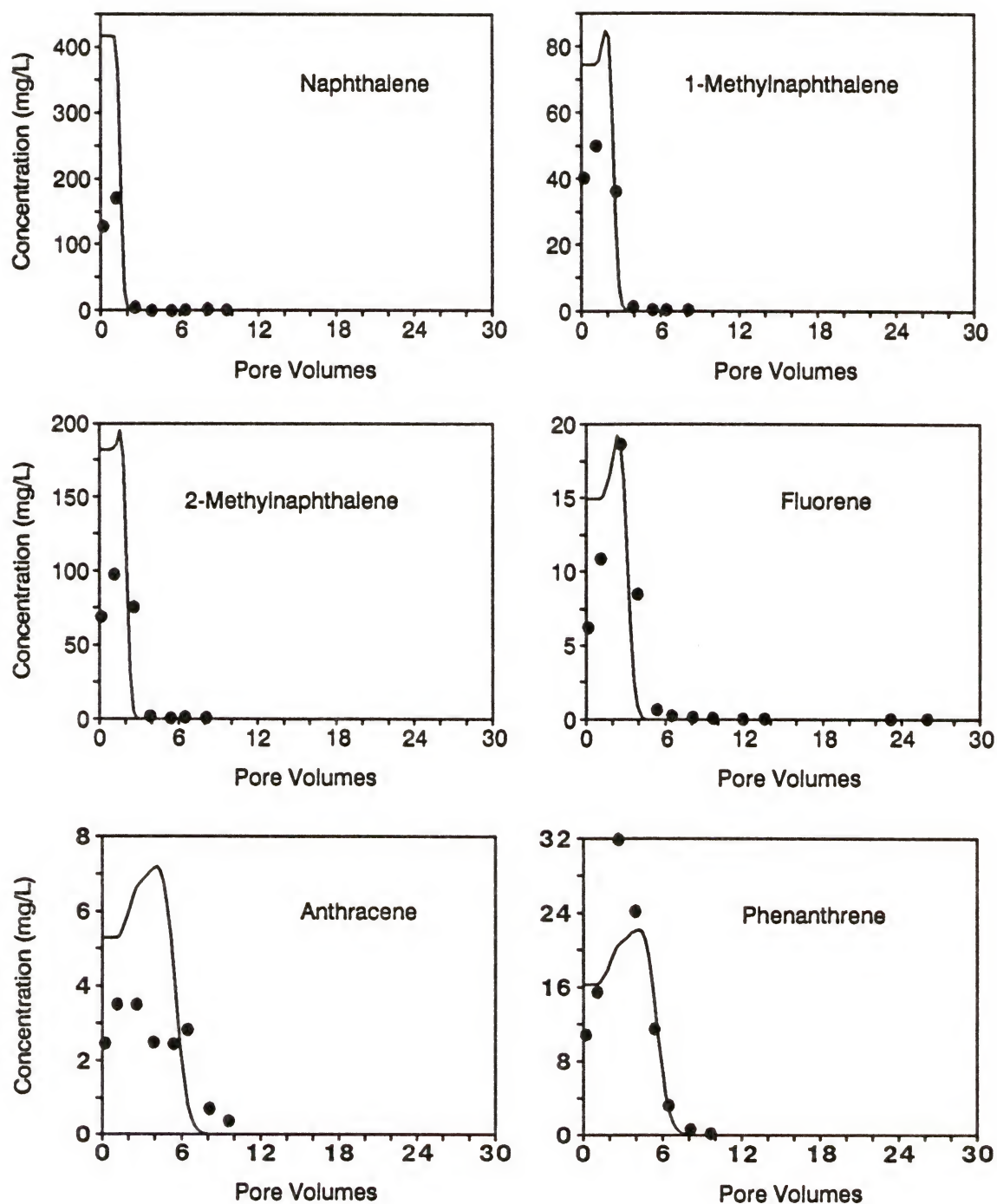


Figure 4-9 Experimental (filled circles) and predicted (lines) elution profiles for six different coal tar constituents and 50% methanol.

fraction of other constituents. This results in lower equilibrium concentrations, as is observed for most compounds. (2) The addition of a cosolvent increases the solubility of all constituents. It is, therefore, expected that significant amounts of more compounds will be removed from the tar phase. The assumption of just ten soluble compounds is therefore less appropriate for elution in cosolvent mixtures. A better qualification and quantification of the coal tar is then necessary to perform more accurate predictions. (3) The effect of cosolvents on nonideality in the tar phase (represented by  $\alpha$  in Equation 4-5) is unknown, and more research is necessary before this effect can be incorporated into models as presented here. Realizing the uncertainties in the composition of coal tar, and assumptions in the model, the independent model predictions may still be considered reasonable.

### Discussion of Solvent Flushing as a Potential Remediation Technique

The model simulations and experimental data discussed in previous sections shows that solvent flushing is an effective technique to remove organic solutes from contaminated soils. Although these results support the potential application of cosolvents in remediation techniques, several factors discussed below need to be considered before field-scale implementation.

#### Hydrologic Considerations

In situ solvent flushing technique is likely to be more successful for contaminated sites with coarse-textured soils (or aquifer solids). Low hydraulic



conductivities for the finer-textured materials would limit the solvent flushing rates, and thus require longer times for complete contaminant elution. One of the major problems with the solvent flushing technique may be the delivery of the cosolvents to the source. The presence of residual OIL reduces the hydraulic conductivity, and likely creates regions of immobile ground water. When the cosolvent is introduced into the subsurface, it may have to diffuse through these immobile water regions before it can change solubility and sorption characteristics. Since cosolvents are generally lighter than water, they tend to float to the top of the saturated zone, and bypass contaminated regions. This problem could be solved by introducing the cosolvent in a gradient. When injecting a cosolvent at a site, caution needs to be taken to avoid leaching of the cosolvent outside the hydraulically-controlled zone that may facilitate off-site transport of the contaminants. Since most cosolvents themselves are hazardous chemicals, they should be prevented from leaving the hydraulically-controlled zone.

### Selection of Cosolvents

Solvent flushing would be more appropriate for more hydrophobic chemicals (high  $\log K_{ow}$ ), such as polychlorinated biphenyls and larger polynuclear aromatic hydrocarbons, for which most other remediation techniques are inefficient. In this study, experiments were performed with methanol as the cosolvent. Other water-miscible cosolvents (e.g., ethanol or acetone) are expected to give similar results. The efficiency of each cosolvent is determined by the value of  $\alpha\beta\sigma$ ; the larger this value, the higher is the recovery efficiency for given cosolvent fraction. In general,

partially-miscible organic solvents, such as butanone, are much stronger solvents (i.e., larger  $\sigma$ ) than completely-miscible organic solvents like methanol (Pinal et al., 1990). A disadvantage of partially-miscible organic solvents, however, is the limited solubility in water: therefore, a mixture of solvents may be most efficient for soil remediation by in situ solvent flushing.

Besides the efficiency, the persistence and toxicity of the cosolvents should also be considered. After the target contaminants have been recovered, the mixed solvent must be displaced from the soil by flushing with water. Since the cosolvent is not retained by the soil, this should not take more than a few pore volumes. Any residual amounts of cosolvent should not create another hazardous problem, and must preferably be biodegraded by native microorganisms, assuming recovery and reestablishment of appropriate microbial consortia.

When the solvent with the dissolved contaminants is extracted from the subsurface, it is preferred that the cosolvent can be recovered from this waste and be reused. The cosolvents for remediation of the site may also determine the type of waste management.

### Heterogeneity

At a contaminated site, heterogeneity can be present in several ways. (1) A heterogeneous flow field may exist as a result of soil heterogeneity. Spatial variations in particle- and pore-size distribution and/or bulk density (e.g., clay lenses, layering, fracturing) will affect local hydraulic conductivity values, influencing the flow field. This type of heterogeneity is often indicated with the term physical nonequilibrium.

(2) A heterogeneous flow field may also result due to the presence of residual OIL. The entrapped OIL phase may block pore spaces causing changes in local pore water velocities. (3) Heterogeneous distribution of the OILs in ganglia and single droplets is also likely. The distribution of the OIL may be quite heterogeneous due to the periodicity of some spill events or due to the heterogeneous characteristics in the OIL entrapment as a result of soil heterogeneity. (4) Heterogeneity in sorption characteristics is yet another factor. The spatial distribution of the amount and type of organic matter in soils or aquifer materials will determine local variations in sorption and mass-transfer rates.

Heterogeneity is often accompanied by uncertainty, since heterogeneity is very difficult to characterize. A common approach to describe heterogeneity in a single dimension is to assume that transport takes place in an ensemble of independent, homogeneous stream tubes (Jury and Roth, 1990). In this section, the stream-tube model will be used to investigate the effects of heterogeneity and uncertainty on the removal of contaminants from the sorbed phase (Case 1). As an example, only the variability in flow velocities will be considered. For a heterogeneous flow field, one stream tube may be considered as a pore network with a single velocity. The porous medium, then, consists of a collection of these stream tubes that have the same volume and are not interconnected. The variability in velocity ( $v$ ) is assumed to have a log-normal distribution. The frequency distribution or density function ( $f$ ) for a log-normal distribution is defined as (Mood et al., 1974):

$$f(x) = \frac{1}{x \sigma \sqrt{2\pi}} \exp\left(-\frac{1}{2\sigma^2}(\ln x - \mu)^2\right) \quad (4-18)$$



where  $x$  is a positive random variable (in this case  $v$ );  $\mu$  is the expected value or mean of  $\ln x$  ( $-\infty < \mu < \infty$ ); and  $\sigma^2$  is the variance of  $\ln x$  ( $\sigma > 0$ ). Note that  $\ln x$  has a normal distribution. The mean and variance of  $x$  are given by:

$$E[x] = \exp\left(\mu + \frac{1}{2}\sigma^2\right) \quad (4-19)$$

$$\text{var}[x] = \exp(2\mu + 2\sigma^2) - \exp(2\mu + \sigma^2) \quad (4-20)$$

A model was developed that generated random numbers with a log-normal distribution. This model was added as a subroutine to the solvent-flushing model discussed for Case 1. Monte Carlo simulations were then performed for naphthalene with  $v$  varying according to a log-normal distribution. From these simulations an average elution profile was calculated, along with the corresponding standard deviations.

For most stream-tube models usually only advective flow is considered, which means that the solution moves through the pores with a sharp front. This also means that the properties affected by the cosolvent have to change as an abrupt step function, which gave a numerically unstable solution. To avoid this problem, the dispersion term was maintained in the model, and assumed to be the same in each stream tube and equal to the overall dispersion coefficient. Dispersion, most likely, also occurs at the pore scale due to molecular diffusion and drag forces on the pore walls, but will probably be different from the large scale dispersion. If the dispersion coefficient is assumed to be linearly related to velocity (Equation 1-5), the Peclet number is independent of velocity. This means that for a variable velocity only the



Damkohler number ( $\omega$ ) changes. Although a relationship between the first-order, mass-transfer rate coefficient ( $k$ ) and velocity is suspected (see Chapter 3), it is assumed here that  $k$  can be treated as a constant over the velocity range covered by the log-normal distribution. The mean velocity was taken from Table 4-2 ( $v=70$  cm/hr), while an arbitrary standard deviations of 70 cm/hr was assumed. The results of the Monte Carlo simulations are shown in Figure 4-10. The top figure shows the elution profile for a  $v=70$  cm/hr and the average elution profile calculated from the Monte by the Monte Carlo simulations. The extreme values for the velocity generated by the log-normal distribution were 0.035 and 769 cm/hr. Even though the equations for the solvent flushing model are strongly nonlinear, a variable velocity does not have a great influence on the elution profile. The effects increase with increasing standard deviation of the velocity. Monte Carlo simulations with a standard deviation of 20 cm/hr showed that the average elution profile was essentially similar to the elution profile simulated with the average velocity. These results suggest that the model simulations presented in Case 1 are a reasonable estimation of the average concentration in a cross sectional area of a plume in a three-dimensional field. In reality, of course, stream-tube models are a poor representation of the heterogeneity, and more complex models need to be developed to get a better understanding of the effects of heterogeneity on the solvent flushing technique. On the other hand, when little information is available on the heterogeneity of the system, the average velocity gives a reasonable first estimation of the expected elution profile.

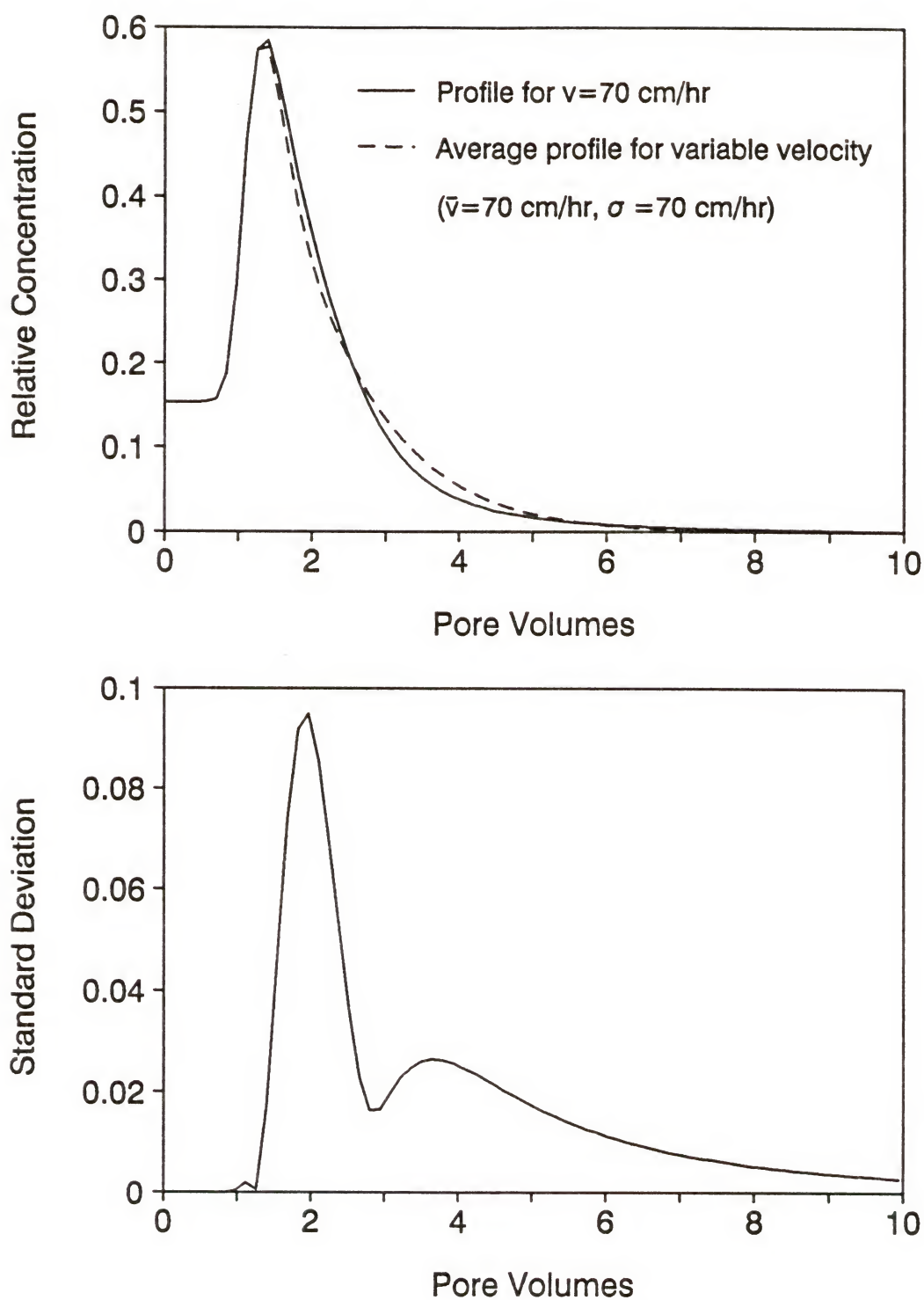


Figure 4-10 Results of Monte Carlo simulations for variable velocity.

The standard deviations associated with the average elution profile are also included in Figure 4-10. It is evident that the uncertainty in the elution profiles is greatest for the peak. The standard deviation is initially zero, because this portion of the curve is only determined by the retardation factor.

### External Factors

The selection of a remediation technique is not only determined by physico-chemical factors of the environment. Political, social and economical factors may in fact carry more weight in the decision-making process. Current political restrictions, for example, do not allow the injection of any foreign additive into the subsurface. The remediation of a site should also have minimum impact on the people living in the surrounding area. Finally, the cost is a very important factor that influences the decision for a particular remediation technique.

The limitations discussed here apply essentially to all remediation techniques that involve the injection of some chemical or microbial additives. Although these limitations seem very severe and more research is required to fully understand, the failure of more traditional techniques, such as pump-and-treat, require new technologies that enhance the remediation of contaminated sites. In that sense, solvent flushing may be considered as a potential alternative in the near future.

The models and experimental data discussed in this chapter oversimplify and even ignore some of the processes that occur in reality. Nevertheless, this study provides a first insight in the effects of cosolvents on the removal of organic chemicals from contaminated soils. More complete models that include three-

dimensional flow, heterogeneity, unsaturated flow conditions, OIL mobilization, etc., need to be developed to evaluate the full range of problems associated with field-scale applications of solvent flushing for remediation of contaminated sites.



## CHAPTER 5

### SUMMARY AND CONCLUSIONS

In this dissertation the chemodynamics of complex waste mixtures were discussed to be able to assess the contamination problem at industrial waste disposal/spill sites. Complex waste mixtures of environmental concern considered here were multi-component, organic immiscible liquids (OILs). Two major processes determine the dynamics of organic chemicals in saturated soils and aquifer media contaminated with OILs: dissolution, and sorption. Dissolution controls the rate at which contaminants are released from regions near the source (near field), while sorption controls the rate of transport of the contaminants in the far-field region. Both processes were discussed at a mechanistic level, and their impact on contamination and remediation was evaluated.

The partitioning between the solution phase and multi-component OILs can be described by Raoult's law, i.e., the equilibrium concentration is equal to the mole fraction in the OIL phase times the (super-cooled) liquid solubility. This means that the concentrations are always below their solubility. Model simulations for multi-component dissolution in a one-dimensional, homogeneous column showed that with a decrease in effluent concentration of one of the constituent, the concentration of

all other constituents increased, as a result of changes in mole fraction. This has an important impact on the evaluation of contaminated sites, since contaminant levels of certain components could increase over time. For nonideal behavior, the activity coefficients in the organic phase exceed one, resulting in higher solute concentrations in the aqueous phase, which is favorable for remediation, but unfavorable for contamination scenarios.

The model was tested for two sets of experimental data: (1) dissolution from a synthetic mixture of decane, tetrachloroethene (PCE), and naphthalene, and (2) dissolution from a sand, artificially coated with a thin film of coal tar. The synthetic mixture showed significant nonideal behavior for naphthalene and PCE, due to the different nature of the three chemicals. The activity coefficients could be reasonably predicted with the UNIFAC model. The column experiment conducted with the decane/PCE/naphthalene exhibited nonequilibrium conditions due to high pore-water velocities. The aqueous elution profiles for six constituents from the tar-contaminated sand, showed good agreement with the model predictions, considering the uncertainty associated with the input data.

The dissolution studies showed that Raoult's law provides a reasonable estimate for the dissolution of complex mixtures in a dynamic system. Nonideal conditions may affect the equilibrium concentrations in the solution phase, but considering the high uncertainty associated with most model parameters, nonideal behavior of the chemicals can be ignored as a first approximation. In realistic field situations, the limited contact area between the OIL and water phases, and/or slow

diffusion of the constituents through the organic phase may cause severe nonequilibrium conditions.

The mechanisms of desorption and multi-component dissolution are very similar. Based on this conclusion, the release of organic contaminants from soils contaminated with complex waste mixtures was evaluated using nonequilibrium sorption models. The mechanism is determined by the location and characteristics of the organic matter or OIL phase. Two primary mechanisms were reviewed: intra-organic matter diffusion, and retarded intra-particle diffusion. Column experiments were conducted to study sorption by three different type of contaminated soils: (1) a decane-treated Eustis fine sand; (2) a soil contaminated with coal tar; and (3) and aged tar-contaminated soil.

For all three sorbents, it was assumed that intra-organic matter diffusion was the rate-limiting mechanism. The bicontinuum first-order mass-transfer model was used to fit the data, and the obtained mass-transfer parameters were compared to a collection of data for natural sorbents. The decane-treated Eustis soil had a much higher sorption capacity than the untreated soil, but the mass-transfer rate parameters were in the same range as observed for natural soils. The observed mass-transfer rate coefficients for the soil contaminated with coal tar were extremely small, indicating that the release of organic contaminants from the tar phase is very slow. The increase in mass-transfer constraints was attributed to the interactions of the coal tar with the soil matrix and other debris, codisposed with the tar. Severe

phase, but also means that it is more difficult to recover the contaminants. For the aged tar-contaminated soil, the mass-transfer coefficients were slightly smaller than for the natural sorbents. It was speculated that with aging, the structure of the tar becomes more open and less hydrophobic, hence the diffusion through the tar is enhanced.

The presence of cosolvents at a site will increase the solubility, decrease sorption, and enhance mass transfer through the sorbent. These properties lead to higher solution concentrations and higher mobility of the contaminants. This is unfavorable for contamination, but favorable for remediation. Solvent flushing was therefore proposed as a potential remediation technique. Several scenarios were evaluated, and showed that cosolvents are a very effective additive to remove organic chemicals from contaminated sites. Several restrictions, however, hinder the current implementation of this technique in the field.

The processes discussed in this dissertation only control the release and transport of organic chemicals at a local scale. Heterogeneity of the subsurface may affect the overall problem of contamination and remediation at a larger scale. Nevertheless, it is important to understand and quantify processes at a local scale to assess their impact on a larger scale, and to be able to extrapolate information to other sites. The rate of these processes is also important to assess the potential for remediation techniques in which local processes play an important role, such as bioremediation. In the near future, more research is needed in prevention, risk analyses, and large scale studies that integrate processes at different levels.



## APPENDIX A NUMERICAL SOLUTION FOR MULTI-COMPONENT ELUTION

### Nondimensional Transport Equation

The one-dimensional solute transport equation for dissolution from a multi-component OIL was derived in Chapter 3. In nondimensional parameters this equation is given by:

$$\frac{\partial C_i}{\partial p} + \frac{MW_i}{\theta S_i} \frac{\partial(N_o C_i)}{\partial p} - \frac{1}{P} \frac{\partial^2 C_i}{\partial X^2} - \frac{\partial C_i}{\partial X} \quad (3-15)$$

Initial condition:

$$C_i = \frac{m_i}{N_o} \frac{S_i}{MW_i} \quad (3-3)$$

Top boundary condition:

$$\left( C_i - \frac{1}{P} \frac{\partial C_i}{\partial X} \right)_{X=0} = 0 \quad (3-18)$$

Bottom boundary condition:

$$\left. \frac{\partial C_i}{\partial X} \right|_{X=1} = 0 \quad (3-19)$$

### Numerical Solution

The differential equations were solved using the Crank-Nicolson central finite difference technique, where

$$\frac{\partial C_i}{\partial p} = \frac{C_{ij}^{t+1} - C_{ij}^t}{\Delta p} \quad (\text{A-1})$$

$$\frac{MW_i}{\theta S_i} \frac{\partial (N_o C_i)}{\partial p} = \frac{MW_i}{\theta S_i \Delta p} (N_{oj}^{t+1} C_{ij}^{t+1} - N_{oj}^t C_{ij}^t) \quad (\text{A-2})$$

$$\frac{1}{P} \frac{\partial^2 C_i}{\partial X^2} = \frac{1}{2P} \left( \frac{C_{ij+1}^{t+1} - 2C_{ij}^{t+1} + C_{ij-1}^{t+1}}{(\Delta X)^2} + \frac{C_{ij+1}^t - 2C_{ij}^t + C_{ij-1}^t}{(\Delta X)^2} \right) \quad (\text{A-3})$$

$$\frac{\partial C_i}{\partial X} = \frac{1}{2} \left( \frac{C_{ij+1}^{t+1} - C_{ij-1}^{t+1}}{2 \Delta X} + \frac{C_{ij+1}^t - C_{ij-1}^t}{2 \Delta X} \right) \quad (\text{A-4})$$

subscript  $j$  refers to the  $j^{\text{th}}$  node, and superscript  $t$  refers to the time step.

Combining Equations A-1 through A-4 with Equation 3-15 gives:

$$\begin{aligned} & \frac{1}{\Delta p} (C_{ij}^{t+1} - C_{ij}^t) + \frac{1}{\theta S_i \Delta p} (N_{oj}^{t+1} C_{ij}^{t+1} - N_{oj}^t C_{ij}^t) \\ & - \frac{1}{2P(\Delta X)^2} (C_{ij+1}^{t+1} - 2C_{ij}^{t+1} + C_{ij-1}^{t+1} + C_{ij+1}^t - 2C_{ij}^t + C_{ij-1}^t) \\ & - \frac{1}{4\Delta X} (C_{ij+1}^{t+1} - C_{ij-1}^{t+1} + C_{ij+1}^t - C_{ij-1}^t) \end{aligned} \quad (\text{A-5})$$

after rearrangement:

$$\begin{aligned}
 & \left( -\frac{1}{2P(\Delta X)^2} - \frac{1}{4\Delta X} \right) C_{i,j-1}^{t+1} + \left( \frac{1}{\Delta p} + \frac{N_{oj}^{t+1}}{\theta S_i \Delta p} + \frac{1}{P(\Delta X)^2} \right) C_{i,j}^{t+1} \\
 & + \left( -\frac{1}{2P(\Delta X)^2} - \frac{1}{4\Delta X} \right) C_{i,j+1}^{t+1} - \left( \frac{1}{2P(\Delta X)^2} + \frac{1}{4\Delta X} \right) C_{i,j-1}^t \quad (A-6) \\
 & + \left( \frac{1}{\Delta p} + \frac{N_{oj}^t}{\theta S_i \Delta p} - \frac{1}{P(\Delta X)^2} \right) C_{i,j}^t + \left( \frac{1}{2P(\Delta X)^2} - \frac{1}{4\Delta X} \right) C_{i,j+1}^t
 \end{aligned}$$

or

$$-a_1 C_{i,j-1}^{t+1} + b_{i,j}^{t+1} C_{i,j}^{t+1} + a_2 C_{i,j+1}^{t+1} - a_1 C_{i,j-1}^t + b_{i,j}^t C_{i,j}^t - a_2 C_{i,j+1}^t \quad (A-7)$$

where:

$$a_1 = \frac{1}{2P(\Delta X)^2} + \frac{1}{4\Delta X} \quad (A-8)$$

$$a_2 = -\frac{1}{2P(\Delta X)^2} + \frac{1}{4\Delta X} \quad (A-9)$$

$$b_{i,j}^{t+1} = \frac{1}{\Delta p} + \frac{N_{oj}^{t+1}}{\theta S_i \Delta p} + \frac{1}{P(\Delta X)^2} \quad (A-10)$$

$$b_{i,j}^t = \frac{1}{\Delta p} + \frac{N_{oj}^t}{\theta S_i \Delta p} - \frac{1}{P(\Delta X)^2} \quad (A-11)$$

The numerical expression for the top boundary condition given by Equation A-18 is:  
after rearrangement:

$$\left( \frac{C_{i,2}^{t+1} + C_{i,1}^{t+1}}{2} \right) - \frac{1}{P} \left( \frac{C_{i,2}^{t+1} - C_{i,1}^{t+1}}{2} \right) = 0 \quad (\text{A-13})$$

$$\left( \frac{1}{2} + \frac{1}{P\Delta X} \right) C_{i,1}^{t+1} + \left( \frac{1}{2} - \frac{1}{P\Delta X} \right) C_{i,2}^{t+1} = 0 \quad (\text{A-12})$$

or

$$d_1 C_{i,1}^{t+1} + d_2 C_{i,2}^{t+1} = 0 \quad (\text{A-14})$$

where

$$d_1 = \frac{1}{2} + \frac{1}{P\Delta X} \quad (\text{A-15})$$

$$d_2 = \frac{1}{2} - \frac{1}{P\Delta X} \quad (\text{A-16})$$

The numerical expression for the bottom boundary condition given by Equation 3-19 is:

$$C_{i,l}^{t+1} - C_{i,l-1}^{t+1} = 0 \quad (\text{A-17})$$

The numerical problem reduces to solving the following system of equations:

$$d_1 C_{i,1}^{t+1} + d_2 C_{i,2}^{t+1} = 0 \quad (\text{A-13})$$



$$- a_1 C_{i,j-1}^{t+1} + b_{i,j}^{t+1} C_{i,j}^{t+1} + a_2 C_{i,j+1}^{t+1} - a_1 C_{i,j-1}^t + b_{i,j}^t C_{i,j}^t - a_2 C_{i,j+1}^t \quad (\text{A-7})$$

$$C_{i,l-1}^{t+1} - C_{i,l}^{t+1} = 0 \quad (\text{A-17})$$

or in matrix form:

$$\begin{bmatrix} d_1 & d_2 & & & \\ -a_1 & b_{i,2}^{t+1} & a_2 & & \\ & -a_1 & b_{i,3}^{t+1} & a_2 & \\ & & \ddots & \ddots & \\ & & & -a_2 & b_{i,l-1}^{t+1} & a_2 \\ & & & & 1 & -1 \end{bmatrix} \begin{pmatrix} C_{i,1}^{t+1} \\ C_{i,2}^{t+1} \\ C_{i,3}^{t+1} \\ \vdots \\ C_{i,l-1}^{t+1} \\ C_{i,l}^{t+1} \end{pmatrix} = \begin{pmatrix} 0 \\ a_1 C_{i,1}^t + b_{i,2}^t C_{i,2}^t - a_2 C_{i,3}^t \\ a_1 C_{i,2}^t + b_{i,3}^t C_{i,3}^t - a_2 C_{i,4}^t \\ \vdots \\ a_1 C_{i,l-2}^t + b_{i,l-1}^t C_{i,l-1}^t - a_2 C_{i,l}^t \\ 0 \end{pmatrix}$$

This system was solved by Thomas algorithm. Since coefficient  $b^{t+1}$  is unknown, an iteration procedure is required. This was performed as follows: the above system was solved for  $C^{t+1}$  using the old value of  $N_o$  ( $N_o^t$ ), then the mass of each compound left in the OIL phase was calculated based on eqn.[4] using the new  $C^{t+1}$  and old  $N_o$  values. Based on the mass, a new  $tmol$  was calculated according to Equation 3-4. This new value is compared to the value for  $tmol$  from the previous iteration. When the difference was smaller than a particular value ( $10^{-18}$ ) the iteration was terminated and the program continued with the next time step.

Table A-1 Computer code for the multi-component dissolution model.

---

```

C      Program DOMCOIL.FOR
C      Dissolution Of Multi-Component Organic Immiscible
C      Liquids      Version 1. Equilibrium Conditions
C
C      This program provides a numerical solution to the
C      one-dimensional solute transport equation including
C      dissolution from a multi-component organic immiscible
C      liquid (OIL). Equilibrium dissolution is described by
C      Raoult's law. Sorption is ignored.
C
C      c = concentration (g/ml)
C      co = c at previous time step
C      c0 = initial equilibrium concentration based on Raoult's
C           law (g/ml)
C      cm = maximum concentration in water (crystal solubility,
C           g/ml)
C      dp = timestep in pore volumes
C      dx = relative distance between each node
C      err = error, change in tmol between iterations
C      filin = input filename
C      filout = output filename
C      insol = mass in solution phase (g/ml)
C      inoil = mass in OIL (g/cm3 soil)
C      l = number of nodes
C      m = mass in OIL phase (g/cm3 soil)
C      mo = m at previous time step
C      m0 = initial mass in OIL (g/cm3 soil)
C      mberr = error in mass balance
C      mp = mass of pitch (g/cm3 soil)
C      mw = molecular weight of compound (g/mole)
C      mwp = molecular weight of pitch (g/mole)
C      n = number of compounds (max. 15)
C      out = cumulative mass in the effluent that left the
C           column (g/cm3 soil)
C      p = help variable
C      pe = Peclet number
C      pv = pore volume
C      pvwrt = counter for written output
C      s0 = (super-cooled) liquid solubility (g/ml)
C      s = (super-cooled) liquid solubility (mol/ml)
C      tm = initial number of moles in OIL (moles/cm3 soil)
C      tm1 = tm from previous iteration
C      tmol = total moles in OIL (moles/cm3 soil)
C      tmolo = tmol from previous time step
C      tmol1 = tmol from previous iteration
C      tot0 = initial total mass (g/cm3 soil)
C      tot = total mass for mass balance (g/cm3 soil)
C      totp = total number of pore volumes to be simulated

```

```

C      tp = total number of time steps
C      wc = water content (ml/cm^3 soil)
C      wrt = time step at which output is desired
C      a,r,a1,a2,b,bo,c1,c2,d1,d2 = elements of matrix system
C
      CHARACTER          filout*12,filin*12
      INTEGER            i,j,p,l,tp,n
      DOUBLE PRECISION   pe,wc,pv,dp,dx,totp,wrt,pvwrt,err,mberr
      DOUBLE PRECISION   s0(15),s(15),mw(15),m(52,15),m0(15)
      DOUBLE PRECISION   mo(52,15),c(52,15),co(52,15)
      DOUBLE PRECISION   c0(15),cm(15)
      DOUBLE PRECISION   mp,mwp,tm,tml,tmol(52),tmol1(52)
      ,tmolo(52)
      D O U B L E          P R E C I S I O N
a(52,3),r(52),a1,a2,b(52),bo(52,15),c1,c2,d1,d2
      D O U B L E          P R E C I S I O N
inoil(15),insol(15),out(15),tot(15),tot0(15)
C
      PRINT *, ' '
      PRINT *, '*****'
      PRINT *, '*'
      PRINT *, '*'
      PRINT *, '          DOMCOIL'
      PRINT *, '*'
      PRINT *, '*'      Dissolution Of Multi-Component OILs
      PRINT *, '*'      1. Equilibrium Conditions
      PRINT *, '*'
      PRINT *, '*'      Soil and Water Science Department
      PRINT *, '*'      University of Florida
      PRINT *, '*'      1992
      PRINT *, '*'
      PRINT *, '*****'
      PRINT *, ' '
C
C      Define input and output file
C
      PRINT *, 'Input file:'
      READ(*,'(A)') filin
      OPEN(4,FILE=filin)
      PRINT *, 'Output file:'
      READ(*,'(A)') filout
      OPEN(5,FILE=filout)
      PRINT *, ' '
C
C      Read input data
C
      READ(4,*) n
      DO 5 j=1,n
          READ(4,*) m0(j),mw(j),s0(j),cm(j)
5  CONTINUE
      READ(4,*) mp
      READ(4,*) mwp
      READ(4,*) wc

```

```

      READ(4,*) pe
      READ(4,*) totp
C
C      Define other parameter values
C
      l=52
      dx=0.02
      wrt=totp/200
      pvwrt=0.0
      pv=0.0
      dp=AMIN1(dx,pe*dx*dx)
      tp=IDNINT(totp/dp)
C
C      Define initial condition
C
      DO 10 j=1,n
          s(j)=s0(j)/mw(j)
          tot0(j)=m0(j)
          out(j)=0.0
10  CONTINUE
      tm=mp/mwp
      DO 15 j=1,n
          tm=tm+m0(j)/mw(j)
15  CONTINUE
C
      1      DO 20 j=1,n
          c0(j)=m0(j)*s(j)/tm
          IF (c0(j).GT.cm(j)) THEN
              c0(j)=cm(j)
          ENDIF
          m0(j)=tot0(j)-wc*c0(j)
20  CONTINUE
      err=0.0
      tml=tm
      tm=mp/mwp
      DO 25 j=1,n
          tm=tm+m0(j)/mw(j)
25  CONTINUE
      err=AMAX1(err,ABS(tml-tm))
      IF (err.GT.1.0E-18) GOTO 1
C
      DO 30 j=1,n
          c(1,j)=(1/(pe*dx)-0.5)*c0(j)/(0.5+1/(pe*dx))
30  CONTINUE
      DO 35 i=2,l
          tmol(i)=tm
          DO 40 j=1,n
              m(i,j)=m0(j)
              c(i,j)=c0(j)
40  CONTINUE
35  CONTINUE

```



```

C
C   Define matrix constants
C
a1=1/(2*pe*dx*dx)+1/(4*dx)
a2=-1/(2*pe*dx*dx)+1/(4*dx)
c1=-1/(pe*dx*dx)+1/dp
c2=-1/(pe*dx*dx)-1/dp
d1=0.5+1/(pe*dx)
d2=0.5-1/(pe*dx)
C
C   Start simulation
C
DO 45 p=1,tp
    pv=p*dp
C
C   Save previous values
C
    DO 50 i=1,l
        tmolo(i)=tmol(i)
        DO 55 j=1,n
            co(i,j)=c(i,j)
            mo(i,j)=m(i,j)
55    CONTINUE
50    CONTINUE
C
C   Define coefficients that are a function of pv and x
C
    DO 60 j=1,n
        DO 65 i=2,l-1
            bo(i,j)=1/dp+tmolo(i)/(wc*dp*s(j))-1/(pe*dx*dx)
65    CONTINUE
60    CONTINUE
C
    2    DO 70 j=1,n
        DO 75 i=2,l-1
            b(i)=1/dp+tmol(i)/(wc*dp*s(j))+1/(pe*dx*dx)
75    CONTINUE
C
C   Solve for concentration
C
a(1,2)=d1
a(1,3)=d2
DO 80 i=2,l-1
    a(i,1)=-a1
    a(i,2)=b(i)
    a(i,3)=a2
80    CONTINUE
a(1,1)=1.0
a(1,2)=-1.0
C
r(1)=0.0

```

```

DO 85 i=2,l-1
    r(i)=a1*co(i-1,j)+bo(i,j)*co(i,j)-
+      a2*co(i+1,j)
85    CONTINUE
    r(1)=0.0

C
    CALL THMS(a,r,c,l,cm,j)
C
C
    If concentration is too small, set to 0
C
DO 90 i=2,l
    IF (c(i,j).LE.1.0E-18) THEN
        c(i,j)=0.0
    ENDIF
90    CONTINUE

C
C
    Calculate mass in OIL
C
DO 95 i=2,l-1
    m(i,j)=mo(i,j)+wc*dp*(a1*(co(i-1,j)+
+      c(i-1,j))+c2*c(i,j)+c1*co(i,j)
+      -a2*(co(i+1,j)+c(i+1,j)))
95    CONTINUE
70    CONTINUE
    err=0.0
DO 100 i=2,l-1
    tmol1(i)=tmol(i)
    tmol(i)=mp/mwp
    DO 105 j=1,n
        tmol(i)=tmol(i)+m(i,j)/mw(j)
105    CONTINUE
    err=AMAX1(err,ABS(tmol1(i)-tmol(i)))
100    CONTINUE
    IF (err.GT.1.0E-18) GOTO 2

C
C
    Mass balance
C
    mberr=0.0
DO 110 j=1,n
    out(j)=out(j)+0.5*dp*wc*(c(1,j)+co(1,j))
    inoil(j)=0.0
    insol(j)=0.0
    DO 115 i=2,l-1
        inoil(j)=inoil(j)+dx*m(i,j)
        insol(j)=insol(j)+dx*wc*c(i,j)
115    CONTINUE
    tot(j)=inoil(j)+insol(j)+out(j)
    mberr=AMAX1((1-tot(j)/tot0(j)),mberr)
110    CONTINUE

C
C
    Write the solution to the output file.

```

```

C      pvwrt=pvwrt+dp
C      IF (pvwrt.GT.wrt) THEN
C          WRITE(5,200) pv,(c(1,j)*1000000, j=1,n)
C          WRITE(*,201) pv,mberr*100
C          pvwrt=0.0
C      ENDIF
C
C      45 CONTINUE
C
C      200 FORMAT(1X,F10.2,15E12.5)
C      201 FORMAT(1X,'PV:',F12.2,5X,'Error in mass balance:',
C          +      F8.3,'%')
C      END
C
C      -----
C      Subroutine THMS
C      This subroutine solves the problem:  $Ax=r$  where A is a
C      tridiagonal matrix (lxl), by Thomas algorithm.
C
C      a = elements of tridiagonal matrix A
C      x = elements of solution vector x
C      r = elements of residual vector r
C
C      SUBROUTINE THMS(a,r,x,l,cm,j)
C
C      INTEGER i,j,k,l
C      DOUBLE PRECISION a(52,3),r(52),x(52,15),s,m,cm(15)
C
C      Thomas algorithm
C
C      DO 10 i=2,l
C          m=a(i,1)/a(i-1,2)
C          a(i,2)=a(i,2)-m*a(i-1,3)
C          r(i)=r(i)-m*r(i-1)
C      10 CONTINUE
C
C      Backward substitution
C
C      DO 20 i=0,l-1
C          k=l-i
C          s=r(k)
C          IF (k.NE.1) THEN
C              s=s-a(k,3)*x(k+1,j)
C          ENDIF
C          x(k,j)=s/a(k,2)
C
C      If concentration exceeds cm, set to cm
C
C      IF (x(k,j).GT.cm(j)) THEN
C          x(k,j)=cm(j)

```

```
      ENDIF  
20  CONTINUE  
    RETURN  
  END
```

---



Table A-2    Input file for the program DOMCOIL used to simulate the data in Figure 3-2 (for clarification of input parameters see computer code).

---

2				
2.00E-02	165.83	2.44E-04	2.44E-04	
4.92E-03	128.16	1.14E-04	3.00E-05	
3.59E-02				
142.28				
0.44				
24.4				
2000				

---

APPENDIX B  
EQUILIBRIUM AND NONEQUILIBRIUM SORPTION PARAMETERS  
COMPILED FROM THE LITERATURE

Sorbent	Compound	$f_{oc}$ (%)	$v$ (cm/hr)	K (ml/g)	F	$k_2$ (hr <sup>-1</sup> )	k (hr <sup>-1</sup> )	log K <sub>oc</sub>	rf <sup>a</sup>
Aquifer	Toluene	0.015	40	0.11	0.22	4.9	6.3	2.87	A
Aquifer	o-Xylene	0.015	40	0.11	0.32	6.9	10.1	2.87	A
Aquifer	m- or p-Xylene	0.015	40	0.16	0.24	6.5	8.5	3.03	A
Aquifer	Ethylbenzene	0.015	40	0.11	0.37	7.5	11.9	2.87	A
Aquifer	n-Propylbenzene	0.015	40	0.24	0.33	9.7	14.6	3.20	A
Aquifer	isopropylbenzene	0.015	40	0.18	0.45	7.1	12.8	3.07	A
Aquifer	2-Ethyltoluene	0.015	40	0.16	0.40	9.2	15.3	3.03	A
Aquifer	3- or 4-Ethyltoluene	0.015	40	0.21	0.36	7.8	12.2	3.14	A
Aquifer	1,2,3-Trimethylbenzene	0.015	40	0.14	0.37	9.8	15.5	2.98	A
Aquifer	1,2,4-Trimethylbenzene	0.015	40	0.19	0.38	7.4	11.9	3.11	A
Aquifer	1,2,5-Trimethylbenzene	0.015	40	0.21	0.40	8.0	13.2	3.14	A
Aquifer	p-Xylene	0.02	89	0.10	0.54	13.8	29.7	2.70	B1
Aquifer	p-Xylene	0.02	5	0.10	0.72	0.5	1.7	2.70	B1
Aquifer	Naphthalene	0.02	45	0.21	0.52	6.2	12.8	3.02	B1
Aquifer	Naphthalene	0.02	5	0.22	0.67	0.3	0.86	3.04	B1
Aquifer	Tetrachloroethene	0.02	45	0.23	0.30	4.9	6.9	3.07	B1
Aquifer	Tetrachloroethene	0.02	5	0.26	0.40	0.2	0.37	3.11	B1
Aquifer	1,4-Dichlorobenzene	0.02	90	0.15	0.71	16.8	58.7	2.88	B1
Aquifer	1,4-Dichlorobenzene	0.02	5	0.10	0.38	0.8	1.4	2.70	B1
Aquifer	Naphthalene	0.1	53	0.22	0.00	4.3	4.3	2.35	B1
Aquifer	Naphthalene	0.1	6	0.19	0.10	0.7	0.8	2.28	B1
Aquifer	Tetrachloroethene	0.03	93	0.24	0.41	11.1	18.7	2.90	B1
Aquifer	Tetrachloroethene	0.03	5	0.24	0.45	0.6	1.0	2.91	B1

Sorbent	Compound	$f_{\infty}$ (%)	$v$ (cm/hr)	K (ml/g)	F	$k_2$ (hr <sup>-1</sup> )	k (hr <sup>-1</sup> )	log K <sub>oc</sub>	rf <sup>a</sup>
Aquifer	Toluene	0.13	90	0.05	0.48	15.1	28.8	1.59	B2
Aquifer	p-Xylene	0.13	90	0.14	0.39	8.4	13.9	2.03	B2
Aquifer	Naphthalene	0.13	90	0.22	0.55	9.5	21.1	2.23	B2
Aquifer	Chlorobenzene	0.13	90	0.09	0.46	10.1	18.7	1.84	B2
Aquifer	1,3-Dichlorobenzene	0.13	90	0.38	0.48	6.1	11.8	2.47	B2
Aquifer	1,2,4-Trichlorobenzene	0.13	90	0.73	0.49	5.5	10.7	2.75	B2
Aquifer	1,1,1-Trichloroethane	0.13	90	0.03	0.50	14.5	28.7	1.36	B2
Aquifer	1,2-trans-Dichloroethene	0.13	90	0.05	0.28	18.8	26.1	1.58	B2
Aquifer	Trichloroethene	0.13	90	0.09	0.32	8.1	11.9	1.84	B2
Aquifer	Tetrachloroethene	0.13	90	0.35	0.20	4.3	5.4	2.43	B2
Aquifer	p-Chlorophenol (pH=2)	0.13	90	0.07	0.73	10.2	38.2	1.73	B2
Aquifer	2,4-Dichlorophenol (pH=2)	0.13	90	0.10	0.71	16.4	56.5	1.89	B2
Aquifer	2,4,6-Trichlorophenol (pH=2)	0.13	90	0.24	0.56	8.4	19.3	2.27	B2
Aquifer	2,3,4,5-Tetrachlorophenol (pH=2)	0.13	90	0.94	0.77	3.9	17.0	2.86	B2
Aquifer	Pentachlorophenol (pH=2)	0.13	90	3.63	0.69	1.4	4.5	3.45	B2
Aquifer	Quinoline	0.13	90	0.45	0.72	7.0	24.8	2.54	B2
Muck	Trichloroethene	18	GP	41		2.7		2.36	B3
Soil	Trichloroethene	0.47	GP	1.1		1.7		2.37	B3
Soil	Trichloroethene	0.85	GP	1.17		1.9		2.14	B3
Soil	Trichloroethene	0.39	GP	0.23		17.1		1.77	B3
Soil	Tetrachloroethene	0.39	GP	0.74		7.2		2.78	B3
Muck	Benzene	18	GP	10		1.3		1.74	B3
Muck	Chlorobenzene	18	GP	22.5		1.5		2.10	B3



Sorbent	Compound	$f_{oc}$ (%)	$v$ (cm/hr)	K (ml/g)	F	$k_2$ (hr <sup>-1</sup> )	k (hr <sup>-1</sup> )	log K <sub>oc</sub>	rf <sup>a</sup>
Muck	1,2-Dichlorobenzene	18	GP	50		0.5		2.44	B3
Muck	1,2,4-Trichlorobenzene	18	GP	96		0.4		2.73	B3
Soil	Benzene	0.39	90	0.08		23.5		1.32	B3
Soil	Chlorobenzene	0.39	90	0.3		17		1.98	B3
Soil	1,2-Dichlorobenzene	0.39	90	0.94		9.8		2.38	B3
Soil	1,2,4-Trichlorobenzene	0.39	90	3.03		3.5		2.89	B3
Soil	Naphthalene	0.39	80	0.94	0.46	7.4	13.7	2.38	B4
Soil	Anthracene	0.39	80	33.7	0.52	0.6	1.3	3.94	B4
Aquifer	Tetrachloromethane	0.015	0.9	0.11	0.46	0.2	0.41	2.86	B5
Aquifer	Trichloroethene	0.015	0.9	0.11	0.43	0.4	0.63	2.86	B5
Aquifer	Tetrachloroethene	0.015	0.9	0.24	0.48	0.2	0.44	3.21	B5
Aquifer	p-Xylene	0.015	0.9	0.26	0.47	0.2	0.30	3.24	B5
Aquifer	1,4-Dichlorobenzene	0.015	0.9	0.79	0.50	0.1	0.13	3.72	B5
Aquifer	1,2-Dichlorobenzene	0.015	0.9	0.85	0.52	0.1	0.11	3.75	B5
Aquifer	Naphthalene	0.025	0.9	0.07	0.62	0.2	0.57	2.48	B5
Aquifer	Biphenyl	0.025	0.9	0.24	0.61	0.3	0.65	2.99	B5
Sediment	4,4'-Dichlorobiphenyl	3.4	GP	33000		0.003		5.99	C
Sediment	2,6,2',6'-Tetrachlorobiphenyl	3.4	GP	11000		0.0009		5.51	C
Sediment	2,4,6,2',4',6'-Hexachlorobiphenyl	3.4	GP	379000		0.0003		7.05	C
Sediment	2,4,5,2',4',5'-Hexachlorobiphenyl	3.4	GP	431000		0.0004		7.1	C

Sorbent	Compound	$f_{oc}$ (%)	$v$ (cm/hr)	$K$ (ml/g)	$F$	$k_2$ (hr <sup>-1</sup> )	$k$ (hr <sup>-1</sup> )	$\log K_{oc}$	rf <sup>a</sup>
Sediment	Phenanthrene	1.5	GP	250	0.40	0.11	0.19	4.22	K1
Sediment	Pyrene	1.5	GP	1260	0.57	0.02	0.046	4.92	K1
Sediment	Naphthalene	1.5	GP	20	0.38	0.62	1.0	3.12	K1
Sediment	Hexachlorobenzene	2.07	GP	7300	0.24	0.003	0.004	5.55	K2
Sediment	Hexachlorobenzene	0.15	GP	1100	0.48	0.026	0.05	5.87	K2
Sediment	Hexachlorobenzene	0.11	GP	1100	0.48	0.02	0.04	6.00	K2
Sediment	Hexachlorobenzene	3.04	GP	30000	0.13	0.001	0.001	5.99	K2
Sediment	Hexachlorobenzene	1.48	GP	2600	0.16	0.009	0.01	5.24	K2
Sediment	Hexachlorobenzene	1.21	GP	3500	0.28	0.02	0.03	5.46	K2
Sediment	Hexachlorobenzene	1.52	GP	2600	0.35	0.004	0.005	5.23	K2
Sediment	Pentachlorobenzene	3.04	GP	7600	0.23	0.004	0.005	5.40	K2
Sediment	Pentachlorobenzene	1.48	GP	2200	0.29	0.009	0.01	5.17	K2
Sediment	Pyrene	3.04	GP	2900	0.36	0.004	0.006	4.98	K2
Sediment	Pyrene	1.48	GP	1300	0.59	0.01	0.03	4.94	K2
Sediment	Trifluralin	0.72	GP	120	0.47	0.11	0.2	4.22	K2
Sediment	Trifluralin	0.11	GP	23	0.50	0.26	0.52	4.32	K2
Sediment	Trifluralin	3.04	GP	950	0.22	0.006	0.008	4.49	K2
Aquifer	Trichloroethene	0.034	24	0.15	0.23	3.0	3.9	2.65	L
Aquifer	Trichloroethene	0.025	24	0.10	0.10	3.8	4.18	2.59	L
Aquifer	p-Xylene	0.034	24	0.41	0.20	1.6	1.98	3.09	L
Aquifer	p-Xylene	0.025	24	0.23	0.13	2.2	2.57	2.96	L

Sorbent	Compound	$f_{oc}$ (%)	$v$ (cm/hr)	$K$ (ml/g)	$F$	$k_2$ (hr <sup>-1</sup> )	$k$ (hr <sup>-1</sup> )	$\log K_{oc}$	rf <sup>a</sup>
Aquifer	Lindane	1.14	2.21	42.4	0.10	0.01	0.016	3.57	M
Aquifer	Nitrobenzene	1.14	6.56	18.6	0.14	0.03	0.04	3.21	M
Aquifer	Bromoform	0.019	12.1	0.04	0.49	1.7	3.4	2.32	P
Aquifer	Carbon tetrachloride	0.019	12.1	0.08	0.33	0.79	1.2	2.62	P
Aquifer	Tetrachloroethene	0.019	12.1	0.1	0.46	1.5	2.7	2.72	P
Aquifer	1,2-Dichlorobenzene	0.019	12.1	0.17	0.44	1.1	1.9	2.95	P
Aquifer	Hexachloroethane	0.019	12.1	0.24	0.56	0.64	1.5	3.10	P
Aquifer	Bromoform	0.019	0.75	0.06	0.31	0.14	0.20	2.50	P
Aquifer	Carbon tetrachloride	0.019	0.75	0.40	0.34	0.11	0.17	3.33	P
Aquifer	Tetrachloroethene	0.019	0.75	0.30	0.46	0.04	0.067	3.19	P
Aquifer	1,2-Dichlorobenzene	0.019	0.75	0.41	0.40	0.05	0.088	3.34	P
Aquifer	Hexachloroethane	0.019	0.75	0.49	0.53	0.05	0.11	3.41	P
Soil	1,2,4-Trichlorobenzene	1.2	6	9	0.011	0.18	0.18	2.88	S
Soil	1,2,3,5-Tetrachlorobenzene	1.2	6	25	0.009	0.13	0.13	3.32	S

<sup>a</sup> References:

A:	Angle et al. (1992)	B5:	Brusseau et al. (1991d)	L:	Lee et al. (1988)
B1:	Brusseau (1992)	C:	Coates and Elzerman (1986)	M:	Miller and Weber (1986)
B2:	Brusseau and Rao (1991)	K1:	Karickhoff (1980)	P:	Ptacek and Gillham (1992)
B3:	Brusseau et al. (1990)	K2:	Karickhoff and Morris (1985)	S:	Southworth et al. (1987)
B4:	Brusseau et al. (1991b)				

## REFERENCE LIST

- Abernethy, S.G., D. Mackay, and L.S. McCarty (1988) "Volume fraction" correlation for narcosis in aquatic organisms: The key role of partitioning. *Environ. Toxic. Chem.* 7:469-481.
- Abriola, L.M. (1989) Modeling multiphase migration of organic chemicals in groundwater systems: A review and assessment. *Environ. Health Perspectives* 83:117-143.
- Abriola, L.M., and G.F. Pinder (1985) A multiphase approach to the modeling of porous media contaminated by organic compounds, 1. Equation development. *Water Resour. Res.* 21:11-18.
- Angle, J.T., M.L. Brusseau, W.L. Miller, and J.J. Delfino (1992) Nonequilibrium sorption and aerobic biodegradation of dissolved alkylbenzenes during transport in aquifer material: Column experiments and evaluation of a coupled-process model. *Environ. Sci. Technol.* 26:1404-1410.
- Augustijn, D.C.M., R.E. Jessup, P.S.C. Rao, and A.L. Wood (1993) Remediation of contaminated soils by solvent flushing. *J. Environ. Eng.* (in press).
- Avnir, D., D. Farin, and P. Pfeifer (1983) Chemistry in noninteger dimensions between two and three, II. Fractal surfaces of adsorbents. *J. Chem. Phys.* 79:3566-3571.
- Ball, W.P., Ch. Buehler, T.C. Harmon, D.M. Mackay, and P.V. Roberts (1990) Characterization of a sandy aquifer material at the grain scale. *J. Contam. Hydrol.* 5:253-295.
- Ball, W.P., M.N. Goltz, and P.V. Roberts (1991) Comment on "Modeling the transport of solutes influenced by multiprocess nonequilibrium" by M.L. Brusseau, R.E. Jessup, and P.S.C. Rao. *Water Resour. Res.* 27:653-656.
- Ball, W.P., and P.V. Roberts (1991) Long-term sorption of halogenated organic chemicals by aquifer material, 2. Intraparticle diffusion. *Environ. Sci. Technol.* 25:1237-1249.



- Banerjee, S. (1984) Solubility of organic mixtures in water. *Environ. Sci. Technol.* 18:587-591.
- Banerjee, S., and P.H. Howard (1988) Improved estimation of solubility and partitioning through correction of UNIFAC-derived activity coefficients. *Environ. Sci. Technol.* 22:839-841.
- Banerjee, P. M.D. Piwoni, and K. Ebeid (1985) Sorption of organic contaminants to a low carbon subsurface core. *Chemosphere* 14:1057-1067.
- Barber, L.B., E.M. Thurman, and D.D. Runnells (1992) Geochemical heterogeneity in a sand and gravel aquifer: Effect of sediment mineralogy and particle size on the sorption of chlorobenzenes. *J. Contam. Hydrol.* 9:35-54.
- Barcelona, M., A. Wehrmann, J.F. Keely, and W.A. Pettyjohn (1990) Contamination of Ground Water; Prevention, Assessment, Restoration. Noyes Data Corp. (Park Ridge, NJ) 213 pp.
- Biggar, J.W., and D.R. Nielsen (1976) Spatial variability of the leaching characteristics of a field soil. *Water Resour. Res.* 12:78-84.
- Borden, R.C., and M.D. Piwoni (1992) Hydrocarbon dissolution and transport: A comparison of equilibrium and kinetic models. *J. Contam. Hydrol.* 10:309-323.
- Bouchard, R.C., C.G. Enfield, and M.D. Piwoni (1989) Transport processes involving organic chemicals. In: B.L. Sawhney, and K. Brown (Eds.) *Reactions and Movement of Organic Chemicals in Soils*. Soil Sci. Soc. Am. (Madison, WI) Special Publication No. 22 p. 349-371.
- Brusseau, M.L. (1992) Nonequilibrium transport of organic chemicals: The impact of pore-water velocity. *J. Contam. Hydrol.* 9:353-368.
- Brusseau, M.L., R.E. Jessup, and P.S.C. Rao (1990) Sorption kinetics of organic chemicals: Evaluation of gas-purge and miscible-displacement techniques. *Environ. Sci. Technol.* 24:727-735.
- Brusseau, M.L. R.E. Jessup, and P.S.C. Rao (1991a) Nonequilibrium sorption of organic chemicals: Elucidation of rate-limiting processes. *Environ. Sci. Technol.* 25:134-142.
- Brusseau, M.L., R.E. Jessup, and P.S.C. Rao (1991c) Reply to W.P. Ball, M.N. Goltz, and P.V. Roberts' comment on "Modeling the transport of solutes influenced by multiprocess nonequilibrium" by M.L. Brusseau, R.E. Jessup, and P.S.C.

Rao. *Water Resour. Res.* 27:657-659.

Brusseau, M.L., T. Larsen, and T.H. Christensen (1991d) Rate-limited sorption and nonequilibrium transport of organic chemicals in low organic aquifer materials. *Water Resour. Res.* 27:1137-1145.

Brusseau, M.L., and P.S.C. Rao (1989a) Sorption nonideality during organic contaminant transport in porous media. *CRC Critical Reviews in Environ. Control* 19:33-99.

Brusseau, M.L., and P.S.C. Rao (1989b) The influence of sorbate-organic matter interactions on sorption nonequilibrium. *Chemosphere* 18:1691-1706.

Brusseau, M.L., and P.S.C. Rao (1991) Influence of sorbate structure on nonequilibrium sorption of organic compounds. *Environ. Sci. Technol.* 25:1501-1506.

Brusseau, M.L., P.S.C. Rao, R.E. Jessup, and J.M. Davidson (1989) Flow interruption: A method for investigating sorption nonequilibrium. *J. Contam. Hydrol.* 4:233-240.

Brusseau, M.L., A.L. Wood, and P.S.C. Rao (1991b) Influence of organic cosolvents on the sorption kinetics of hydrophobic organic chemicals. *Environ. Sci. Technol.* 25:903-910.

Cameron, D.R., and A. Klute (1977) Convective-dispersive solute transport with a combined equilibrium and kinetic adsorption model. *Water Resour. Res.* 13:183-188.

Chatzis, I., N.R. Morrow, and H.T. Lim (1983) Magnitude and detailed structure of residual oil saturations. *Soc. Petrol. Eng. J.* 22:311-326.

Chen, C.S. (1993) Partitioning of Motor Oil Components Into Water. Master Thesis, University of Florida.

Chiou, C.T. (1989) Theoretical considerations of the partition uptake of nonionic organic compounds by soil organic matter. In: B.L. Sawhney, and K. Brown (Eds.) *Reactions and Movement of Organic Chemicals in Soils*. Soil Sci. Soc. Am. (Madison, WI) Special Publication No. 22 p. 1-29.

Chiou, C.T. (1990) Roles of organic matter, minerals, and moisture in sorption of nonionic compounds and pesticides by soil. In: P. MacCarthy, C.E. Clapp, R.L. Malcolm, and P.R. Bloom (Eds.) *Humic Substances in Soil and Crop Sciences; Selected Readings*. Am. Soc. Agron. (Madison, WI) p. 111-160.

- Cline, P.V., J.J. Delfino, and P.S.C. Rao (1991) Partitioning of aromatic constituents into water from gasoline and other complex solvent mixtures. *Environ. Sci. Technol.* 25:914-920.
- Coates, J.T., and A.W. Elzerman (1986) Desorption kinetics for selected PCB congeners from river sediments. *J. Contam. Hydrol.* 1:191-210.
- Corapcioglu, M.Y., and A.L. Baehr (1987) A compositional multiphase model for groundwater contamination by petroleum products, 1. Theoretical considerations. *Water Resour. Res.* 23:191-200.
- Corey, A.T. (1986) *Mechanics of Immiscible Fluids in Porous Media.* Water Resources Publications (Littleton, CO) 255 pp.
- Crank, J. (1975) *The Mathematics of Diffusion.* Oxford University Press (Oxford) 2nd edition, 414 pp.
- Davidson, J.M., P.S.C. Rao, and P. Nkedi-Kizza (1983) Physical processes influencing water and solute transport in soils. In: D.W. Nelson, D.E. Elrick, and K.K. Tanji (Eds.) *Chemical Mobility and Reactivity in Soil Systems.* Soil Sci. Soc. Am. (Madison, WI) Special Publication No. 11 p. 35-47.
- De Smedt, F., and P.J. Wierenga (1984) Solute transfer through columns of glass beads. *Water Resour. Res.* 20:225-232.
- EPRI (1993) *Chemical and Physical Characteristics of Coal Tar From Selected Manufactured Gas Plant (MGP) sites.* EPRI-RP2879-01,12 (In press).
- Falta, R.W., I. Javandel, K. Pruess, and P.A. Witherspoon (1989) Density-driven flow of gas in the unsaturated zone due to evaporation of volatile organic compounds. *Water Resour. Res.* 25:2159-2169.
- Fried, J.J., P. Muntzer and L. Zilliox (1979) Ground-water pollution by transfer of oil hydrocarbons. *Ground Water* 17:586-594.
- Fu, J., and R.G. Luthy (1986a) Aromatic compound solubility in solvent/water mixtures. *J. Environ. Eng.* 112:328-345.
- Fu, J., and R.G. Luthy (1986b) Effect of organic solvent on sorption of aromatic solutes onto Soils. *J. Environ. Eng.* 112:346-366.
- Gerstl, Z. (1990) Estimation of organic chemical sorption by soils. *J. Contam. Hydrol.* 6:357-375.



- Hansen, H.K., P. Rasmussen, A. Fredenslund, M. Schiller, and J. Gmehling (1991) Vapor-liquid equilibria by UNIFAC group contribution, 5. Revision and extension. *Ind. Eng. Chem. Res.* 30:2352-2355.
- Hoag, G.E., and M.C. Marley (1986) Gasoline residual saturation in unsaturated uniform aquifer materials. *J. Environ. Eng.* 112:586-604.
- Huling, S.G., and J.W. Weaver (1991) Dense Nonaqueous Phase Liquids. Ground Water Issue, Environmental Protection Agency (Ada, OK) 21 pp.
- Hunt J.R., N. Sitar, and K.S. Udell (1988) Nonaqueous phase transport and cleanup, 1. Analysis of mechanisms. *Water Resour. Res* 24:1247-1258.
- Jury, W.A., and K. Roth (1990) Transfer Functions and Solute Movement Through Soil. Birkhäuser Verlag (Basel) pp. 226.
- Kaluarachchi, J.J., and J.C. Parker (1990) Modeling multicomponent organic chemical transport in three-fluid-phase porous media. *J. Contam. Hydrol.* 5:349-374.
- Karickhoff, S.W. (1980) Sorption kinetics of hydrophobic pollutants in natural sediments. In: R.A. Baker (Ed.) *Contaminants and Sediments, Vol. 2. Analysis, Chemistry, Biology.* Ann Arbor Science Publishers, Inc. (Ann Arbor, MI) p. 193-205.
- Karickhoff, S.W. (1985) Pollutant sorption in environmental systems. In: W.B. Neely, and G.E. Blau (Eds.) *Environmental Exposure from Chemicals, Vol 1.* CRC Press (Boca Raton, FL) p. 49-64.
- Karickhoff, S.W., D.S. Brown, and T.A. Scott (1979) Sorption of hydrophobic pollutants on natural sediments. *Water Res.* 13:241-248.
- Karickhoff, S.W., and K.R. Morris (1985) Sorption dynamics of hydrophobic pollutants in sediment suspensions. *Environ. Toxic. Chem.* 4:469-479.
- Koorevaar, P., G. Menelik, and C. Dirksen (1983) *Elements of Soil Physics.* Elsevier (Amsterdam) 228 pp.
- Lane, W.F., and R.C. Loehr (1992) Estimating the equilibrium aqueous concentrations of polynuclear aromatic hydrocarbons in complex mixtures. *Environ. Sci. Technol.* 26:983-990.
- Lee, L.S., M. Hagwall, J.J. Delfino, and P.S.C. Rao (1992a) Partitioning of polynuclear aromatic hydrocarbons into water from diesel fuel. *Environ. Sci.*



Technol. 26:2104-2110.

- Lee, L.S., P.S.C. Rao, M.L. Brusseau, and R.A. Ogwada (1988) Nonequilibrium sorption of organic contaminants during flow through columns of aquifer material. *Environ. Toxic. Chem.* 7:779-793.
- Lee, L.S., P.S.C. Rao, and I. Okuda (1992b) Equilibrium partitioning of polynuclear aromatic hydrocarbons from coal tar into water. *Environ. Sci. Technol.* 26:2110-2115.
- Leenheer, J.A. (1991) Organic substance structures that facilitate contaminant transport and transformations in aquatic sediments. In: R.A. Baker (Ed.) *Organic Substances and Sediments in Water*, Vol 1. Lewis Publishers, Inc. (Chelsea, MI) p. 3.
- Leinonen, P.J., and D. Mackay (1973) The multicomponent solubility of hydrocarbons in water. *Can. J. Chem. Eng.* 51:230-233.
- Lenhard, R.J., J.C. Parker, and J.J. Kaluarachchi (1989) A model for hysteretic constitutive relations governing multiphase flow, 3. Refinements and numerical simulations. *Water Resour. Res.* 25:1727-1736.
- Lion, L.W., T.B. Stauffer, and W.G. MacIntyre (1990) Sorption of hydrophobic compounds on aquifer materials: Analysis methods and the effect of organic carbon. *J. Contam. Hydrol.* 5:215-234.
- Little, Arthur D., Inc. (1981) Reference constants for priority pollutants and selected chemicals. Report to Wald, Harkrader, and Ross (Washington, DC) Reference No. 84204.
- Mackay, D.M., J.A. Cherry (1989) Groundwater contamination: Pump-and-treat remediation. *Environ. Sci. Technol.* 23:630-636.
- Mackay, D., W.Y. Shiu, A. Maijanen, and S. Feenstra (1991) Dissolution of non-aqueous phase liquids in groundwater. *J. Contam. Hydrol.* 8:23-42.
- Mandelbrot, B.B. (1982) *The fractal geometry of nature*. Freeman (San Francisco) 460 pp.
- Means, J.C., S.G. Wood, J.J. Hassett, and W.L. Banwart (1980) Sorption of polynuclear aromatic hydrocarbons by sediments and soils. *Environ. Sci. Technol.* 14:1524-1528.
- Mendoza, C.A., and E.O. Frind (1990) Advective-dispersive transport of dense

organic vapors in the unsaturated zone, 1. Model development. *Water Resour. Res.* 26:379-387.

Mercer, J.W., and R.M. Cohen (1990) A review of immiscible fluids in the subsurface: Properties, models, characterization, and remediation. *J. Contam. Hydrol.* 6:107-163.

Mihelcic, J.R. (1990) Modeling the potential effect of additives on enhancing the solubility of aromatic solutes contained in gasoline. *Ground Water Monitoring Review* 10(3):132-137.

Miller, C.T., M.M. Poirier-McNeill, and A.S. Mayer (1990) Dissolution of trapped nonaqueous phase liquids: Mass transfer characteristics. *Water Resour. Res.* 26:2783-2796.

Miller, C.T. and W.J. Weber (1986) Sorption of hydrophobic organic pollutants in saturated soil systems. *J. Contam. Hydrol.* 1:243-261.

Mingelgrin, V., and Z. Gerstl (1983) Reevaluation of partitioning as a mechanism of nonionic chemicals adsorption in soils. *J. Environ. Qual.* 12:1-11.

Mood, A.M., F.A. Graybill, and D.C. Boes (1974) *Introduction to the Theory of Statistics*. McGraw-Hill (New York, NY) 3rd edition, 564 pp.

Morris, K.R., R. Abramowitz, R. Pinal, P. Davis, and S.H. Yalkowsky (1988) Solubility of aromatic pollutants in mixed solvents. *Chemosphere* 17:285-298.

Nkedi-Kizza, P., J.W. Biggar, H.M. Selim, M.Th. van Genuchten, P.J. Wierenga, J.M. Davidson, and D.R. Nielsen (1984) On the equivalence of two conceptual models for describing ion exchange during transport through an aggregated oxisol. *Water Resour. Res.* 8:1123-1130.

Nkedi-Kizza, P., M.L. Brusseau, P.S.C. Rao, and A.G. Hornsby (1989) Nonequilibrium sorption during displacement of hydrophobic organic chemicals and <sup>45</sup>Ca through soil columns with aqueous and mixed solvents. *Environ. Sci. Technol.* 23:814-820.

Nkedi-Kizza, P., P.S.C. Rao, and A.G. Hornsby (1985) Influence of organic cosolvents on sorption of hydrophobic organic chemicals by soils. *Environ. Sci. Technol.* 19:975-979.

Nkedi-Kizza P., P.S.C. Rao, and A.G. Hornsby (1987) Influence of organic cosolvents on leaching of hydrophobic organic chemicals through soils. *Environ. Sci. Technol.* 21:1107-1111.

- Nkedi-Kizza, P., P.S.C. Rao, R.E. Jessup, and J.M. Davidson (1982) Ion exchange and diffusive mass transfer during miscible displacement through an aggregated oxisol. *Soil Sci. Soc. Am. J.* 46:471-476.
- Passioura, J.B. (1971) Hydrodynamic dispersion in aggregated media, 1. Theory. *Soil Sci.* 111:339-344.
- Palmer, C.D., and W. Fish (1992) Chemical Enhancements to Pump-and-Treat Remediation. EPA/540/S-92/001, R.S. Kerr Env. Res. Lab., U.S. EPA, Ada, OK.
- Parker, J.C., and A.J. Valocchi (1986) Constraints on the validity of equilibrium and first-order kinetic transport models in structured soils. *Water Resour. Res.* 22:399-407.
- Parker, J.C., and M.Th. Van Genuchten (1984) Determining Transport Parameters from Laboratory and Field Tracer Experiments. Virginia Agricultural Experiment Station Bulletin 84-3, 96 pp.
- Pennell, K.D., R.D. Rhue, P.S.C. Rao, and C.T. Johnston (1992) Vapor-phase sorption of p-xylene and water on soils and clay minerals. *Environ. Sci. Technol.* 26:756-763.
- Pfannkuch, H.-O. (1984) Ground water contamination by crude oil at the Bemidji, Minnesota research site: U.S. Geological Survey toxic waste-ground water contamination study. Paper presented at Toxic-Waste Technical Meeting, U.S. Geol. Surv. (Reston, VA).
- Pfeifer, P. (1987) Characterization of surface irregularity. In: P. Laszlo (Ed.) *Preparative Chemistry Using Supported Reagents*. Academic Press (San Diego) p. 13-33.
- Pignatello, J.J. (1990) Slowly reversible sorption of aliphatic halocarbons in soils. I. Formation of reversible fractions. *Environ. Toxic. Chem.* 9:1107-1115.
- Pinal, R., L.S. Lee, and P.S.C. Rao (1991) Prediction of the solubility of hydrophobic compounds in nonideal solvent mixtures. *Chemosphere* 22:939-951.
- Pinal, R., P.S.C. Rao, L.S. Lee, and P.V. Cline (1990) Cosolvency of partially miscible organic solvents on the solubility of hydrophobic organic chemicals. *Environ. Sci. Technol.* 24:639-647.
- Poulsen, M., L. Lemon, and J.F. Barker (1992) Dissolution of monoaromatic hydrocarbons into groundwater from gasoline-oxygenate mixtures. *Environ.*



Sci. Technol. 26:2483-2489.

- Powers, S.E., L.M. Abriola, and W.J. Weber (1992) An experimental investigation of nonaqueous phase liquid dissolution in saturated subsurface systems: Steady state mass transfer rates. *Water Resour. Res.* 28:2691-2705.
- Powers, S.E., C.O. Loureiro, L.M. Abriola, and W.J. Weber (1991) Theoretical study of the significance of nonequilibrium dissolution of nonaqueous phase liquids in subsurface systems. *Water Resour. Res.* 27:463-477.
- Ptacek, C.J., and R.W. Gillham (1992) Laboratory and field measurements of nonequilibrium transport in the Borden aquifer, Ontario, Canada. *J. Contam. Hydrol.* 10:119-158.
- Prausnitz, J.M. (1969) *Molecular Thermodynamics of Fluid Phase Equilibria*. Prentice Hall (Englewood Cliffs, NJ).
- Rao, P.S.C., A.G. Hornsby, D.P. Kilcrease and P.J. Nkedi-Kizza (1985) Sorption and transport of hydrophobic organic chemicals in aqueous and mixed solvent systems: Model development and preliminary evaluation. *J. Environ. Qual.* 14:376-383.
- Rao, P.S.C., R.E. Jessup, and T.M. Addiscott (1982) Experimental and theoretical aspects of solute diffusion in spherical and nonspherical aggregates. *Soil Sci.* 133:342-349.
- Rao, P.S.C., L.S. Lee, P. Nkedi-Kizza, and S.H. Yalkowsky (1989) Sorption and transport of organic pollutants at waste disposal sites. In: Z. Gerstl, Y. Chen, U. Mingelgrin, and B. Yaron (Eds.) *Toxic Organic Chemicals in Porous Media*. Springer-Verlag (Berlin) *Ecological Studies* 73, p.176-192.
- Rao, P.S.C., L.S. Lee and R. Pinal (1990) Cosolvency and sorption of hydrophobic organic chemicals. *Environ. Sci. Technol.* 24:647-654.
- Rao, P.S.C., L.S. Lee, and A.L. Wood (1991) Solubility, sorption, and transport of hydrophobic organic chemicals in complex mixtures. *Environ. Research Brief*, EPA-600/M-91/009, U.S. EPA (Ada, OK).
- Rao, P.S.C., D.E. Rolston, R.E. Jessup, and J.M. Davidson (1980) Solute transport in aggregated porous media: Theoretical and experimental evaluation. *Soil Sci. Soc. Am. J.* 44:1139-1146.
- Rappoldt, C. (1990) The application of diffusion models to an aggregated soil. *Soil Sci.* 150:645-661.



- Rhue, R.D., K.D. Pennell, P.S.C. Rao, and W.H. Reve (1989) Competitive adsorption of alkylbenzene and water vapors on predominantly mineral surfaces. *Chemosphere* 18:1971-1986.
- Rice, J.A. and J.-S. Lin (1993) Fractal nature of humic material. *Envir. Sci. Technol.* 27:413-414.
- Rullkotter, J., and W. Michaelis (1990) The structure of kerogen and related materials: A review of recent progress and future trends. *Org. Geochem.* 16:829-852.
- Schnitzer, M. (1978) Humic substances: Chemistry and reactions. In: M. Schnitzer and K.S.U. Khan (Eds.) *Soil Organic Matter*. Elsevier (Amsterdam) *Developments in Soil Sci.* 8 p. 1-64.
- Schwarzenbach, R.P., and J. Westall (1981) Transport of nonpolar organic compounds from surface water to groundwater: Laboratory sorption studies. *Environ. Sci. Technol.* 15:1360-1367.
- Schwille, F. (1984) Migration of organic fluids immiscible with water in the unsaturated zone. In: B. Yaron, G. Dagan, and J. Goldshmid (Eds.) *Pollutants in Porous Media, the Unsaturated Zone Between Soil Surface and Groundwater*. Springer-Verlag (Berlin) *Ecol. Studies* 47 p. 27-48.
- Schwille, F. (1988) *Dense Chlorinated Solvents in Porous and Fractured Media*. Lewis (Chelsea, MI) 146 pp.
- Seagren, E.A., B.E. Rittmann, and A.J. Valocchi (1993) Quantitative evaluation of flushing and biodegradation for enhancing in situ dissolution of nonaqueous-phase liquids. *J. Contam. Hydrol.* 12:103-132.
- Selim, H.M., J.M. Davidson, and R.S. Mansell (1976) Evaluation of a two-site adsorption-desorption model for describing solute transport in soils. In: *Proc. Summer Computer Simulation Conf.*, Washington, DC.
- Sleep, B.E., and J.F. Sykes (1989) Modeling the transport of volatile organics in variably saturated media. *Water Resour. Res.* 25: 81-92.
- Snyder, L.R., and Kirkland, J.J. (1979) *Introduction to Modern Liquid Chromatography*. Wiley & Sons, Inc. (New York, NY) 2nd edition.
- Southworth G.R., K.W. Watson, and J.L. Keller (1987) Comparison of models that describe the transport of organic compounds in macroporous soil. *Environ. Toxic. Chem.* 6:251-257.

- Starr, J.L., and J.-Y. Parlange (1979) Dispersion in soil columns: The snow plow effect. *Soil Sci. Soc. Am. J.* 43:488-450.
- Stevenson, F.J. (1985) Geochemistry of soil humic substances. In: G.R. Aiken, D.M. McKnight, R.L. Wershaw, and P. MacCarthy (Eds.) *Humic Substances in Soil, Sediment, and water*. John Wiley & Sons (New York, NY) p. 13-52.
- Sun, S., and S.A. Boyd (1991) Sorption of polychlorobiphenyl (PCB) congeners by residual PCB-oil phases in soils. *J. Environ. Qual.* 20:557-561.
- Travis, C.C., and E.L. Etnier (1981) A survey of sorptive relationships for reactive solutes in soil. *J. Environ. Qual.* 10:8-17.
- U.S. EPA (1990) Solvent Extraction Treatment. EPA/540/2-90/013, Office of Emergency and Remedial Response, U.S. EPA (Washington, DC).
- U.S. EPA (1991) In Situ Solvent Flushing. EPA/540/2-91/021, Office of Emergency and Remedial Response, U.S. EPA (Washington, DC).
- Vadas, G.G., W.G. MacIntyre, and D.R. Burris (1991) Aqueous solubility of liquid hydrocarbon mixtures containing dissolved solid components. *Environ. Toxic. Chem.* 10:633-639.
- Valocchi, A.J. (1985) Validity of the local equilibrium assumption for modeling sorbing solute transport through homogeneous soils. *Water Resour. Res.* 21:808-820.
- Van Dam, J. (1967) The migration of hydrocarbons in a water-bearing stratum. In: P. Hepple (Ed.) *The Joint Problems of the Oil and Water Industries*. Inst. Pet. (London) p. 55-88.
- Van der Waarden, M., A.L.A.M. Bridié, and W.M. Groenewoud (1971) Transport of mineral oil components to groundwater, 1. Model experiments on the transfer of hydrocarbons from a residual oil zone to trickling water. *Water Res.* 5:213-226.
- Van Genuchten, M.Th., and F.N. Dalton (1986) Models for simulating salt movement in aggregated field soils. *Geoderma* 38:165-183.
- Van Genuchten, M.Th., and P.J. Wierenga (1976) Mass transfer studies in sorbing porous media, 1. Analytical solutions. *Soil Sci. Soc. Am. J.* 40:473-480.
- Van Genuchten, M.Th., and P.J. Wierenga (1977) Mass transfer studies in sorbing porous media, 2. Experimental evaluation with tritium ( $^3\text{H}_2\text{O}$ ). *Soil Sci. Soc.*

Am. J. 41:272-278.

Verschuieren, K. (1983) Handbook of Environmental Data on Organic Chemicals. Van Nostrand Reinhold (New York, NY) 2nd edition, 1310 pp.

Wang, H.F., M.P. Anderson (1982) Introduction to groundwater modeling; Finite difference and finite elements methods. Freeman (New York, NY) 237 pp.

Weber, W.J., and C.T. Miller (1988) Modeling the sorption of hydrophobic contaminants by aquifer material, 1. Rates and equilibrium. Water Res. 22:457-464.

Wershaw, R.L. (1986) A new model for humic materials and their interactions with hydrophobic organic chemicals in soil-water or sediment-water systems. J. Contam. Hydrol. 1:29-45.

Wilson, J.L., S.H. Conrad, W.R. Mason, W. Peplinski, and E. Hagan (1990) Laboratory Investigation of Residual Organics from Spills, Leaks, and the Disposal of Hazardous Wastes in Groundwater. EPA/600/6-90/004 U.S. EPA 267 pp.

Wise, W.R., G.C. Robinson, and P.B. Bedient (1992) Chromatographic evidence for nonlinear partitioning of aromatic compounds between petroleum and water. Ground Water 30:936-944.

Wood, A.L., D.C. Bouchard, M.L. Brusseau and P.S.C. Rao (1990) Cosolvent effects on sorption and mobility of organic contaminants in soils. Chemosphere 21:575-587.

Wu, S.C., and P.M. Gschwend (1986) Sorption kinetics of hydrophobic organic compounds to natural sediments and soils. Environ. Sci. Technol. 20:717-725.

Wu, S.C., and P.M. Gschwend (1988) Numerical modeling of sorption kinetics of organic compounds to soil and sediments particles. Water Resour. Res. 24:1373-1383.

Yalkowsky, S.H. (1979) Estimation of entropies of fusion of organic compounds. I&EC Fundam. 18:108-111.

Yalkowsky, S.H. and T. Roseman (1981) Solubilization of drugs by cosolvents. In: Yalkowsky S.H. (Ed.) Techniques of Solubilization of Drugs. Marcel Dekker Inc. (New York, NY) p. 91-134.

Zalidis, G.C., M.D. Annable, R.B. Wallace, N.J. Hayden, and T.C. Voice (1991) A

laboratory method for studying the aqueous phase transport of dissolved constituents from residually held NAPL in saturated soil columns. *J. Contam. Hydrol.* 8:143-156.

Zielinski, J.M. and J.L. Duda (1992) Predicting polymer/solvent diffusion coefficients using free-volume theory. *Am. Inst. Chem. Eng. J.* 38:405-415.



## BIOGRAPHICAL SKETCH

Dionysius (Denie) C.M. Augustijn was born on November 7<sup>th</sup> 1964 in Etten-Leur, The Netherlands. He was the 4<sup>th</sup> out of 5 children born to a miller's family. After graduating from high school in 1983, he went to the Agricultural University Wageningen, and it was there that he decided to become a soil scientist. In 1987 he spent 7 months at the University of Florida in Gainesville, as part of his graduate program. Two years later, in the summer of 1989, he received the Dutch "ingenieurs" degree, which is equivalent to the American master's degree. Shortly after his graduation he married, and returned to the University of Florida, together with his wife Ellen-Wien, to start a Ph.D. In May 1993 he will start a new position at Shell Research Ltd., Sittingbourne, England.

I certify that I have read this study and that in my opinion it conforms to acceptable standards of scholarly presentation and is fully adequate, in scope and quality, as a dissertation for the degree of Doctor of Philosophy.



---

P.S.C. Rao, Chair  
Professor of Soil and Water Science

I certify that I have read this study and that in my opinion it conforms to acceptable standards of scholarly presentation and is fully adequate, in scope and quality, as a dissertation for the degree of Doctor of Philosophy.



---

P. Nkedi-Kizza  
Associate Professor of Soil and Water  
Science

I certify that I have read this study and that in my opinion it conforms to acceptable standards of scholarly presentation and is fully adequate, in scope and quality, as a dissertation for the degree of Doctor of Philosophy.



---

R.D. Rhue  
Associate Professor of Soil and Water  
Science


I certify that I have read this study and that in my opinion it conforms to acceptable standards of scholarly presentation and is fully adequate, in scope and quality, as a dissertation for the degree of Doctor of Philosophy.



---


W.D. Graham  
Assistant Professor of Agricultural  
Engineering

I certify that I have read this study and that in my opinion it conforms to acceptable standards of scholarly presentation and is fully adequate, in scope and quality, as a dissertation for the degree of Doctor of Philosophy.

  
\_\_\_\_\_  
K. Hatfield  
Assistant Professor of Civil Engineering

This dissertation was submitted to the Graduate Faculty of the College of Agriculture and to the Graduate School and was accepted as partial fulfillment of the requirements for the degree of Doctor of Philosophy.

August 1993

  
\_\_\_\_\_  
Dean, College of Agriculture

\_\_\_\_\_  
Dean, Graduate School